4th International Conference on Engineering and Formal Sciences

Amsterdam, 14-15 December 2018

Venue

Amsterdam Science Park

Conference Proceedings

ISBN 978-88-909700-4-7

REVISTIA

PUBLISHING AND RESEARCH

Amsterdam, 14-15 December 2018

ISBN 9788890970047

Venue

Amsterdam Science Park

Typeset by Revistia

Printed in Amsterdam

Address: 11, Portland Road, London, SE25 4UF, United Kingdom
Tel: +44 2080680407
E-Mail: office@revistia.com

International Scientific and Advisory Board

Emilian Dobrescu, PhD, Academia Romana, Bucharest

Misu Jan Manolescu, PhD, Rector, University of Oradea

Nik Maheran, PhD, Director, GERIC - University of Malaysia

Siniša Opić, PhD, University of Zagrep

Mixhait Reci, PhD, President Iliria College, Pristina-Kosovo

Catalin Zamfir, PhD, Director, ICCV, Academia Romana

İsmail Hakki Mirici, PhD, President, WCCI, Turkiye

Rodica Sirbu, PhD, Ovidius" University of Constanţa, Faculty of Pharmacy, Romania

M. G. Varvounis, PhD, Democritus University of Thrace, Greece

Sohail Amjad, PhD, University of Engineering and Technology, Mardan

Miriam Aparicio, PhD, National Scientific and Technical Research Council - Argentina

Manasi Gore. PhD, Pune University, Maharashtra, India

Sri Nuryanti, PhD, Indonesian Institute of Sciences, Indonesia

Gani Pllana, PhD, Faculty of Mechanical Engineering, University of "Hasan Prishtina", Kosovo

Siew Hong Lam, PhD, Department of Biological Sciences, National University of Singapore

Basira Azizaliyeva, PhD, Azerbaijan National Academy of Sciences, Baku, Azerbaijan

Ahmet Ecirli, PhD, INSOC, Romanian Academy, Bucharest

Sokol Pacukaj, PhD, MCSER, Italy

TABLE OF CONTENTS

Virtual Learning Environments Practices, in the students of System Engineering of the Tecnologico Nacional de Mexico, Campus Mexicali

Jesus Francisco Gutierrez Ocampo

Corina Araceli Ortiz Perez

M.C. Jose Antonio Camaño Quevedo

Abstract.

The virtual learning environment is not just about taking a course and placing it on a computer, it deals with a combination of resources, interactivity, support and activities of structured learning. To carry out this process it is necessary to know the possibilities and limitations that the computer support or virtual platform offers us, so that the students achieve their study objective more adequately, for that reason its use is studied in the students of computer systems engineering career of the Tecnologico Nacional de Mexico, Campus Mexicali.

Keywords: Virtual Learning Environments, TECNM, Ingenieria de sistemas.

Introduction

This 2018 participates in the entrance exam to the Tecnologico Nacional de Mexico, Mexicali campus, and as a tutor I have to deliver the results of this to a group of students of the Systems Engineering Career of this school, this process is not New, but increasingly it is more important for the results offered by this test to the student and the teacher, to be delivering the results to students, I realized that I was missing information on virtual learning environments, because they are currently used in the vast majority of educational institutions, and I took on the task of researching on this topic that I consider that boosts the competitiveness of the institutions that use them.

Methodology

explaining how this research was carried out, based on the conception of the idea, and its problematic, we defined the objectives and formulated the questions, then we defined the study population, indicating the main factors for which it has been delimited, including the formula statistics used to determine the sample, the instrument used for compiling the information was designed, which forms the sample, basically focusing on the survey. And, finally, we will detail the assumptions used in the investigation, as well as the statistical results.

n = 75

N = 417

Zα = 1.96

p = .17

q = .17

e = .17

$$n = \frac{417\,(3.8416)\,(0.5)\,(0.5)}{(417-1)(0.0025)+(3.8416)(0.17)(0.17)} = 75$$

Survey:

1. The virtual learning environment, which is used in the subjects of the career of Computer Systems Engineering at the TECNM Campus Mexicali, are known by students.

2. The virtual learning environment, which is used in the subjects of the career of Computer Systems Engineering at the TECNM Campus Mexicali, is useful for the student.

3. The virtual learning environment, which is used in the subjects of the career of Computer Systems Engineering at the TECNM Campus Mexicali, is used regularly in classes.

4. The virtual learning environment, which is used in the subjects of the career of Computer Systems Engineering at the TECNM Campus Mexicali, are known by students, will be recommended to other students.

5. The virtual learning environment, which is used in the subjects of the career of Computer Systems Engineering at the TECNM Campus Mexicali, are known by students, considers them necessary for a better learning.

6. The virtual learning environment, which is used in the subjects of the career of Computer Systems Engineering at the TECNM Campus Mexicali, are known by students, Apart from the use in class you have seen them being used in some other career.

7. The virtual learning environment, which is used in the subjects of the career of Computer Systems Engineering at the TECNM Campus Mexicali, are known by students, In the last 12 months you have used them.

8. The virtual learning environment, which is used in the subjects of the career of Computer Systems Engineering at the TECNM Campus Mexicali, are known by students, If you had the opportunity to use this technology you would use it.

9. The virtual learning environment, which is used in the subjects of the career of Computer Systems Engineering at the TECNM Campus Mexicali, are known by students, considers them reliable for use in the classroom.

10. The virtual learning environment, which is used in the subjects of the career of Computer Systems Engineering at the TECNM Campus Mexicali, are known by students, You consider yourself an enthusiast of the virtual learning environment.

With the following multiple choice answers:

a) Strongly Disagree

b) Disagree

c) I slightly disagree

d) A little agreement

e) Agree

f) Totally agree

Result:

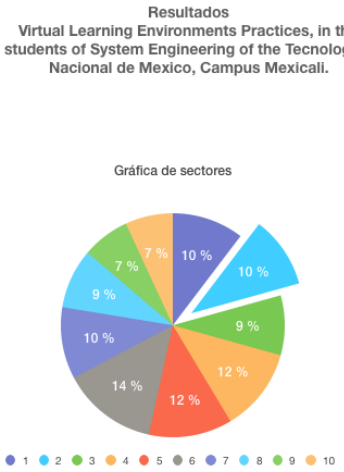

Resultados

CUESTION	ANSWER 1	ANSWER 2	ANSWER 3	ANSWER 4	ANSWER 5	ANSWER 6
1	6	4	5	4	5	7
2	6	7	7	4	7	7
3	5	6	6	3	6	8
4	7	5	7	5	7	8
5	7	5	7	5	7	6
6	8	8	4	6	8	7
7	6	7	3	6	8	7
8	5	4	5	6	5	7
9	4	5	6	7	5	6
10	4	4	4	5	4	6

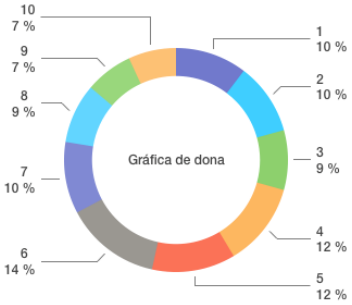

Conclusion

The virtual learning environment, which is used in the subjects of the career of Computer Systems Engineering at the TECNM Campus Mexicali on the answers obtained it is known by the students, besides being considered useful, and is used regularly in classes, and students recommend it to other students, and consider them necessary for a good learning, it was detected that not all the students use the virtual learning environment.

References

[1] Cabero, J. y Llorente, M.C. (2005). Las plataformas virtuales en el ámbito de la teleformación, en Revista electrónica Alternativas de Educación y Comunicación. Disponible en http://tecnologiaedu.us.es/cuestionario/bibliovir/plataformas_virtuales_tel eformacion_2005.pdf

[2] 2-9th annual International Conference of Education, Research and Innovation p. 816-825

[3] Michael porter. (1983). Cases in Competitive Strategy. usa: the free press.

The Principles of Energy Efficient Microclimate Provision in the Skyscraper "Biotecton" of 1 km Height

Krivenko O.
PhD, associate professor, Department of Architectural Constructions
Kyiv National University of Construction and Architecture, Kyiv, Ukraine

Mileikovskyi V.
PhD, associate professor, Department of Heat Gas Supply and Ventilation
Kyiv National University of Construction and Architecture, Kyiv, Ukraine

Tkachenko T.
PhD, associate professor, Department of Labor Protection and Environment
Kyiv National University of Construction and Architecture, Kyiv, Ukraine

Abstract

The article deals with the formation of a healthy human living environment in superstructure buildings with the requirements of indoor air quality, environmental and constructive safety. The results of the development of "Biotecton" - an ultra-high-rise multi-functional building (the height is 1000 m) are presented. In order to effectively overcome the wind and seismic loads, the principles of the structure of the natural form (Gramineae stems, Triticale) are used. It is a multi-tiered spatial structure, in the nodes of which there are dampers for limiting oscillatory movements. For solving the problems of increasing the energy efficiency of ventilation and air conditioning, the use of air from height 1000 m with the minimum of anthropogenic pollution is investigated. Two mechanisms of the movement of air in a superstructure were investigated: natural impulses (under the action of gravitational pressure and wind) and mechanical (fans). It is shown that the natural pressure is insufficient for air movement. The mechanical impulse is necessary, but its energy requirement can be compensated by a renewable energy source - wind turbines with a total capacity of 5.3 MW. For high air quality, the use of "oxygen gardens" in green areas, which are evenly spaced along the entire height of the building, is explored. The study proposed a list of plants that effectively clean air from pollution, sequestrate excess CO_2, enrich the air with oxygen and release phytoncides that effectively fight against pathogenic microorganisms.

Keywords: superstructure building, skyscraper, indoor air quality, ventilation, oxygen gardens

1. Introduction

In connection with the consolidation of the development of cities-metropolises throughout the world, the active implementation of the "fabric" of the city is not only high-rise buildings but also tall buildings (above 75 m). Every year, the number of high-rise buildings in the world is growing, which is due to the demand for such types of objects and the development of the latest architectural, engineering, engineering and design solutions.

Skyscrapers bring people very high above the surface of the earth, which separates them from the natural environment. There is a need for an artificial microclimate of skyscraper premises with the requirements of temperature, humidity, gas composition of air, environmental safety of premises, intellectualizing of the building, etc. The energy component of the maintenance of a skyscraper is growing, which complicates the balance of the relations of natural and artificially created environment.

The task of creating vertical spatial structures based on natural forms capable of interacting with the environment to ensure their viability was the basis for the development of the skyscraper "Biotecton", capable of overcoming the height of 1000 m, conducted by scientists and students of the Kyiv National University of Construction and Architecture since 2015. As a basis, the stem of cereals has been taken as a shape-forming architectural and constructive element. The constructive shape of the *Gramineae* stems has the same effects of natural influences and mechanical forces as acting on the

skyscraper. Stems of cereals with an average diameter of the base of 3 mm can reach a height of 1500 mm. When the coefficient of harmony is 1:500, the rye stem carries a spike, which is 1.5 times heavier than the weight of the stem itself.

2. Previous studies

Previous anatomical studies conducted by scientist Alexey Lazarev (*Lazarev A, 1985*) confirmed that the internal structure and relationships between the structural elements of stems can effectively bear the loads on the vertical spatial structure (Fig. 1).

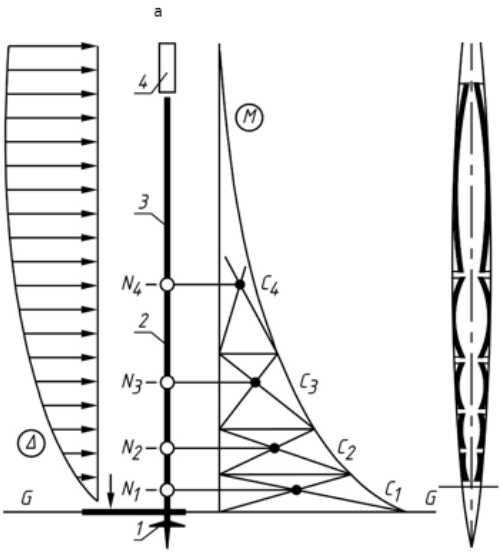

Figure 1 Features of the structure of the stem of wheat:
a – scheme of static work of the wheat stem by the architect A. Lazarev and the engineer G. Sarkisian;
b – structure of the stem of wheat:
1 – root; 2 – internode; 3 – stem; 4 – spike; N_1 ... N_4 – stem nodes; $G – G$ – the ground level $C_1 ... C_4$ – centres of equal planes on the diagram M of bending moments; Δ – the displacement diagram

As a result of anatomical studies of *Gramineae* stems, *Triticale*, the following features of the shape of its structure were determined:

• a stem of cereals is a multi-tier structure, which is divided into a number of internodes, which reduce the force of wind pressure and the load;

• internodes of stems have a spindle-like shape, which reduces the deflection;

• at the nodes of the stem there are dampers – elastic hinges that form a dynamic damping system to limit the oscillatory movements of the stem;

• additional stability is provided by a mutual arrangement in the stem of firm and soft tissues, their ability to work both on compression, and on stretching;

• the cereal root system is a strong complex system, which consists of the main vertical root, lateral roots, more roots developing in different directions.

3. The basis of the "Biotecton" structure

The three-dimensional shape of the ultra-high-rise building "Biotecton" of height 1000 m is based on the tectonic structure of rye, which is musty-tier and multi-functional structure. The effectiveness and efficiency of the bearing system of "Biotecton" are achieved by separating the structure of the building by three dampers, spindle-like shape with minimal reliance area, the system of braces, stiffening core and root-like foundations to ensure effective mounting of the structure.

The damper is a dynamic shock absorber system, which allows fading of the amplitude of oscillation and increasing of seismic resistance. The model of the damping system (Fig. 2) of "Biotecton" is based on the results of anatomical studies and experimental tests on the vibrating bench in the laboratory of aerodynamics. The damping effect (quenching) fluctuations in the model "Biotecton" has been confirmed using devices Bruhl and Kyer (Denmark).

Multi-tiered, multifunctional structure "Biotecton" has free spaces, allowing their free use while ensuring efficiency and economy.

4. The grounding of air exchange principles

4.1. Main principles

An important principle of designing "Biotecton" was the creation of a comfortable environment for people. One of the main factors of comfort is the provision of air exchange for the organization of a healthy microclimate in premises with suitable heat-humidity conditions.

A significant part of the glazing of the facades and the impossibility of traditional ventilation of the premises through open windows leads to a significant increase in power demand for air conditioning. These and other factors cause special design of air exchange in "Biotecton" and require researches of energy-efficient solutions. At the level of 1 km, there is fresh, cool and clean air independently of artificial pollutions at the Earth's surface. Therefore, it is a good idea to take the air from the upper levels of "Biotecton". The air will move down (Fig. 3) by a duct in the inner stiffening core and after that will be distributed by premises. At the altitude of 1 km, the air temperature during the warm period of the year is lower (ICAO, 1993) than on the surface of the Earth by 6.49 °C/km (averaged value), which reduces the energy consumption for air cooling.

In this great building, there is a necessity for high air exchange amount. For energy efficiency, we need to search for ways of reducing the air demand, decreasing the energy for air movement and treatment.

4.2. The grounding of the air movement motive

Two options for air movement motive are used in ventilation and air conditioning: natural (under the action of gravitational pressure and wind) and mechanical (fans). If the temperature of the external air near to the ground level is 32 °C (305.15 K), the temperature of the intake air at the level of 1 km will be t_{ext} = 32 – 6.49 = 25.51 °C or T_{ext} = 298.66 K. The density of this air coerced to the standard atmospheric pressure is (Mileikovskyi & Klymenko, 2016) ρ_{ext} = 353 / 298,66 = 1,1819 kg/m^3. Comfortable air temperature during a warm period of a year for the design of buildings and microclimate systems (EN 15251:2011 (2011) in residential buildings, office space, conference halls, classrooms, restaurants is t_{wz} = 26 °C. (T_{wz} = 299.15 K) The corresponding air density is ρ_{wz} = 353 / 299.15 = 1.1800 kg/m^3. Gravitational pressure on the ground floor (height between the air intake and the premises is about H = 1000 m) at gravitational acceleration g = 9,80665 m/s^2 is $\Delta P_{gr} = (\rho_{wz} - \rho_{in})\, g\, H$ = = (1,1819 – 1,1800)·9,80665·1000 = 19 Pa, which is not enough for a kilometre network of air ducts. Another negative aspect of the use of gravitational pressure was studied by the authors in the paper (Mileikovskyi & Klymenko, 2016): natural ventilation has low energy efficiency. Energy (heat) of exhaust air (total energy) is [W]

$$E_{tot} = \Delta Q = c_p\, \rho_\ell\, L\, (T_\ell - T_{ext}), \qquad (1)$$

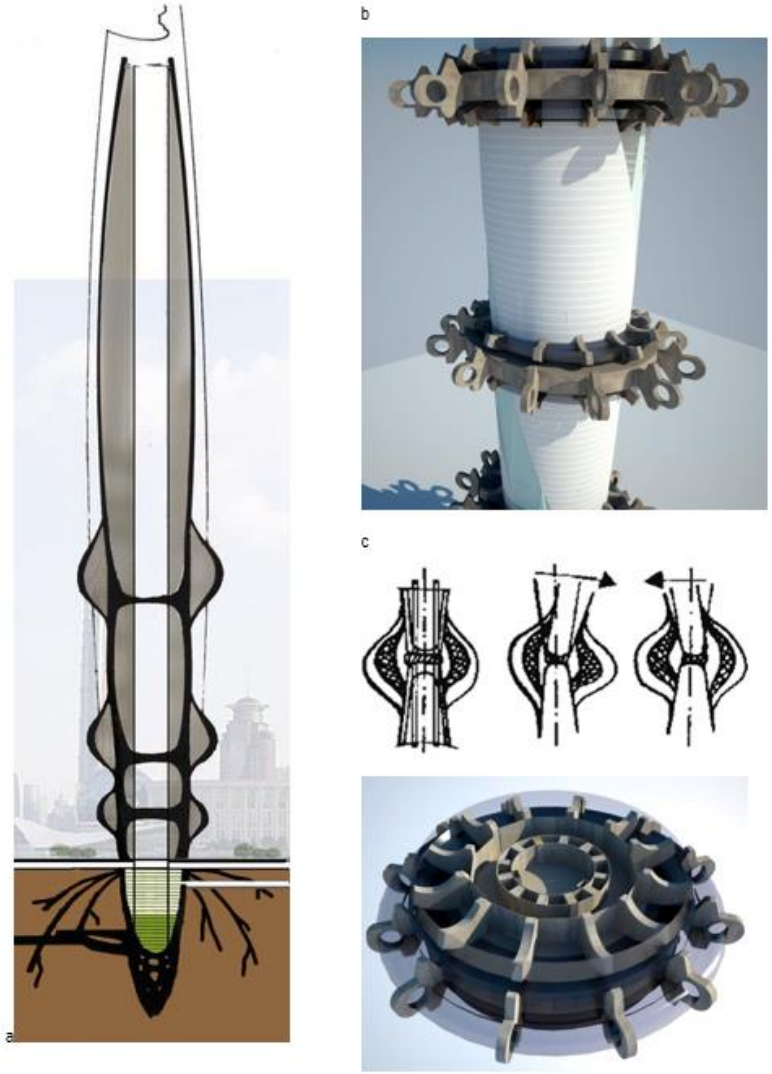

Figure 2

Demonstration system "Biotecton":
a – sketch of placement, b – general view of the damping system, c – wheat stem damper,
d – an element of the damper

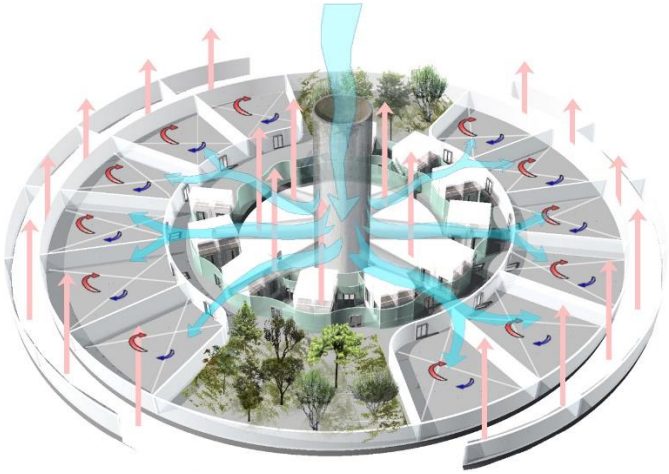

Figure 3 Spatial scheme of the ventilation system in "Bietekoton"

where c_p = 1006 J/(kg·K) – isobar heat capacity of air (Mileikovskyi & Klymenko, 2016); L – volume flow rate of air, m^3/s. For simplicity, sensible heat is used, which leads to a certain underestimation of the heat supply and an overestimation of the efficiency of the system. Useful energy is the energy that is used for the movement of air through the air ducts (with pressure losses equal to the gravitational pressure [Pa]) [W]:

$$E_{usef} = \Delta P L. \qquad (2)$$

The effectiveness $\eta_{v,g}$ of the natural ventilation is determined (Fig. 4) as the ratio of the useful energy E_{usef} [W] to the total E_{tot} [W] taking into account the formulas (1...3):

$$\eta_{v,g} = E_{usef} / E_{tot} = g H / (c_p T_{ext}) = 9{,}75 \cdot 10^{-3} H / T_{ext}. \qquad (3)$$

By Fig. 4 the effectiveness of natural ventilation in the cold period of the year is only 3.5%. Therefore, the mechanical ventilation with the heat (cold) utilization from exhaust air should be preferred. For this purpose, it is proposed to use mechanical combined extract and input ventilation units with heat pumps located in technical spaces. They take air from the duct, located on the axis of the building. For disposing the exhaust air, other airline in the stiffening core can also be used. Air release can be carried out under the facade glazing to transport it to the top of the building. The condition of using this space is to prevent the condensation of moisture on the glass in the cold season for these climatic conditions. Condensation worsens the operating conditions of the enclosing structures and distorts the view from the windows.

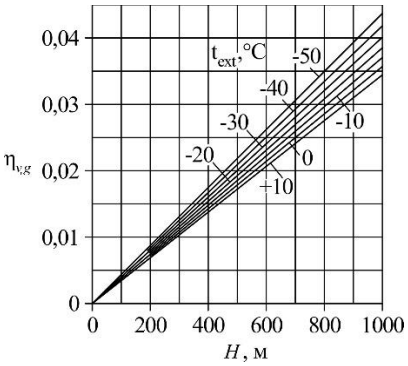

Fig. 4. Schedule of the coefficient of efficiency of natural ventilation

(Mileikovskyi & Klymenko, 2016), extended to 1 km

Typically, the pressure of embedded fans in the standard combined ventilation units is not sufficient to provide the movement of air by kilometre air ducts. Therefore, we should install an additional fan or fans that will create sufficient pressure and air flow in the air ducts. At the top of the buildings, we should use wind turbines to utilize the energy of winds, which are significant at such level. According to preliminary data of mathematical modelling, the wind turbines provide 5.3 MW of energy, which at properly designed airlines and air ducts should be sufficient for air movement.

4.3. Biotechnical method of improving air quality

To improve the quality of the internal air, green zones (Fig. 5) are designed in "Biotecton", which can be used for ventilation on each floor. Interior landscaping of skyscrapers provides an opportunity for improvement of ecological and psychological comfort of a person. Landscaping zones in the vertical spatial structure of "Biotecton" make it possible to give access to the natural environment. In "Biotecton", planting is the basis of the architectural and planning decision. The green interior band may spirally wrap the building. Green areas of common use in "Bietecton" are located one per five floors. The proposed solution gives an opportunity to provide 30 % landscaped volume of the skyscraper and to ensure its even placement in the height of "Biotecton". In fact, thanks to the projected planting system in Bietekoton, a person has access to the natural environment on every floor of the building.

In order to improve the air exchange in the premises of "Biotecton", it is proposed to use "oxygen gardens", which are envisaged by the project in "green zones". Most "oxygen gardens" are above the cloud level. Therefore, they are under the constant influence of solar radiation, which allows obtaining a stable photosynthesis during the year. There are two options for using "oxygen gardens":

1. The inflow air with the flow rate G_{ext} [kg/s] and the concentration of CO_2 q_{ext} [ppm] is fed to oxygen gardens, where it is further enriched with oxygen, and after that, the air will be supplied to other premises. This solution allows getting the best conditions for people to rest in the "oxygen gardens";

2. Some part of the exhaust air with flow rate G_R [kg/s], and CO_2 concentration q_ℓ [ppm] from the premises without the possibility of release of harmful and odoriferous substances is recirculated to oxygen gardens, which, through sequestration of CO_2 will be enriched with oxygen and becomes re-usable. Due to the increased concentration of CO_2 in the exhaust air, plant growth improves.

Figure 5 A three-dimensional planning solution of the biotecton planting system: a – general view of "Biotecton", b – floors with greening; c – section of greening; d – general view of "green zones"; e – turn of greening zones on different floors

For the accepted assortment of plants, it is possible to calculate the total sequestration of CO_2 ΔS [mg/s]. Then the decrease in the concentration of CO_2 [ppm] in the air passing through an "oxygen garden" with the flow rate G [kg/s] is [ppm]

$$\Delta q = 1000\ \Delta S / G. \quad (4)$$

Air and CO_2 balance in the "oxygen garden" [kg/s, mg/s]

$$G_{ext} + G_R = G_{in}. \quad (5)$$

$$G_{ext}\, q_{ext} + G_R\, q_\ell - \Delta S = G_{in}\, q_{in}. \quad (6)$$

Required flow rate by of external and recirculated air in the "oxygen garden" using equations (5) and (6)

$$G_{ext} = G_{in}\,(q_\ell - q_{in}) / (q_\ell - q_{ext}); \quad (7)$$

$$G_R = G_{in}\,(q_{in} - q_{ext}) / (q_\ell - q_{ext}). \quad (8)$$

If recirculation is not used, the reducing of the standard sanitary norm G_{norm} [kg/s] of external air can be achieved up to [kg/s]:

$G_{ext} = G_{norm} (q_{ext} – \Delta q) / q_{ext}$. (9)

Thus, "oxygen gardens" reduce the need for outdoor air, and thus increase the energy efficiency of ventilation and air conditioning. They are a biotechnical method for energy-efficient indoor air quality achievement.

4.4. Plant assortment for air quality control

Although plants have no specialized respiratory organs, they are actively taking part in gas exchange. This phenomenon is based on two of the most important physiological processes: photosynthesis and breathing. For photosynthesis, plants absorb CO_2 from the ambient air. One of the final products of photosynthesis is oxygen, without which the existence of all living things on our planet would be impossible. The process of respiration of plants in many respects is the opposite to photosynthesis.

Unlike many animals, plants do not have adaptations that would provide an active flow of gases. They penetrate into plants solely by osmosis, that is through passive diffusion along the formed gradients of concentration. The gases contained in the tissues of a leaf, in a cortex, in a stalk and in a root, are also passively moved by the special intercellular moves. These "gas pipelines" are combined with ambient air with the help of stomata that are located on the surface of leaf plates. Plant cells can be considered as tiny water containers. Many gases are well soluble in the aqueous phase. Thanks to this, the absorption of gases by plants is very fast. It is known that many harmful substances cause plants to intensify the processes of respiration. Consequently, plants react actively to them. It is logical to assume that in the process of the long evolution in plants, they implemented protective mechanisms that allow neutralizing harmful substances and gases entering the tissue together with carbon dioxide. This assumption is confirmed in (*Yan Van der Neer (2005)*. Specialists of NASA have derived a generalized coefficient of air purification efficiency of plants (Table 1). It was calculated taking into account the degree of danger of absorbed gases, the breadth of their spectrum, and the rate of their absorption. This coefficient is expressed in terms of units and is located on a numerical axis in the range from 0 to 10.

For qualitative air, it is also recommended to use phytoncide plants, through which the air of the premises is restored. For "oxygen gardens" it is recommended to additionally use plants with CAM-metabolism, which contributes to limiting the loss of moisture during nights. As a result, in these plants, stomata are opened at night to absorb CO_2 and store it in the form of organic acid in vacuoles of cells. At day, the stomata are closed. The organic acid decarboxylates again to CO_2. Such plants include, for example, species of the genus *Sedum*, which may be promising for the "green vertical" walls in the rooms.

Thus, "oxygen gardens" reduce the need for outdoor air, and increase the energy efficiency of ventilation and air conditioning.

Conclusions

For the provision of a stable and healthy operation of skyscrapers, it is possible to use natural shapes. "Biotecton" - a building with high of 1 km – is stable and can provide high indoor air environment quality due to use of the shape of rye. The calculations presented have shown that natural ventilation is not able to provide normative air exchange in the premises of "Biotecton" during the warm period of the year due to low natural pressure – less than 20 Pa.

Table 1.

Absorption by plants of poisonous substances

Appointment	Absorbed substance	Cleaning quality	Recommended use for premises
Aglaonema	Benzene, toluene	6,8 P	with artificial carpeting
Azalea	Formaldehyde	6,3	in rooms of any type
Aloe	Formaldehyde, tobacco smoke	6,5	in recently built or renovated
Anturium	Formaldehyde, ammonia, toluene	7,2	of any type
Araucaria	Various impurities	7,0 P	offices and halls
Musa	Formaldehyde	6,8	greenhouses and winter gardens
Begonia	Volatile chemical compounds	6,9	of any type
Guzmania	Formaldehyde, toluene	6,0	of any type
Dendrobium	Methanol, acetone, formaldehyde, ammonia, toluene	6,0	offices
Dieffenbachia	Formaldehyde	7,3	of any type, except children's
Dracaena	Formaldehyde, benzene, trichlorethylene	7,8	of any type
Kalanchoe	Formaldehyde	6,2 P	of any type
Calathea	Formaldehyde	7,1	selectively in offices and rooms
Codiaeum	Volatile chemical compounds	7,0	selectively in offices and rooms
Maranta	Various impurities	6,6	in the winter gardens; in largely backlit aquariums
Neoregelia	Toluene, various impurities	6,4	of any type
Nephrolepis	Formaldehyde	7,5	in the dark with high air humidity
Peperomia	Formaldehyde	6,2	of any type
Hedera	Formaldehyde, trichlorethylene, benzene	7,8	of any type
Sansevieria	Formaldehyde, trichlorethylene, benzene	6,8	of any type
Syngonium	Formaldehyde	7,0	of any type
Spathiphyllum	Formaldehyde, acetone, trichlorethylene, benzene	7,5	of any type
Scindapsus	Formaldehyde, benzene	7,5	of any type
Tradescantia	Formaldehyde	7,8	of any type
Phalaenopsis	Formaldehyde, toluene	6,3	of any type
Ficus	Formaldehyde, trichlorethylene, benzene	8,0 P	of any type
Philodendron	Formaldehyde	7,0	of any type
Phoenix	Toluene	7,8	of any type
Chlorophytum	Formaldehyde, carbon monoxide, tobacco smoke	7,8 P	of any type
Chrysalidocarpus	Formaldehyde, trichlorethylene, benzene	8,5	with high air humidity
Cyclamen	Летючі органічні сполуки	6,0	with high air humidity
Cissus	Volatile Organic Compounds	7,5	in semi-oiled spaces of any type
Schefflera	Formaldehyde, benzene, toluene	8,0	in rooms of any type
Schlumbergera	Volatile chemical compounds	5,6	in well-lit rooms any type
Aechmea	Formaldehyde, volatile organic compounds	6,8	in rooms of any type

Remark. P - phytoncides emissive plant

In the cold season, natural ventilation has a low efficiency of 3.5%. Therefore, the advantage must be given to mechanical ventilation with the utilization of heat (cold) of exhaust air. At the same time, it is recommended to use a renewable energy source – wind turbines with a total capacity of 5.3 MW. It is expedient to remove air from the upper part of the building through clean air and more moderate parameters than in the surface layer. It is a good idea to use "oxygen gardens" with plants that clean air from pollution, to sequester excess CO_2, enrich the air with oxygen, and release phytoncides that effectively fight against pathogenic microorganisms, in order to decrease the necessary airflow.

References

[1] EN 15251:2011(2011) Indoor environmental input parameters for design and assessment of energy performance of buildings addressing indoor air quality, thermal environment, lighting and acoustics.

[2] ICAO (1993) *Doc 7488-CD. Manual of the ICAO Standard Atmosphere (extended to 80 kilometres (262 500 feet)) (Third ed.). Montreal: International Civil Aviation Organization. ISBN 92-9194-004-6.*

[3] Lazarev A. Biotekton – the project of the city of the future. – Kiev, 1985 (In Ukrainian)

[4] *Mileikovskyi V. & Klymenko H. (2016) Analytical Researches of the Energy Efficiency of Natural Ventilation. Ventyliatsiia, Osvitlennia ta Teplohazopostachannia, 20, 39-45 (In Ukrainian)*

[5] *Yan Van der Neer (2005) All about Houseplants that are Clean Air. Sanct-Petersburg: «SZKEO «Kristall»*

Study on Urban Sustainable Restructuring of Leinefelde, Germany and Revealing the Important Strategies for Environmental Well-Being for Shrinking Cities

Sri Charan P

Assistant Professor, Faculty of Architecture,
Manipal Academy of higher education, India

Abstract

Why habitat Mars when you can make earth livable. Demographic change led to the shrinking of the city and also aging native population were big problems in leinefelde. Sustainable urban structures, housing affordability and availability was a big criteria. The political and economic change in the eastern Germany after reunification in 1989, anticipated and intensified the problems. By 1993 municipality realized that it should develop strategies and policies to stop the breakdown of economic and political breakdown of the city. As a result of the actions taken, leinefelde has become successful transformation of shrinking cities in the world. This research paper finds the problems led to shrinking of the city and then focuses on the different parameters and strategies like project context, social aspects, environmental aspects, economic aspects, organizational aspects, sustainable aspects that were carried out in order to have a successful transformation of leinefelde. And finally list down the key indicator for project being successful as a conclusion.

Keywords: Restructuring, project context, social characteristics, environmental features, economic aspects, organizational aspects, sustainable and innovation.

Introduction

Until 1960s leinefelde was a small village in the rural eichsfeld region. The division after World War II led the village separated from its traditional markets and West Germany economy. Subsequently, in 1960 East Germany government began a large industrialization for the region "Eichsfeld Plan". Which led to the village from 2500 habitants to 16500 modern industrial town. In corresponding to the construction of textile industries in leinefelde, a new town was developed – Sudstadt. Sudstadt town was designed to the predominant ideal socialist town: blocks of pre-fabricated flats set in a green landscape, sports fields and infrastructure facilities. In 1969, Leinefelde was given an eminence of an urban municipality, with responsibilities and rights of East Germany's German democratic republic (GDR). After twenty years, the reunification of Germany gave leinefelde status as urban municipality and in 1990 municipal council and mayor were elected in the first free vote after the world war[1].

In 1993, lot of local population was leaving leinefelde to find the fortune somewhere else. The main reason is because of the reunification of Germany led to change from an organized to a market economy, this in general has changed the value system and socialist housing policy. The main reason is the lack of sustainability, soon it became evident and downfall of textile branch after reunification destroyed the economics of the town. This led to the growing unemployment rates in the city and many people left to the most prosperous regions in Germany which led to the vacant flats. And in the competitive housing market, standardized pre-fabricated units with low quality were rejected which were the major housing units. People who are better off moved out from the apartments and owned their new houses. This directed to the depopulation of

leinefelde and sudstadt, native population is decreasing and aging population added more to collapse of the city.

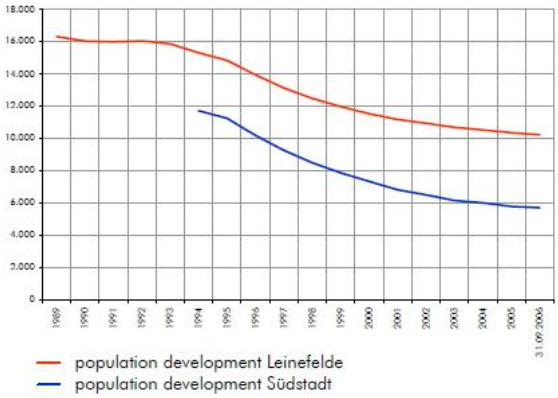

Graph 1: Depopulation in leinefelde and sudstadt

By analyzing the graph it is evident that the demand for rental property in the city was decreased by 50 percent.

But 1993, Mayor and administration took the following first steps towards sustainable urban development of the city:

Subsidy program run cooperatively by the German federal government and the state of Thuringia.

Authorizing an urban development master-plan in order to explore the potentials of the sudstadt district.

Implementing an initial pilot project “the refurbishment of boniftius square”- Public open square.

Municipality with its responsibility for urban and social enhancements had been involved in number of actions, Such as:

Establishing a participative development process.

Encouraging economic development.

Public subsidies for transformation processes.

Commencing quality and quarter management.

Renewing flats.

Renovating all social and technical infrastructures under public responsibilities.

Main Aims and Strategies of the Project:[1][2]

Maintaining balance between employment capacities, number of habitants, urban structures and housing volumes.

Improving surroundings, environment and living conditions.

Promote affordable and attractive housing.

Progress social, economic and community life in the city.

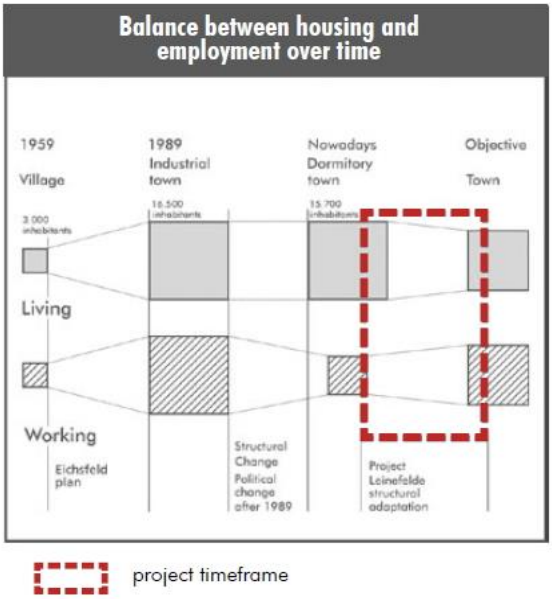

Fig 1: Balance between housing and employment over time.

The above mentioned aims were achieved by following strategies:

Sustainability through contribution.

Sustainability from employment and a diversified economy.

Sustainability through energy conservation and recycling of building materials.

The master plan as an apparatus of direction.

High excellence public amenities and infrastructure to make town attractive.

Demolition of empty apartment building to offer new urban potentials and market steadiness.

Improvement of the housing surroundings.

Making difference between private and public space to have “ownership”.

Different housing typologies as a means of social amalgamation.

2.1 Sustainability through contribution.

Photo 1: Communal participation in the project

Main idea for all the activities to be based on coordination between stakeholders and the target groups in order to promote ownership. Active local participatory is important for establishing sustainable investment in housing renovation.

2.2 Sustainability from employment and a diversified economy.

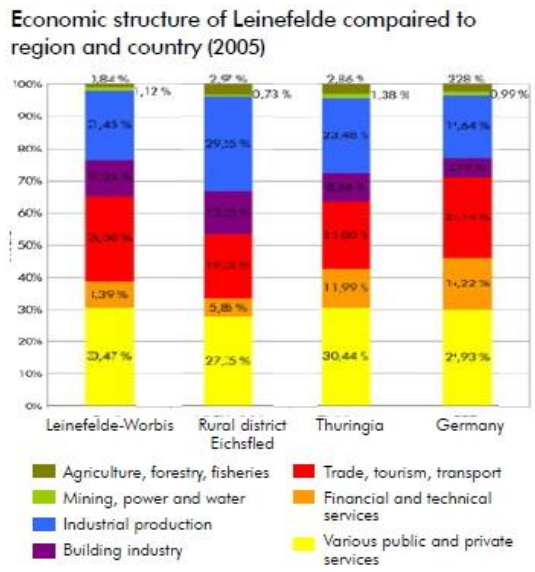

Graph 2: Economic structure of Leinefelde

The reason for unemployment and migration in the city was because due to one-dimensional structure of the economy. To solve this, the municipality promoted the establishment of new enterprises with a different range of activities. Empty textile factory was converted into accommodation facilities, newly designed industrial area and trading estates provided complementary opportunities.

2.3 Sustainability through energy conservation and recycling of building materials.

Photo 2: Recycling and reuse.

The demolition and the dismantling of prefabricated concrete slab construction from housing units helped to procure the transformation process with raw materials which are reused both in construction and landscaping. As a result, it reduced transportation and dumping cost. Interesting landscaped almost free of cost.

2.4 The master plan as an apparatus of direction.

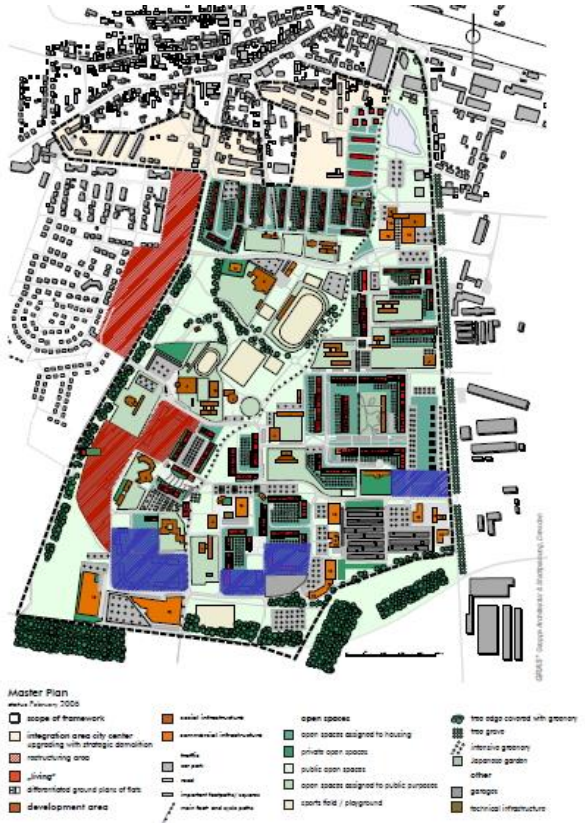

Photo 3: Master plan of leinefelde

First stage of the project included master plan drawn and agreed in 1995. It basically established guidelines for renewal and in particular to the core area. Master plan is a result of discussion between stakeholders.

2.5 High excellence public amenities and infrastructure to make town attractive.

Photo 4: New swimming pool

To stop the outward migration, municipality with partners offered high quality facilities and infrastructure like new swimming pool, kindergartens and public transport system. Public investment is for communal good and also provide sustainable private investment in the city.

2.6 Demolition of empty apartment building to offer new urban potentials and market steadiness.[3]

Photo 5: Dismantling of prefabricated houses.

It was decided that 50% of the existing housing will be demolished and the remaining renovated in order to improve urban quality and to have healthy housing market. Reducing density, improving and opening urban spaces will revitalize the core area.

2.7 Improvement of the housing surroundings.

The project ensured different types of open spaces for private, semi private and public use. Variety of flora and fauna in open spaces improve the ecology of the surroundings. Parking, courtyards and accessibility were designed for easement.

Photo 6: Urban landscape near housing.

2.8 Making difference between private and public space to have "ownership".

Photo 7: Private, semi private and public space.

A very clear divisions were made between private, semi private and public spaces. Giving spatial transition when accessing different spaces. Special importance to the public squares as it is more intensifies public life and civic individuality.

2.9 Different housing typologies as a means of social amalgamation.

City had different social categories with a features in socialist housing schemes. To preserve the mixture in a market economy, a variety of housing typologies were designed and constructed. Renovation projects aimed at individualize flats, building and housing area.

Photo 8: Successful reconstruction of apartments.

Photo 9: Successful renovation of apartments.

3.0 Financial Aspect:

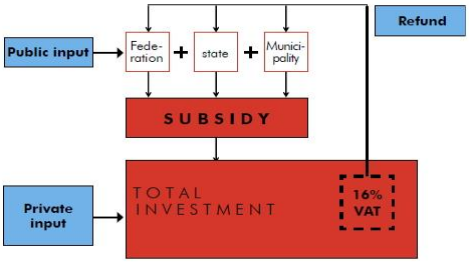

Flow Chart 1: All the aspects of finances for the project. [1]

The project financed according to the renovation and renewal of the following facilities:

Housing renovation generally offer finance with interest rates to cover nonprofit yielding expenditure.

Urban renewal is mainly to target public facilities. The municipality bears almost 25 to 30% of the cost.

In 2002, a new program was offered that aims to associate market by financing the demolition of vacant flats. 100% subsidy in case of simple demolition.

Since 1993, a total of 140 million euros has been invested in refurbishment, new construction and private green space.

Average investment for renovation varies from 470 euro/meter square to 820 euros, which is still less than the half of the construction of new building.

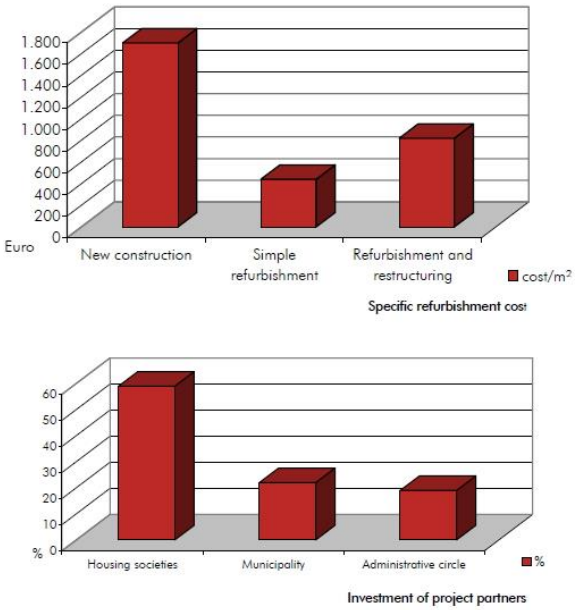

Graph 3: Cost per square meter and investment of project partners.

4.0 Social Aspects [1][6]:

The integrated approach helped develop employment opportunities and town with great levels of urban quality. This allowed inhabitants to develop social and physical environment. The following have proven for encouraging social sustainability and community empowerment:

Discussions between municipality, landlords and tenants.

Survey on residents for their current state and their hopes and expectations.

A regular newspaper for the updates.

Workshops for particular project for tenants and stake holders.

Social service center offers assistance to problem groups.

Different standards of renovation: no exclusion for low or high income group.

5.0 Environmental aspects [1]:

To improve environmental quality is important factor for sustainability and helped in the transformation process in leinefelde and the principles followed are as follows:

Diversity and intensity by planting different local species of trees and vegetation.

Established biological links and micro climatic exchanges in landscape areas.

Improvement of the energy efficiency of buildings by modern heating, technologies and renewable fuel.

The reuse of concrete slabs and pieces for landscape architecture and allow of entire concrete slabs for the construction of detached houses.

Reconstitution of ground water is important for sustainable bio diversity.

Improving pedestrian areas and cycle paths.

6.0 Organizational aspects:

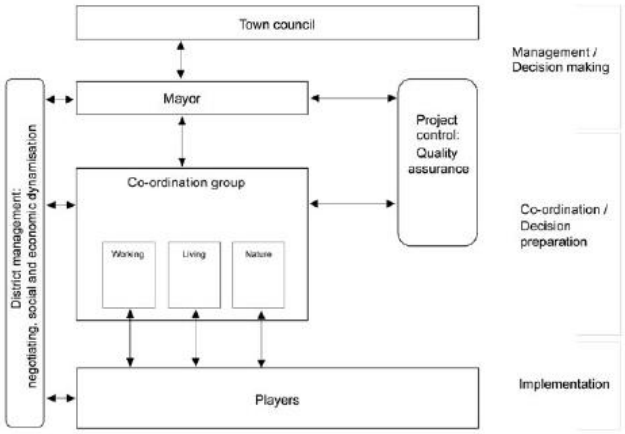

Flow Chart 2: Organizational chart for entire project

Organizational setup of the project places all the different stakeholders under common leader. The key factor is the balance between individuals, common interests and project decisions.

Regular meetings, guarantee coordination and quality management is necessary for the whole transformation process. District management provides link between habitats and the project. It collects and distributes information both direction. It works actively to improve social situations of long term unemployment, lack of qualification and family troubles. From the start, municipality engaged an external consultant for strategic planning, coordination and quality management. The consultant closely works with mayor and head of the urban development.

7.0 Monitoring and evaluating [5].

The project was regularly monitored using global indicators: demographic data, urban development, housing supply & demand and the financial & economic situation. These data could be used for the adjustments of the master plan. Two surveys (1994 and 2001) analyzed inhabitant's responses to the project. It confirmed the fundamental change in social attitude, perception of quality.

Conclusions

Key indicators of the projects success are conclusion and are as follows [7]:

Demographic and social development: demographic erosion has been slowed and 150 inhabitants are lost per year.

Urban development: 1764 apartments have been demolished, 4 years ahead of the project initial schedule, thus anticipating the future reduction in subsides.

Economic development: There are currently 1200 businesses in the city and the regional unemployment rate in 2005 was 15% significantly lower than the state of Thuringia average of 18%.1300 people commute to city for employment opportunities.

Financial situation of municipality: Leinefeldes's municipality debt is 650 euros per inhabitant despite its below average per capita tax income, which is lower than the average in state of Thuringia i.e. 960 euros per inhabitant.

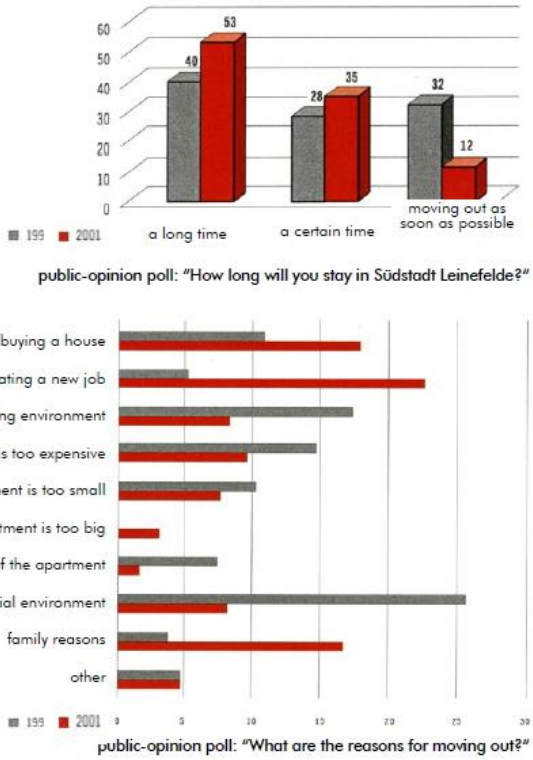

Graph 4: Comparison of parameters of 1991 and 2001

References

[1] World habitat award 2007 report, vol 1, pp 8-26, January 2007.

[2] Bundesministerium für Verkehr, Bau- und Wohnungswesen. Dokumentation zum Bundeswettbewerb "Stadtumbau Ost", pp 11-47, (2003).

[3] Cepl, J. Oswald Mathias Ungers's Urban Archipelago for Shrinking Berlin. In P. Oswalt, ShrinkingCities, Volume 1: International Research (pp. 187-195), (2005).

[4] Gruppe Architektur & Stadtplanung (GRAS).Rahmenplan Südstadt Leinefelde: Aktualisierte Städtebauliche Entwicklungskonzeption. (1999)

[5] Hesse, M, The Compact City: A Model for Eastern German Cities In P. Oswalt, Shrinking Cities,Volume 1: International Research (pp. 180-183), (2005).

[6] Kil, W. "Flaggschiff" des Stadtumbaus. Deutsches Architektenblatt , pp. 26-29, (2007, April)..

[7] Leinefelde. (2005). Rahmenplan Leinefelde-Südstadt. Leinefelde-Worbis: Leinefelde-Worbis.

[8] Reinhardt, G. Stadtumbau Ost - Revitalisierung in Leinefelde. Forum Wohneigentum , pp.135-140, (2003, Heft 3)

Analysis of Dimensional Variations of Precision Gear Forging Die Geometry Due to Shrink Fit

Prof. Dr. Omer Eyercioglu

Gaziantep University, Faculty of Engineering, Mech. Eng. Dept., 27310 Gaziantep, Turkey

Abstract

The usual way to shrink fit design for precision forging dies are made by thick wall cylinder approach; i.e., taking the pitch diameter of the gear as bore diameter of the die insert without considering gear tooth shape. However, the compressive pre-stress due to the shrink fitting causes dimensional variations on the gear profile of the die insert. The dimensional accuracy of the final product is dependent on the accuracy of the gear die. Therefore, the dimensional variations due to shrink fit must be pre-determined and the gear tooth profile on the die insert modified accordingly. In this study, the dimensional variations of the precision spur gear forging die because of shrink fitting are analyzed by finite element method and the results are compared with the experimental ones. The results show that the FE model is successful to simulate the cylindrical die and agree well with thick wall cylinder approach and the experimental measurements. However, both the experimental measurements and the finite element results of gear die predict much higher radial displacements than the results of cylindrical die. Therefore, the determination of shape change of the gear die profile is beyond the capability of the thick wall cylindrical approach.

Keywords: Precision Gear Forging, Die Design, Shrink Fit, Finite Element

Introduction

The technology of precision forging has attained great commercial success in recent years. The major application is the forging of gears for high volume commercial sectors such as automobile and truck transmissions (Behrens BA, 2007). The process has been successively applied for straight and spiral bevel gears at first then spur and helical gears have been forged with functional surfaces which can be finished in one operation (Eyercioglu O, 1996, Dean TA, 2000). The current studies are focused on increasing the quality of the precision forged gears for high quality gear transmission applications such as turboprop gearboxes (Eyercioglu, O, 2018). One of the important problems in precision gear forging is the dimensional change of the die components during forging. They subjected to high loads in a very short period of time and should withstand to high static and impact pressures, friction forces between surfaces, and both mechanical and thermal fatigue (Yilmaz. NF and Eyercioglu O, 2018).

As an engineering practice, the die insert is shrunk fit into one or more shrink rings in order to increase the resistance of the die insert against forging pressure. A compressive hoop (tangential) pre-stress on the die insert is created by interference between mating diameters of adjacent rings. The compressive hoop stress imposed by shrink ring has a cumulative effect at the bore of the die insert. Consequently resultant tensile hoop stress on the bore, caused by the forging loads can be substantially reduced. The usual way to calculate the interference allowance between the die insert and the shrink ring is to use thick wall cylinder approach (Parsons and Cole, 1968). The approach is given in detail by Lame (1852). This approach is also used for design of precision spur gear forging dies (Eyercioglu O and Dean TA, 1997) by considering the die assembly as a short cylinder if the facewidth of the gear is not too long. In this case, the die is considered as a cylinder with an inside (bore) diameter equal to the pitch circle of the gear and the actual gear tooth shape is neglected.

However, the compressive pre-stress due to the shrink fitting causes dimensional variations on the gear profile of the die insert. The dimensional accuracy of the final product is dependent on the accuracy of the gear die. Therefore, the dimensional variations due to shrink fit must be pre-determined and the gear tooth profile on the die insert modified accordingly. For this purpose many researcher have been worked on the dimensional accuracy of the gear forging dies (Eyercioglu O 1994, Sadeghi MH 2003, Yilmaz NF, 2009, Eyercioglu, O. 2009). Pederson (2006) suggest two methods (classical plane analysis and a super element technique) to obtain a direct solution without iteration to determine the shape

of a shrink fit surface result in a prescribed distribution of contact pressure due to the shrink fit. A theoretical model is presented for predicting involute profile deflection in hot precision forging of gears was presented by Zuo (2017).

In this study, the dimensional variations of the precision spur gear forging die because of shrink fitting are analyzed by finite element (FE) method and the results are compared with the experimental ones. The FE model is verified with thick wall cylinder approach and the experimental results for cylindrical die.

Shrink Fit Design

The thick wall cylinder equations formulated by Lame (1852) are generally used in most shrink fit applications. The interference pressure (p) between die and the ring due to shrink fitting in terms of radial interference, (z), is given as:

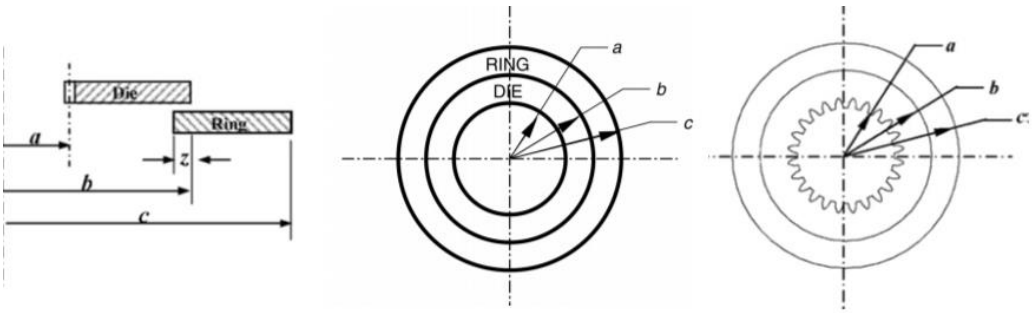

Figure 1. Shrink fit models for cylindrical and gear dies

$$p = \frac{Ez(b^2 - a^2)(c^2 - b^2)}{2b^3(c^2 - a^2)} \quad (1)$$

where (E) Young's Modulus, (a) and (b) are the inner and outer diameter of the die insert, respectively. The die insert that is shrink fitted by the ring, seen in figure 1, is exposed to an external pressure p due to the shrink-fit between die and ring. The tangential (hoop) (σ_t) and radial stresses (σ_r) on the die insert can be calculates as:

$$\sigma_t = -\frac{pb^2}{b^2 - a^2}\left(1 + \frac{a^2}{r^2}\right) \quad (2)$$

$$\sigma_r = -\frac{pb^2}{b^2 - a^2}\left(1 - \frac{a^2}{r^2}\right) \quad (3)$$

and the radial displacement (u_d) is given as:

$$u_d = -\frac{pb^2}{E(b^2 - a^2)}\left[(1 - v)r + (1 + v)\frac{a^2}{r}\right] \quad (4)$$

here the variable r varies between limits a and b, and(v) is Poisson's ratio.

Similar equations can be used for the ring can be for the stresses and the radial deflections (u_r) of the ring are written as: (where r varies now between b and c)

$$\sigma_t = \frac{pb^2}{c^2 - b^2}\left(1 + \frac{c^2}{r^2}\right) \quad (5)$$

$$\sigma_r = \frac{pb^2}{c^2 - b^2}\left(1 - \frac{c^2}{r^2}\right) \quad (6)$$

$$u_r = \frac{pb^2}{E(c^2 - b^2)}\left[(1-v)r + (1+v)\frac{c^2}{r}\right] \quad (7)$$

The optimised values of (*b, c, z*) are determined based on the procedures given in Handbook of Metal Forming (Lange K, 1985). For a known die inner radius *a*, radial interference *z*, die outside radius *b* and ring outside radius *c* are given as:

$$z = \frac{b.S_y}{\mathrm{E}}\left(\frac{1}{K_1} - Q_1^2\right) \quad (8)$$

$b=a/Q_1$ (9)

$c=a/Q$ (10)

where;

$$Q_1 = \sqrt{\frac{1}{2}\left(1 + \frac{1}{K_1}\right) - p'} \quad (11)$$

$$Q_2 = Q_1\sqrt{K_1} \quad (12)$$

$Q = Q_1 Q_2$ (13)

$p' = p_i/S_y$ (14)

$K_1 = S_{y(ring)}/S_{y(die)}$ (15)

here (Sy) is the yield strength.

In the case of gear forging die, the shrink fitting is designed based thick wall cylindrical approach by considering the pitch diameter of the gear is the inner diameter of the die insert. Therefore, the Equations 8-15 are used however, it may be expected that the profile of the gear tooth may cause stress concentrations on the inside surface of the die.

Experimental Procedure

Forging Gear Die

The gear in the study is a 3 mm module (m), 28 teeth (N) and 20° pressure angle standard spur gear (i. e. addendum is equal to module and the dedendum is 1.25 times module). The corresponding pitch diameter is equal to 84 mm (a=42 mm). The height of the inner die and the outer ring is selected as 50 mm. The internal pressure encountered during precision

forging of the gear used in this study was taken as 620 MPa from the previous study of the author (Eyercioglu O, 2018). The corresponding die geometry parameters (*b, c* and *z*) were calculated by using Equations 8-15 and shown in Table 1. For validating the analytical, simulation (FEM) and experimental results a cylindrical die having 42 mm bore radius was also manufactured. The gear die assembly is given in figure 2.

Table 1. The die geometry parameters

m (mm)	*N*	*E* (GPa)	*Sy* (MPa)	*v*	*p (MPa)*	*a* (mm)	*b* (mm)	*c* (mm)	*z* (mm)
3	28	210	1030	0.3	133	42	66.42	105.05	0.2

Figure 2. The gear die assembly

Die Material, Manufacturing and Shrink Fitting

AISI H13 hot work tool steel was used for inner die and the outer ring materials. The die components are hardened and tempered to obtain 52-55 HRC. The cylindrical inner die and the outer rings for cylindrical and gear dies are machined to required diameters using a CNC lathe and grinding machine in the accuracy of ±0.01 mm. The gear tooth profile was cut by using wire electro discharge machine (WEDM). The inner die and the outer ring were shrunk by cooling the inner die in liquid nitrogen and heating the outer ring to a temperature of about 200^{o} C.

Profile Measurements

The dimensions of the die components and the gear profile before and after shrink fitting were measured by Kemco 3D Coordinate Measuring Machine (CMM) using a 1 mm ruby touch probe of Renishaw. The measurements repeated at least three times to ensure the results.

Finite Element Modeling

For the gear die, a 3D single tooth a model was created in SolidWorks and exported to Simufact Forming FE package. The generated mesh type and the number of elements were tetrahedral and 180000, respectively. Symmetry plane boundary condition applied to the both side of the model. A uniform friction (0.2) and interference z=0.2 mm was applied between the die and the ring. The cylindrical die model was created similarly. The 3D FE models of the gear and cylindrical dies are shown figure 3.

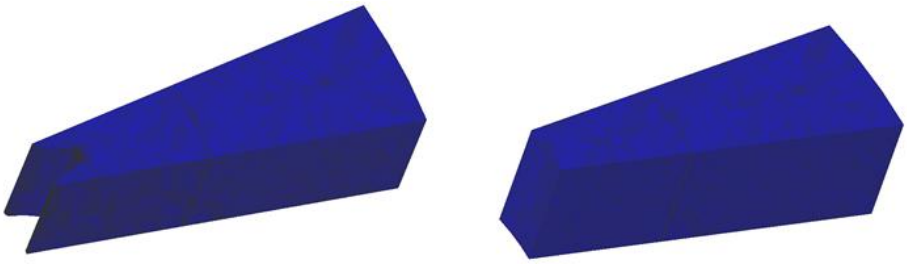

Figure 3. 3D FE models of the gear and cylindrical dies.

Results and Discussion

The Cylindrical Die

The radial displacement (contraction) of the inner die bore radius is calculated as -0.0886 mm by using equation 4. The finite element results (see figure 4) and the 3D CMM measurements given in Table 2 are in well agreement with the analytical one. The 3D CMM measurements of the inner die radius is scattering between 41.909 mm to 41.914 mm, the corresponding radial displacement is in between -0.091 to -0.086 mm. The FE results show a uniform distribution over inner surface with a radial displacement value of -0.0879 mm. The slight differences among analytical, CMM and FEM are coming from the nature of the measurement and truncated values during re-meshing. These results show that the FE model is successful to simulate the thick wall cylinder approach and it is validated with the experimental ones (CMM).

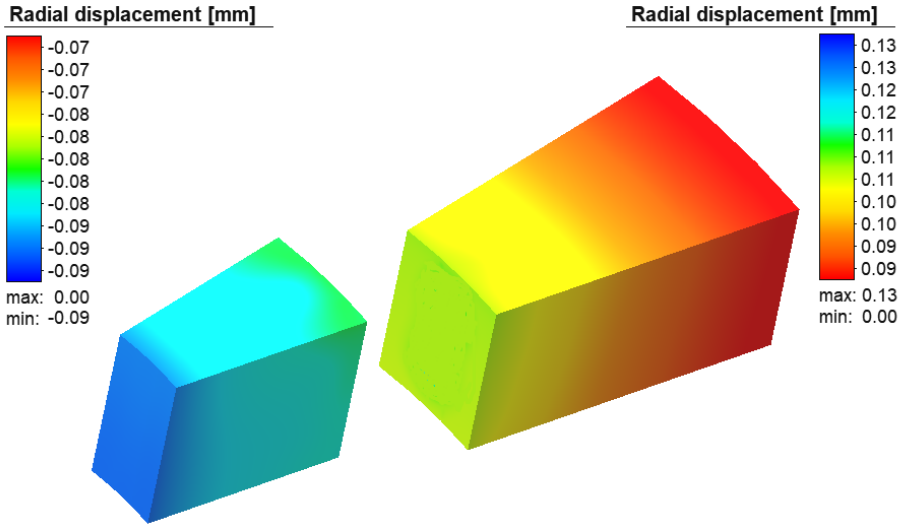

Figure 4. FE results of cylindrical die.

The Gear Die

The radial distance (r) and the corresponding radial displacement (u_r) of the gear profile are given in Table 2. The radial displacement calculated from 3D CMM measurements is scattering between -0.105 mm to -0.114 mm. The FE result shows a uniform distribution over inner surface with a radial displacement value of -0.110 mm as shown in figure 5 and Table 2. The CMM and FE results are in well agreement. However, both the experimental (CMM) and the finite element results of gear die predict much higher radial displacements than the results of cylindrical die (-0.0886 mm). Therefore, the shape change of the gear die profile is beyond the capability of the thick wall cylindrical approach. The gear profiles measured by CMM before and after shrink fit are shown in figure 6. In the design of gear forging die, the gear tooth profile have to be

modified before cutting according to obtain the standard gear after shrink fitting. This can be done by adding radial displacement due to shrink fit on the radial distance of tooth profile ($r + u_r$).

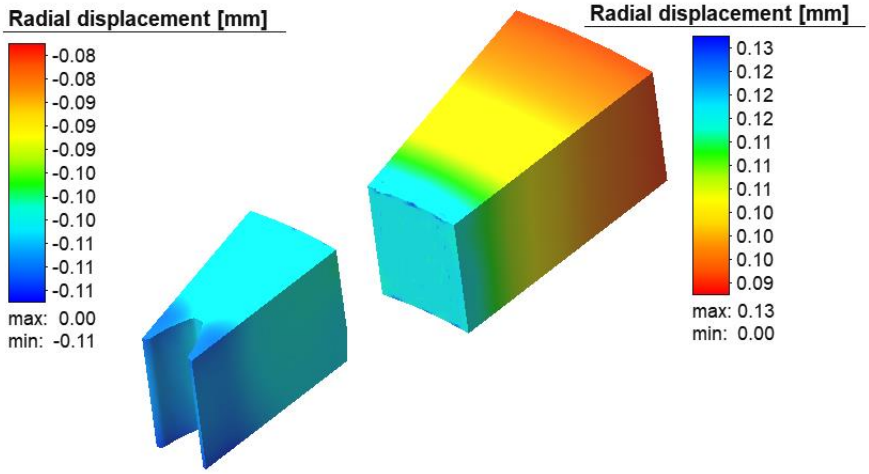

Figure 5. FE results of gear die

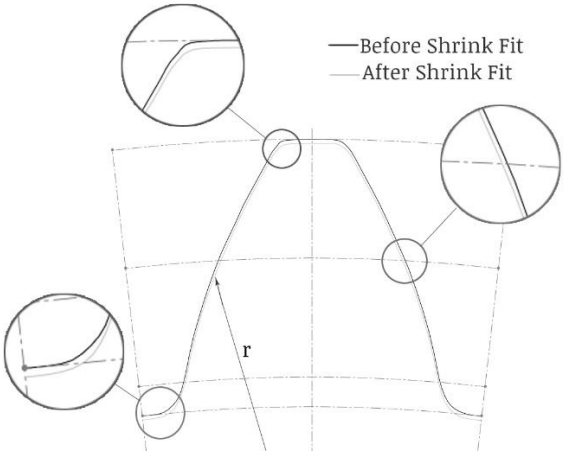

Figure 6. Gear tooth profile before and after shrink fitting.

Table 2. Radial displacement of the inner surfaces

Clylindrical Die			Gear Die		
a CMM (mm)	u_r CMM (mm)	u_r FEM (mm)	r (mm)	u_r CMM (mm)	u_r FEM (mm)
41,912	-0,088	-0,088	38,152	-0,105	-0,110
41,912	-0,088	-0,088	38,158	-0,107	-0,110
41,911	-0,089	-0,088	38,197	-0,108	-0,110
41,914	-0,086	-0,088	38,279	-0,113	-0,110
41,913	-0,087	-0,088	38,487	-0,106	-0,110

41,911	-0,089	-0,088	38,850	-0,107	-0,110
41,911	-0,089	-0,088	39,298	-0,114	-0,110
41,913	-0,087	-0,088	39,780	-0,113	-0,110
41,911	-0,089	-0,088	40,247	-0,108	-0,110
41,914	-0,086	-0,088	40,709	-0,111	-0,110
41,910	-0,09	-0,088	41,160	-0,114	-0,110
41,914	-0,086	-0,088	41,610	-0,113	-0,110
41,911	-0,089	-0,088	42,051	-0,111	-0,110
41,912	-0,088	-0,088	42,474	-0,111	-0,110
41,913	-0,087	-0,088	42,893	-0,106	-0,110
41,910	-0,09	-0,088	43,281	-0,113	-0,110
41,912	-0,088	-0,088	43,639	-0,112	-0,110
41,909	-0,091	-0,088	43,949	-0,108	-0,110
41,913	-0,087	-0,088	44,192	-0,111	-0,110
41,912	-0,088	-0,088	44,409	-0,109	-0,110
41,911	-0,089	-0,088	44,589	-0,105	-0,110
41,912	-0,088	-0,088	44,725	-0,112	-0,110
41,912	-0,088	-0,088	44,834	-0,106	-0,110
41,911	-0,089	-0,088	44,884	-0,109	-0,110
41,912	-0,088	-0,088	44,892	-0,107	-0,110
41,913	-0,087	-0,088	44,893	-0,105	-0,110
41,910	-0,09	-0,088	44,893	-0,104	-0,110

Conclusions

In general practice, shrink fit design for precision forging dies are made by thick wall cylinder approach; i.e., taking the pitch diameter of the gear as bore diameter of the die insert without considering gear tooth shape. However, the compressive pre-stress due to the shrink fitting causes dimensional variations on the gear profile of the die insert. The amount of radial displacement of the gear tooth profile must be predetermined and the profile has to be modified accordingly to manufacture the forged gear in required accuracy. The followings can be concluded from the analytical calculations, experimental work and FE analyses performed in this study:

For cylindrical die insert, the experimental results (CMM measurements) show that the thick wall cylinder approach formulated by Lame well predicts the radial displacement of the inner die radius.

The FE model is successful to simulate the cylindrical die and agree well with thick wall cylinder approach and the experimental ones (CMM).

Both the experimental (CMM) and the finite element results of gear die predict much higher radial displacements than the results of cylindrical die. Therefore, the determination of shape change of the gear die profile is beyond the capability of the thick wall cylindrical approach.

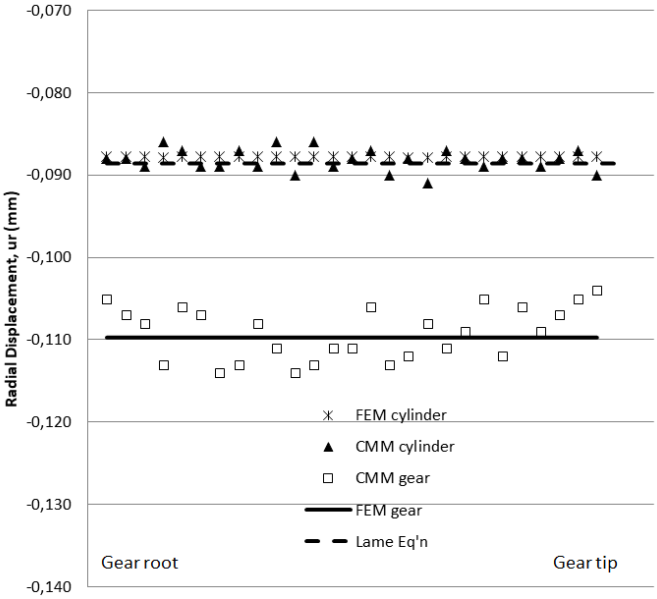

Acknowledgements

The author would like to thank The Scientific and Technological Research Council of Turkey (Tubitak Grand No: MAG-217M063) and BAPYB of Gaziantep University for their financial supports.

References

[1] Behrens BA, Doege E, Reinsch S, Telkamp K, Daehndel H, Specker A, (2007) Precision forging processes for high-duty automotive components. J Mater Proc Tech 185:139–146.

[2] Dean TA (2000) The Net-Shape Forming of Gears. Mater Des 21:271–278.

[3] Eyercioglu, O., Dean, T. A. and Walton, D. (1994) Dimensional accuracy of hot precision forged spur gears. In 1994 International Gearing Conference, Newcastle Upon Tyne, pp. 285–290.

[4] Eyercioglu O, Dean TA, Walton D, (1996) "Precision Forging of Gears," presented at the 7th Int. Machine Design and Production Conference, Ankara, Turkey.

[5] Eyercioglu, O. and Dean, T. A. (1997) Design and manufacture of precision gear forging dies. In CIRP International Conference on Design and Production of Dies and Molds, Istanbul, Turkey, pp. 311–316.

[6] Eyercioglu,O., Kutuk, M. A. and Yilmaz, N. F.(2009) Shrink fit design for precision gear forging dies, Journal of Materials Processing Technology, vol. 209, no. 4, pp. 2186–2194.

[7] Eyercioglu O. (2018) Precision Forging of Asymmetric Spur Gears, Tubitak-MAG 217M063.

[8] Lame, G., (1852). Lecons sur la Theorie Mathematique del Elasticite des Corps Solides, Bachelier, Paris, Septieme Lecon.

[9] Lange, K., (1985) Handbook of Metal Forming. McGraw-Hill, New York, pp. 15–88.

[10] Parsons, B., Cole, B.N., (1968). A generalized approach to the optimum design of short composite cylinders, Proc. Inst. Mech. Eng. 182.

[11] Pederson, P. (2006) On Shrink Fit Analysis and Design Comput Mech (2006) 37: 121–130 DOI 10.1007/s00466-005-0664-7

[12] Sadeghi MH (2003) Gear forging: mathematical modeling and experimental validation. J Manuf Sci E-T ASME 125:753–762

[13] Yilmaz NF, Eyercioglu O (2009) An integrated computer-aided decision support system for die stresses and dimensional accuracy of precision forging dies. Int J Adv Manuf Technol 40:875–886.

[14] Yilmaz. N. F. and Eyercioglu, O., (2018) Near Net Shape Spur Gear Forging Using Concave Preform, MECHANIKA. 2018 Volume 24(2): 268–277.

[15] Zuo B., Wang, B., Li, Z., Li, N., and Lin, J., An investigation of involute and lead deflection in hot precision forging of gears Int J Adv Manuf Technol (2017) 88:3017–3030 DOI 10.1007/s00170-016-9003-8.

Inverse Brillouin Function and Demonstration of Its Application

Aleksandr Hayrapetyan

Faculty of Physics, Yerevan State University, Armenia

Abstract

The Brillouin function arises in the quantum theory of paramagnetic materials, where it describes the dependence of the magnetization on the externally applied magnetic field and on the temperature of the system. There is no closed form exact analytical expression for the inverse Brillouin function, however, there have been several approximations proposed. In this work, we first compare relative errors and simplicity of several approximations for the inverse Brillouin function. Next, we demonstrate the application of the inverse Brillouin function by determining the Hamiltonian of the system using the simulation data of the magnetization dependence on the temperature. Then we compare the Hamiltonian that was used to set up the simulation with the Hamiltonian determined from the magnetization temperature dependence and an approximation to the inverse Brillouin function. We found that some of the approximations for the inverse Brillouin function can be used to accurately predict the Hamiltonian of the system given the magnetization dependence on temperature.

Keywords: inverse, brillouin, function, demonstration, application

Introduction

To study different paramagnetic phenomena in the classical and quantum theory of paramagnetism, two special functions are used. The first of these is the Langevin function [1]. This function appears when calculating the magnetization if there is a medium in which N atoms is contained in a unit volume. Magnetization takes place in cases where atoms have magnetic moments μ that are oriented to an external magnetic . Several mathematical calculations will be shown in the next section of this paper.

Another special function, which is applied while considering various problems related to the quantum theory of paramagnetism, is the Brillouin function [1]. In the contemporary professional literature not only the direct Brillouin function is used, but also its inverse function. These functions are normally mentioned in the following contexts: polymer science, molecular dynamics modeling, magnetism, rubber theory, etc. But unfortunately, the inverse Brillouin and Langevin functions cannot be calculated analytically, so their approximations are taken, in which the relative error tends to the minimum.

It is noteworthy to mention a few words about paramagnetism, in which we use the above-mentioned special functions. These atoms and molecules have an uncompensated spin magnetic moment. Other examples include free atoms and ions with incomplete inner shells, some molecules with an even number of electrons, lattice defects with an odd number of electrons, metals, other types of atoms and molecules. For the first time, the theory of paramagnetic susceptibility was created by P. Langevin and was used in the above mentioned problem.

In modern literature, one may find the inverse Langevin function, has a wide range of uses. But the quest for the inverse Brillouin function, has not yet been crowned with success. Currently, the existing approximations of the inverse Brillouin function are being improved every day. In the sections below, we consider the Langevin and Brillouin functions, their existing approximations, their negative and positive sides, and their applications.

I would like to mention some works related to the above-mentioned functions, their inverse functions and their areas of application. These topics were discussed in the works of the following authors: A.S. Arrott [2], Martin Kröger [3], M.I. Darby [4], and others whose research we will quote in this paper.

At the end of this paper, a inference will be made about all the above mentioned in very detail, which will allow us to contemplate the indicated functions from new perspectives.

Brillouin and Langevin functions and their applications

Langevin function, it's inverse function and their applications

Let's recall the above mentioned task. Suppose we have an environment that contains N molecules per unit volume. Magnetization arises only when the magnetic moments are oriented under the action of an external field. The energy U, which describes the interaction of magnetic moments (μ) with external field (B), is described by the following scalar product (1):

$$U = -\boldsymbol{\mu} * \boldsymbol{B} \quad (1)$$

This scalar product can be represented as follows (2):

$$U = -\mu B \cos\theta \quad (2)$$

where θ is the angle between the moment vector and the direction of the field.

Within this problem, the field magnetization is calculated by the following equation (3)

$$M = N\mu\langle\cos\theta\rangle \quad (3)$$

where N, as mentioned above, is the concentration, 〈cosθ〉 is the average value of cos θ taken from the spatial distribution of magnetic moments in the state of thermal equilibrium.

If in this problem we use the Boltzmann distribution, then we can count the probability that the moment of the molecule is located in an element of a given solid angle $d\Omega$. This probability is proportional to $exp\ (-U/k_BT)$, and therefore the average value of cosθ (〈cosθ〉) can be calculated by the following equation (4)

$$\langle\cos\theta\rangle = (\int e^{-\beta U}\cos\theta\, d\Omega) * (\int e^{-\beta U} d\Omega)^{-1} \quad (4)$$

here, $\beta \equiv 1/k_BT$ designation is inserted, and $d\Omega = \sin\theta d\varphi d\theta$. In the above equation, integration is performed over all values of φ and over all values of θ. For all values of φ, we get 2π, a θ varies from 0 to π (5):

$$\langle\cos\theta\rangle = \frac{\int_0^\pi 2\pi \sin\theta\cos\theta e^{\beta\mu B\cos\theta} d\theta}{\int_0^\pi 2\pi\sin\theta e^{\beta\mu B\cos\theta} d\theta} \quad (5)$$

For simplicity, let's introduce the following reductions (6)

$$s \equiv \cos\theta\ ,\ x \equiv \frac{\mu B}{k_BT} \quad (6)$$

and after integration we get the following equation (7)

$$\langle\cos\theta\rangle = \left(\int_{-1}^{1} exp(sx)\, sds\right) * \left(\int_{-1}^{1} exp(sx)\, ds\right)^{-1} =$$

$$= \frac{d}{dx} ln \int_{-1}^{1} exp(sx)\, ds = \frac{d}{dx} ln(exp(x) - exp(-x)) - \frac{d}{dx} ln(x) = cthx - \frac{1}{x} \equiv L(x) \quad (7)$$

The resulting function is called the Langevin function. It has the following form (8)

$$L(x) = cth(x) + \frac{1}{x} \quad (8)$$

The final calculation of the magnetization field is made by the following formula (9)

$$M = N\mu L(x) = N\mu(cth(x) + \frac{1}{x}) \quad (9)$$

This function can be regarded in two cases. When $\mu B \gg k_BT$ and when $\mu B \ll k_BT$. In the first case, saturation can be found in the graph of the function, and the second case is of great interest for experimenters when calculating various kinds.

Let's look at some approximations of the Langevin function.

If in the Langevin function we expand in the series $cth\ (x)$ then for small values of x we get the following expression (10)

$$cth(x) \approx \frac{1}{x} + \frac{x}{3} - \frac{x^3}{45} + \cdots \quad (10)$$

Putting this expression into the Langevin function, we obtain the following approximation (11)

$$L(x) \approx \frac{x}{3} \quad (11)$$

For magnetization, we obtain the following expression (12)

$$M \approx \frac{N\mu^2 B}{3k_B T} = \frac{C}{T}B \quad (12)$$

Where C stands for Curie (13)

$$C = \frac{N\mu^2}{3k_B} \quad (13)$$

Let's discuss another approximation of the Langevin function. If we decompose the Langevin function in a Taylor series for small values of x, we get the following result (15)

$$L(x) = \frac{1}{3}x - \frac{1}{45}x^3 + \frac{2}{945}x^5 - \frac{1}{4725}x^7 + \cdots \quad (14)$$

This approximation method is an alternative approximation of the $cth(x)$ approximation. From the point of view of numerical calculation, both approximations are equivalent to each other and are more demanded than direct evaluation of an analytical expression.

It can be said that the Langevin function has been fully investigated and is widely used in describing various tasks.

Below we will discuss the Brillouin function.

Brillouin function , it's inverse function and their applications

Brillouin function, inverse function and its applications

We shall first and foremost recall the formula (15)

$$B_J(x) = \frac{2J+1}{2J} coth\left(\frac{2J+1}{2J}x\right) - \frac{1}{2J} coth\left(\frac{1}{2J}x\right) \quad (15)$$

In which J is a positive integer or half-integer number,

x stands for the relation of Zeeman energy ratio of the magnetic moment in an internal field to the heat energy. (16)

$$x = \frac{g\mu_B JB}{k_B T} \quad (16)$$

in which g is factor g, μ_B is Bohr magneton, J is the full angular momentum, B is the applied magnetic field, k_B is Boltzmann constant, and T is the temperature.

Brillouin function changes by taking values from -1 to 1, reaching +1 if $x \to \infty$ and -1 if $x \to \infty$. Brillouin function has a wide range of utilization, but most often it is used for calculating the magnetization of an ideal paramagnet. It describes the dependency of M from the applied magnetic field B and the total angular momentum J. Magnetization is expressed through the formulum (17)

$$M = Ng\mu_B JB_J(x) \quad (17)$$

in which N stands for the quantity of the atoms per unit volume. The Brillouin function turns into that of Langevin in the range of $J \to \infty$ (8). If $x \to \infty$, then $B_J(x) \to 1$. This means that the magnetization gets saturated and the magnetic moments become totally aligned in the direction of the applied field. (18)

$$M = Ng\mu_B J \quad (18)$$

And now we shall talk about how one should find the inverse function of Brillouin. It is impossible to achieve analytically, but one can throw some approximations apropos the $coth\ (x)$ function and find the Brillouin inverse function with some

accuracy. If the error of this accuracy does not exceed the applied limit (~5%), then the given approximation can be safely used in different calculations.

The first approximation can be done in case if $J = 1/2$, and then $B_J(x) \to tanh\ (x)$. If we are to take this approximation into account, then we can safely write the following expression (19)

$$B_J(x) \approx tanh\ (nx) \quad (19)$$

in which n is the coefficient dependent solely on J . The absolute and relative mistakes depend on this coefficient. We shall turn to the works of Jeno Takacs in order to demonstrate the most precise result possible [5]. Here we have a result which is currently seen as the most precise and recent one, and it is presented as follows (20)

$$n \approx \frac{1}{2{,}667J} + 0.2 \quad (20)$$

Given the value of n, the relative miscalculation makes about 4%. If we are to use the given approximation for $B_J(x)$, then we will get the following result for the inverse function [5] (21)

$$B_j(x)^{-1} \approx \frac{axJ^2}{1-bx^2} \quad (21)$$

a and b are the coefficients that have the following form (22)

$$a = \frac{0.5(1+2J)(1-0.055)}{J-0.27} + \frac{0.1}{J^2} \quad b = 0.8 \quad (22)$$

J changes from 1 to 10 . Model (21) is still relevant outside of these values, but with much less accuracy which means that the error value increases.

Let us discuss yet another version of Brillouin inverse function, and then we shall further discuss its use. This other version of Brillouin inverse function reappears when $J = 1/2$ which resembles the original function by its graph and predicts a quite low range of miscalculation. It is as follows: (23) [6]

$$B_J(x)^{-1} \approx ln\ (\frac{1+2s}{1-2s}) \quad (23)$$

s stands for magnetization. s changes from 0 to ½ . This function cannot be used for other values, as there is a logarithm in the function: when the numerator has a negative sign, the function loses its physical meaning.

Now let us discuss its use. The Brillouin inverse function is used in non-iterative mean field theory. Thus, the mean field equation for an arbitrary isotropic spin Hamiltonian of infinite range will be as follows (24)

$$s = \sigma B_J(-\beta\sigma \frac{\partial H}{\partial s});\ \ \beta = \frac{1}{k_B T} \quad (24)$$

The given equation can be rewritten in the wollowing manner (25)

$$kT = -\frac{\frac{\partial H}{\partial s}}{B_J(x)^{-1}} \quad (25)$$

One can calculate the dependence of T from s using this equation.

The magnetic entropy can be presented in the following form using the Brillouin inverse function (26)

$$\Delta S = -k_B \int_0^s B_J(s')^{-1} ds' \quad (26)$$

ΔS is to represent the decrease in entropy relative to the paramagnetic phase.

Conclusion

To sum up, we can claim that the Brillouin inverse function is hard to compute in mathematical calculations. Various approximations are put forward in order to overcome this problem. We have mentioned some of them above. One of these is the approximation $tanh\ (x)$ (19), and another one is the approximation $ln\ (x)$ (23). In the approximation $tanh(x)$,

the obtained function works with a small admissible error in practice. In the approximation, the obtained function in practice works with a small admissible error. The proof of that is the fact that $B_J(x)$ moves toward $tanh\ (x)$ when $J = 1/2$.

The analytical form of Brillouin inverse function has not yet been found. The abovementioned approximate Brillouin inverse functions work within the operating limits of the quantum number of angular momentum. The majority of materials have J from 1 to 10 in engineering practice. This is why many approximations of the Brillouin inverse function have a great demand in current studies.

Acknowledgment

I would like to thank Rafayel Petrosyan for valuable discussions.

References

[1] C. Kittel ,1963, Introduction to Solid State Physics, 4th edition (New York: John Wiley and Sons, Inc.), pp. 518–523.

[2] A. S. Arrott, J. Appl. Phys. 103, 07C715 (2008).

[3] M. Kröger, Simple, admissible, and accurate approximants of the inverse Langevin and Brillouin functions, relevant for strong polymer deformations and flows, J. NonNewtonian Fluid Mec. 223 (2015) pp. 77–87.

[4] Darby, M.I. (1967). "Tables of the Brillouin function and of the related function for the spontaneous magnetization". Br. J. Appl. Phys. **18** (10): 1415–1417

[5] Takacs, Jeno (2016). "Approximations for Brillouin and its reverse function". COMPEL. **35** (6): 2095.

[6] J. Katriel Continued-fraction approximation for the Brillouin function Phys. Stat. Sol., 189 (1987), p. 308

Anomaly-Based Intrusion Detection*:* Feature Selection *and* Normalization Influence *to the* Machine Learning Models Accuracy

Danijela Protić, MSc

Center for Applied Mathematics and Electronics, Belgrade, Serbia

Miomir Stanković, PhD

Matematical Institute, Serbian Accademy of Science and Arts, Belgrade, Serbia

Abstract

Anomaly-based intrusion detection system detects intrusion to the computer network based on a reference model that has to be able to identify its normal behavior and flag what is not normal. In this process network traffic is classified into two groups by adding different labels to normal and malicious behavior. Main disadvantage of anomaly-based intrusion detection system is necessity to learn the difference between normal and not normal. Another disadvantage is the complexity of datasets which simulate realistic network traffic. Feature selection and normalization can be used to reduce data complexity and decrease processing runtime by selecting a better feature space This paper presents the results of testing the influence of feature selection and instances normalization to the classification performances of k-nearest neighbor, weighted k-nearest neighbor, support vector machines and decision tree models on 10 days records of the Kyoto 2006+ dataset. The data was pre-processed to remove all categorical features from the dataset. The resulting subset contained 17 features. Features containing instances which could not be normalized into the range [-1, 1] have also been removed. The resulting subset consisted of nine features. The feature 'Label' categorized network traffic to two classes: normal (1) and malicious (0). The performance metric to evaluate models was accuracy. Proposed method resulted in very high accuracy values with Decision Tree giving highest values for not-normalized and with k-nearest neighbor giving highest values for normalized data.

Keywords: feature selection, normalization, k-NN, weighted k-NN, SVM, decision tree, Kyoto 2006+

Introduction

Over the past decades the network security has changed with threats becoming far more complex moving from basic attacks against one device to network intrusion attacks against organizations networks. A network intrusion attack is defined as any use of a computer network that compromises network security. Intruders try to gain unauthorized access to files or privileges, modify and destroy the data, or render the computer network unreliable (Aissa & Guerroumi, 2016, 1091). The goal of intrusion detection is to build a system which would scan network activities and generate alerts if either a specific attack occurred or an anomaly in the network behavior detected. Intrusion detection system (IDS) monitors the computer network searching for any suspicious activities that indicate intrusions. In anomaly-based detection base line is what is considered a 'normal' traffic and then flag anything that is not normal as 'abnormal'. The mechanism of anomaly-based IDS depends on the observation to classify input data into classes by adding labels. In a binary classification problem, a single instance can only be divided into two classes. Machine Learning (ML) - based IDS use ML classifiers to learn system normal behavior and build models that help in classifying inputs into the two classes: normal (1) or potentially malicious anomaly (0).

A supervised ML algorithm takes a known set of input data and known responses to generate reasonable predictions for unknown data. In this paper we present four ML algorithms: Gaussian Support Vector Machine (SVM) (Burgess, 1998, 291), Decision Tree (Sebastiani, 2002, 13), k-Nearest Neighbors (k-NN) and weighted k-Nearest Neighbors (wk-NN) (Hechenbichler & Schliep, 2004). k-NN predictions assume that objects near each other are similar. Euclidean distance metric is used to find nearest neighbor. SVM classifies data by finding the linear decision boundary that separates all data points of one class from those of another class. A decision tree predicts responses to data by following the decisions in the tree from the root down to a leaf node. A tree consists of branching conditions where the value of predictor is compared

to a trained weight. However, ML algorithms are computationally expensive if they are trained with the set that has a large number of features. The solution to this problem is to reduce feature space and train classifiers only with the reduced subset. In this paper we present algorithms for feature selection based on preprocessing the Kyoto 2006+ dataset. All categorical features are removed, as well as all features related to the duration of the connection and number of bytes transmitted from source to destination and vice versa. Also, all features containing instances which could not be normalized into the range [-1,1] are cut. Two subsets are generated one consisting of 17 features which contain not-normalized instances and another consisting of nine features of normalized instances. After the training and testing the datasets, accuracy is used to determine performances of the models.

1 Anomaly-Based Intrusion Detection Systems

Anomaly-based IDS monitors computer network to detect intrusion based on irregularities in the pattern with the respect to the normal pattern. It creates a model behavior of the system and then looks for activities that differ from the created model. The anomaly detection approach looks for variations and deviations from an established baseline behavior which might indicate malice. If any anomaly in network activities occurs the IDS warns the system administrator of potentially intrusive action. Anomaly detection can be split into two main methods: machine learning method and rule-based method. ML methods are used to train classifiers in order to recognize what is the notion of normality and then rule-based methods identify abnormal network traffic and flag anomaly.

The main advantage of anomaly based IDS is its ability to detect new attacks even when there is no complete information about the type of attack (Modi et al., 2013, 46). The second advantage is that profile of normal activity is customized for particular computer network and therefore making it very difficult for attacker to know what is certainly what activities it can carry out without getting detected (Patcha & Park, 2007, 3449). One of the biggest advantages of anomaly-based IDS is its ability to detect zero-day attacks since it does not depend on an established signature dataset. The most fundamental challenge is to identify what is normal. Another issue is that even if everything seems like normal over time there are some legitimate anomalies that can be identified as abnormal. Moreover, triage is complex. If one wants to identify an attack an anomaly-based IDS may be very hard to figure out what caused the trigger happened. Furthermore, anomaly-based IDS generates a large number of false positive alarms, since user or network behavior is not always known in advance (Kajal & Devi, 2013, 16). It also requires time to establish baseline behavior when it is first placed in a new network environment or host device. One of the main problems of anomaly-based technique is the selection of the appropriate set of system features because the activities are mostly ad hoc and experience based. Finally, the drawback is also their expensive nature (Garcia-Teodoro et al., 2009, 21).

2 Feature Selection and Instances Normalization

For the purpose of this study two datasets were generated, both based on feature selection and transformation of the Kyoto 2006+ dataset. The Kyoto 2006+ dataset contains daily records of real network traffic data recorded from 2006 to 2009. Each instance in the dataset is labeled with 14 statistical features derived from the KDD Cup '99 dataset (KDD CUP '99 dataset, 1999) and 10 additional features which can be used for further analysis and evaluation of the anomaly-based IDS (Protić, 2018, 587-588). The Kyoto 2006+ dataset is given in the Table 1.

Table 1 goes here

The Kyoto 2006+ dataset was captured using honeypots, darknet sensors, e-mail servers, web crawler and other computer network security systems deployed on five networks inside and outside Kyoto University. During the observation period 50.033.015 sessions of normal traffic, 43.043.225 sessions of known attacks and 425.719 sessions of unknown attack were recorded. The dataset consists of both numerical and categorical features.

Complexity of the Kyoto 2006+ dataset is reduced by elimination of irrelevant features and normalization of instances. In this research normalization executed the following transformation on original instance values

$$tansig(n) = \frac{2}{1 + \mathrm{e}^{-2 \cdot n}} - 1$$

where n represents the number of instances.

The following preprocessing scheme is proposed:

Cut all categorical features - resulting subset contains 17 features (1, 3, 4-17, 24);

Remove statistical features related to the duration of the connection and the number of Source↔Destination bytes (1, 3, 4, 14),

Cut all the features used for further analysis and evaluation of the models (15-17, 24);

Remove features containing instances which could not be normalized into the range [-1, 1] - resulting subset contains nine features (5-13);

Feature 18 ('Label') is used to categorize network traffic into two categories: normal (1) and anomalous (0).

Experiments were carried out on both generated subsets. Number of features in the first subset is approximately three quarters the size of features in the Kyoto 2006+ dataset. Number of features in the second subset contains less than 40% of the original dataset size and is almost a half the size of features in the first subset.

3 Results

In the experiments Classification Learner is used to train and test Gaussian SVM, Decision Tree, k-NN and wk-NN models. Models are chosen because of the following characteristics: prediction speed, memory usage, interpretability and flexibility of the model. (See Table 2)

Table 2 goes here

Experiments were carried out on 10 daily records from the Kyoto 2006+ dataset. The minimum number of records per day was 57.287, while the maximum number of records per day was 158,572.

After the training and testing accuracy was used to determine performances of the models. Accuracy represents the overall success rate, i.e. the ratio between numbers of correct predictions to the total number of classifications, which can be calculated as

$$Accuracy = \frac{TP + TN}{TP + TN + FP + FN}$$

where:

TP (True Positive) represents the number of correctly classified anomaly as anomaly;

FN (False Negative) occurs when classifier incorrectly classifies anomaly as normal behavior;

FP (False Positive) occurs when classifier incorrectly classifies normal behavior as anomaly;

TN (True Negative) represents the number of correctly classifies normal behavior as normal;

Table 3 shows the results of the accuracy for datasets containing nine and 17 features, respectively.

Table 3 goes here

Results show very high accuracy with decision tree giving high values for not-normalized data. In this case accuracy varies from 99.4% to 99.8%. wk-NN gives the highest value for normalized data (99.5%) followed by decision tree (99.3%), Gaussian SVM (98.3%) and k-NN (98.2%) models (see Table 4).

Table 4 goes here

Results show the highest accuracy of the decision tree model and 17 features selected. wk-NN gives the highest value for the second subset. Runtime of the decision tree models is significantly shorter than runtime of other models. Runtime of the second subset is up to four times shorter than runtime of the first subset.

4 Conclusions

Feature selection and instances normalization were used to preprocess Kyoto 2006+ dataset. Two subsets were built, one containing 17 features and not-normalized instances and another containing nine features and normalized instances. Classification Learner was used to train k-NN, wk-NN, Gaussian SVM and the decision tree models. Proposed methods resulted in very high accuracy with decision tree giving the highest accuracy value and the shortest runtime for the subsets containing 17 features. wk-NN method resulted in the highest accuracy value and four times shorter runtime for the subsets consisting nine features.

References

[1] Aissa, N.B. & Guerroumi, M. (2016). Semi-Supervised Statistical Approach for Network Anomaly Detection. Procedia Computer Science, 83, 1090-1095.

[2] Burgess, M. (1998). Computer Immunology. 12th USENIX Conference on System Administration, Boston, MA, USA, 06-11 December 1998, 283-298.

[3] Garcia-Teodoro, P., Diaz-Verdejo, J., Macia-Fernandez, G. & Vasquez, E. (2009). Anomaly-based network intrusion detection: Techniques, systems and challenges. Computers & Security 28(2009), 8-28.

[4] Kajal, R. & Devi, S. (2013). Intrusion Detection Systems: A Review. Journal of Network and Information Security, 1(2), 15-21.

[5] KDD CUP '99 dataset. (1999, October 28). Retrieved from http://kdd.ics.uci.edu/databases/kddcup99/kddcup99.html

[6] Hechenbichler, K. & Schliep, K. (2004). Weighted k-Nearest-Neighbor Techniques and Ordinal Classification. Sonderforschungsbereich 386, Paper 399 (2004). Retrieved from https://epub.ub.uni-muenchen.de/1769/1/paper_399.pdf

[7] Modi, C., Patel, D., Borisaniya, H., Patel, A. & Rajaran, M. (2013). A survey of intrusion detection techniques in Cloud. J. Netw. Comput. App. 36(1), 42-57.

[8] Patcha, A. & Park, J.-M. (2007). An overview of anomaly detection techniques: Existing solutions and latest technological trends. Computer Networks 51(2007), 3448-3470.

[9] Protić, D. (2018). Review of KDD Cup '99, NSL-KDD and Kyoto 2006+ datasets. Vojnotehnički glasnik/Military Technical Courier, 66(3), 580-596. DOI: 10.5937/vojteh-16670.

[10] Sebastiani, F. (2002). Machine learning in automated text categorization. ACM Comput.Surv. 34(1),1-47.

[11] Song, J., Takakura, H., Okabe, Y., Eto, M., Inoue, D. & Nakao, K. (2011). Statistical Analysis of Honeypot Data and Building of Kyoto 2006+ Dataset for NIDS Evaluation. In: Proc.1st Work-shop on Building Anal. Datasets and Gathering Experience Returns for Security. Salzburg. April 10-13, 29-36.

Tables

Table 1 The Kyoto 2006+ dataset

No	Feature	Description
1	Duration – basic	The length of the connection (seconds).
2	Service – basic	The connection's server type (dns, ssh, other).
3	Source bytes – basic	The number of data bytes sent by the source IP address.
4	Destination bytes – basic	The number of data bytes sent by the destination IP address.
5	Count	The numbers of connections whose source IP address and destination IP address are the same to those of the current connection in the past two seconds.
6	Same_srv_rate	% of connections to the same service in the Count feature.
7	Serror_rate	% of connections that have 'SYN' errors in Count feature.
8	Srv_serror_rate	% of connections that have 'SYN' errors in Srv_count (% of connections whose service type is the same to that of the current connections in the past two seconds) features.
9	Dst_host_count	Among the past 100 connections whose destination IP address is the same to that of the current connection, the number of connections whose source IP address is also the same to that of the current connection.
10	Dst_host_srv_count	Among the past 100 connections whose destination IP address is the same to that of the current connection, the number of connections whose service type is also the same to that of the current connection.
11	Dst_host_same_src_port_rate	% of connections whose source port is the same to that of the current connection in Dst_host_count feature.

12	Dst_host_serror_rate	% of connections that have 'SYN' errors in Dst_host_count feature.
13	Dst_host_srv_serror_rate	% of connections that have 'SYN' errors in Dst_host_srv_count feature.
14	Flag	The state of the connection at the time of connection was written (tcp, udp).
15	IDS_detection	Reflects if IDS triggered an alert for the connection; '0' means any alerts were not triggered and an Arabic numeral means the different kind of alerts. Parenthesis indicates the number of the same alert.
16	Malware_detection	Indicates if malware, also known as malicious software, was observed at the connection; '0' means no malware was observed, and string indicates the corresponding malware observed at the connection. Parenthesis indicates the number of the same malware.
17	Ashula_detection.	Means if shellcodes and exploit codes were used in the connection; '0' means no shellcode or exploit code was observed, and an Arabic numeral means the different kinds of the shellcodes or exploit codes. Parenthesis indicates the number of the same shellcode or exploit code
18	Label	Indicates whether the session was attack or not; '1' means normal. '-1' means known attack was observed in the session, and '-2' means unknown attack was observed in the session.
19	Source_IP_Address	Means source IP address used in the session. The original IP address on IPv4 was sanitized to one of the Unique Local IPv6 Unicast Addresses. Also, the same private IP addresses are only valid in the same month; if two private IP addresses are the same within the same month, it means their IP addresses on IPv4 were also the same, otherwise are different.
20	Source_Port_Number	Indicates the source port number used in the session.
21	Destination_IP_Address	It was also sanitized.
22	Destination_Port_Number	Indicates the destination port number used in the session.
23	Start_Time	Indicates when the session was started.
24	Duration	Indicates how long the session was being established.

(Source: Song et al., 2011)

Table 2 Classifiers characteristics

Model	Prediction speed	Memory usage	Interpretability	Model Flexibility
Tree	Fast	Low	Easy	Medium. Medium number of leaves for finer distinctions between classes (maximum number of splits is 20).
SVM	Fast	Medium	Hard	Medium. Medium distinctions, with kernel scale set to `sqrt(P)`.
k-NN	Medium	Medium	Hard	Medium. Medium distinctions between classes. The number of neighbors is set to 10.
wk-NN	Medium	Medium	Hard	Medium. Medium distinctions between classes using a distance weight. The number of neighbors is set to 10.

(Source: MathWorks, 2016.)

Table 3 Accuracy of medium k-NN, wk-NN, medium Gaussian SVM and medium decision tree models

No	Size	Model	Accuracy - 9 features	Runtime	Accuracy - 17 features	Runtime
1	158572	k-NN	98.3%	275.72s	99.0%	1000.8s
		wk-NN	98.4%	277.32s	99.1%	1019.15s
		SVM	98.1%	449.35s	98.4%	467.7s
		Tree	97.2%	3.8452s	98.4%	14.241s
2	129651	k-NN	91.8%	175.84s	98.8%	695.88s
		wk-NN	91.8%	173.32s	99.0%	691.08s
		SVM	98.3%	254.32s	98.4%	304.56s
		Tree	97.3%	3.3104s	99.7%	9.4989s
3	128740	k-NN	98.2%	193.82s	98.6%	682.07s
		wk-NN	98.1%	194.81s	98.8%	690.58s
		SVM	97.8%	280.82s	97.9%	379.61s
		Tree	97.2%	3.3033s	99.8%	9.5367s
4	136625	k-NN	99.3%	194.83s	99.5%	782.1s
		wk-NN	99.4%	194.23s	99.7%	788.11s

		SVM	99.1%	217,32s	99.3%	234.59s
		Tree	98.3%	8.3169s	99.7%	10.001s
5	90128	k-NN	99.0%	101.28s	98.5%	731.2s
		wk-NN	99.1%	101.753s	99.6%	744.15s
		SVM	99.0%	86.283s	99.3%	230.33s
		Tree	98.4%	2.2308s	99.7%	10.855s
6	93999	k-NN	96.5%	109.25s	99.4%	354.09s
		wk-NN	96.5%	108.77s	99.5%	351.55s
		SVM	98.0%	111.83s	98.4%	149.03s
		Tree	97.5%	2.2613s	99.5%	6.9921s
7	80807	k-NN	98.8%	91.25s	99.4%	285.77s
		wk-NN	98.8%	91.267s	99.5%	285.25s
		SVM	97.9%	227.28s	98.1%	125.25s
		Tree	98.9%	2..2615s	99.4%	6.2339s
8	57278	k-NN	99.6%	42.704s	99.3%	77.224s
		wk-NN	99.3%	43.235	99.3%	77.121s
		SVM	99.2%	33.754s	99.1%	31.211s
		Tree	99.3%	1.743s	99.4%	3.7448s
9	58317	k-NN	99.1%	31.714s	99.3%	133.92s
		wk-NN	99.2%	31.738s	99.4%	134.4s
		SVM	99.1%	34.234s	99.2%	36.907s
		Tree	98.9%	1.7482s	99.5%	4.4372s
10	57278	k-NN	99.4%	43.734s	99.6%	129.99s
		wk-NN	99.5%	43.272s	99.6%	130.88s
		SVM	99.2%	30.239s	99.3%	37.894s
		Tree	99.4%	1.7489s	99.7%	4.4535s

Table 4 The highest accuracy of k-NN, wk-NN, Gaussian SVM and decision tree models

Model	Accuracy - 9 features	Runtime	Accuracy - 17 features	Runtime
k-NN	98.2%	193.82s	99.6%	129.99
wk-NN	99.5%	43.272s	99.7%	788.11s
SVM	98.3%	254.32s	99.3%	37.894s
Tree	99.3 %	1.743s	99.8%	9.5367s

Experimental and Numerical Investigation for Mechanical Ventilated Greenhouse (Comparison between Different Turbulence Models)

Ahmed E. Newir

Mechatronics Engineering Department, Faculty of Engineering, October 6 University, Egypt.

Mohamed A. Ibrahim

Mechatronics Engineering Department, Faculty of Engineering, October 6 University, Egypt.

Abstract

Using computational fluid dynamics (CFD) in agriculture field especially in designing greenhouses is becoming ever more important to reduce the energy consumption, wherefore a comparison between the experimental and numerical results increasing the credibility of theoretical studies and therefore depending on it. Forced ventilation greenhouse has been used in even span greenhouse to study the experimental measurements of temperature distribution in summer rush hours, the experiment has been performed in October 6 University, Giza, Egypt. More than one turbulence models (Standard K-ε, RNG K- ε, Reynolds Stress Model (RSM), Transition Shear-Stress Transport (SST), Standard K-ω and K-KL-ω) are used for the (CFD) numerical study implemented for comparison between the experimental and numerical measurements. After this study can get that SST turbulence model is the most efficient numerical solution for this case, a good qualitative and quantitative agreement found between the numerical results and the experimental measurements.

Keywords: Greenhouse; Mechanical ventilation; CFD.

Introduction

Operating mechanical ventilation effects on the yield and quality of almost all greenhouse crops. Mechanical ventilation is used to reduce the greenhouse effect inside the greenhouse during the hot days, which leads to attain the optimum crops temperature with minimum power. The numerical solution allows to make changes to the geometrical shape and method of mechanical ventilation by computational fluid dynamics (CFD) to reach the ideal solution for mechanical ventilation which provides better efficiency.

The first user for an early version of a CFD model to predict the distributions of climatic factors inside and outside small naturally ventilated greenhouses is Okushima (Okushima, Sase, & Nara, 1989). Two equation K-ϵ model is used to computed air flow distributions compared with the wind–tunnel results of S. Sase et al. (Sase & Takakura, 1984), which made different openings in the roof and side walls. While the experimental results showed little correlation with the computational model, the study demonstrated the possibility of using a CFD model to predict environmental distributions for naturally ventilated greenhouses.

I. B. Lee and T. H. Short (Lee & Short, 2000) studied two-dimensional K-ϵ model to validate the experimental data for multi-span greenhouse in different velocity inlet at 0.9 m/s and 2.5 m/s, validation made with only four air temperatures sensors across the 33 m * 35 m multi-span greenhouse, which means a simple understanding of temperature distribution in the greenhouse. The maximum error between the experimental measurements and numerical data was 3.2%.

Campen et al. (Campen & Bot, 2003) show that the three-dimensional calculations are preferable over the two-dimensional calculations, for computational assessment of ventilation rate with wind direction. Crop not considered in the model since no crop grown during the experiments. The calculations resembled experimental data within 15%. The wind speed correlated linearly with ventilation rate for both configurations without the buoyancy effect, which goes with the basic theory on ventilation. The CFD calculations used the standard K-ϵ model and indicated that ventilation rate for both configurations is largely dependent on wind direction, which is also observed in the experimental investigation.

The results for four different configurations of ventilators in different ventilation rates and different airflow and temperatures patterns is investigated by T. Bartzanas et al. (Bartzanas, Boulard, & Kittas, 2004). The presented results indicate that the highest ventilation rates are not always the best criterion for evaluating the performance to the agriculture crops in the greenhouses. The standard K-ϵ model remains the standard model used in the modeling of agricultural structures and applications.

J. Flores-Velazquez et al. (J. Flores, Montero, Baeza, & Lopez, 2014) used CFD with a standard K-ϵ model to study more than one aspect, the rate of air change with different ventilation opening in the roof, air speed, humidity and temperature distribution. The temperature measurements inside the greenhouse with three sensors for the greenhouse area 7.5 * 28 m. This area is large to monitor the change in temperature, which is observed in the theoretical study that there is a temperature difference of almost 15 k and these difference could not predict in the experimental measurements, due to the limitation of temperature measuring instruments. Increasing the speed of mechanical ventilation not recommended because it may lead to loss of crops.

Previous studies have studied the natural and mechanical ventilation in terms of different air speeds, air change rates, roof and side walls openings, but did not sufficiently studied the temperature distribution in experimental and numerical investigations, which is the direct effect on plants and crops in the greenhouse. In previous works computational fluid dynamics (CFD) is used in mechanical and free ventilation of the greenhouses, found some time gaps in the literature CDF studies due to low computational capability of the CFD programs and the limited computing power available at that time. Especially, they failed to describe in detail the effects of fluctuating turbulent airflow and the temperature distribution on the air exchange of the greenhouses with their CFD model.

The objectives of the present study are to verify three-dimensional CFD numerical simulations for different turbulence models (Standard K-ε, RNG K- ε, Reynolds Stress Model (RSM), Transition Shear-Stress Transport (SST), Standard K-ω and K-KL-ω) with air temperature distributions along the greenhouse axis and to compare experimental temperature measurements in a full–scale, mechanical ventilated, even–span greenhouse. Verification tests are during summer day for hot and clear sky.

Experimental Setup

The experiments located at October 6 University, Giza, Egypt (longitude angle of 29.98°and latitude angle of 30.95°). The measurements are conducted during peak sunshine hours between 10:00 AM and 5:00 PM. The greenhouse has inclined roof type even span greenhouse. The frame is made of rectangular iron pipes and Polycarbonate sheets covering material. The greenhouse with an effective floor 3.6x2.4 m^2 with central height 2.4 m and side walls height 1.8 m as shown in figure 1.

A fan of 350 mm sweep diameter and 1360 rpm with a rated air volume flow rate of 3200 m^3/h is provided on the south wall of the greenhouse for the forced convection experiments.

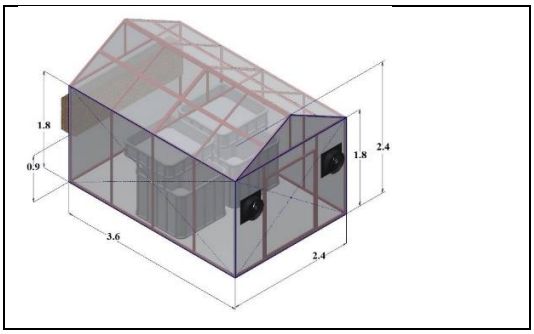

Figure 1 Schematic diagram of the greenhouse (dimensions are in m).

Temperature measurement is the most important parameter in the greenhouse. Therefore, good distribution of the position of the temperature measurement sensors is necessary to study the temperature variation inside the greenhouse.

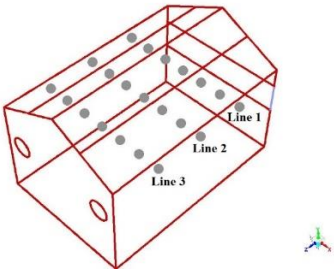

Horizontal Measurements Lines

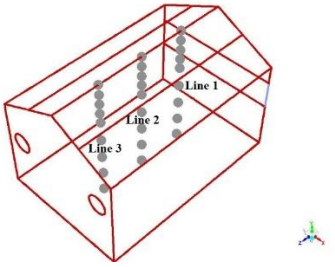

Vertical Measurements Lines

Figure 2 Horizontal and vertical measurements lines.

The temperature sensors are installed in vertical and horizontal lines as shown in figure 2. The positions are 1.6 m and 1.2 m for the horizontal and vertical lines respectively. The vertical and horizontal lines distributed inside the greenhouse in three positions; the first quarter, middle and third quarter sections.

Greenhouse walls temperature measured by 7 (DS18B20) temperature sensor one for each wall and two for the even span roof. In each horizontal line locate seven temperature sensors 0.4 m apart and for the vertical line 9 temperature sensors distributed in two parts, five sensors are used for the bottom part the distance between each of them is 0.4 m, and the top part consists of 4 sensors with 0.2 m apart. Two temperature sensors are used to measure outside and inside temperature.

Mathematical modelling

The three-dimensional model of greenhouse structure is established in this study. The cooling pads shape in the ventilation opening and the internal support structure have a small effect on the internal greenhouse temperature, so they are ignored in simplification processing. The ventilation opening placed on the northern wall to reach the maximum cooling effect using the minimum ventilation. The temperature environments for simulation calculation are in hot summer with no wind. Forced ventilation is performed by fan for greenhouses cooling. Entire greenhouse model is divided into 2 million elements. The grid test results show good grid quality. Iterative calculation is conducted using two CPU 3.07 GHz quad-core workstation in simulation.

The governing equations of fluid flow and heat transfer can considered as mathematical formulations of the conservation laws that govern all associated phenomena. These conservation laws describe the rate of change of a desired fluid property as a function of external forces and can written as:

Continuity equation: the mass flows entering a fluid element must balance exactly with those leaving.

$$\frac{\partial \rho}{\partial t} + \nabla \cdot [\rho \vec{V}] = S_m$$

Where ρ is the air density, t is the time, $\vec{v}$ is the velocity vector and S_m is the source term.

Conservation of momentum (Newton's second law): the sum of the external forces acting on the fluid particle is equal to its rate of change of linear momentum.

$$\frac{\partial}{\partial t}(\rho \vec{v}) + \nabla \cdot (\rho \vec{V} \vec{V}) = -\nabla p + \rho \vec{g} + \vec{F}$$

Where **p** is the static pressure and $\vec{\mathbf{g}}$ and $\vec{\mathbf{F}}$ are the gravitational body force and external body forces respectively.

Conservation of energy (the first law of thermodynamics): the rate of change of energy of a fluid particle is equal to the heat addition and the work done on the particle.

$$U_j \frac{\partial \mathrm{T}}{\partial \mathrm{x_j}} = \frac{\partial}{\partial \mathrm{x_j}} (\alpha \frac{\partial \mathrm{T}}{\partial \mathrm{x_j}} - \overline{\mathrm{u_j t}})$$

The solution method is run to make the control parameter settings of model in the requirement section. The SIMPLE scheme is used in this study in order to make computing convergence faster. Pressure, momentum, turbulent kinetic energy, turbulent dissipation rate, energy and radiation (discrete ordinate) all used second-order upwind for more accurately calculate, and relaxation factor settings are as shown in Table 1.

Table 1 Relaxation factor settings of the solution method.

Pressure	Density	Body Force	Momentum	Turbulent Kinetic Energy	Turbulent Dissipation Rate	Turbulent Viscosity	Energy	Discrete Ordinate
0.4	1	1	0.7	0.8	0.8	0.9	0.9	0.9

The starting point for all problems is a “geometry.” Geometries can created using the ANSYS ©17.1 DESIGN MODULER pre-processor software, which is used to create the grid.

A good quality mesh verifies the fast and accurate solution. Therefore, more than one mesh type is tested and compared with each other to attain a good computational fluid dynamics solution. The different mesh methods are multi-zone, automatic, tetrahedral patch conforming and tetrahedral patch independent. Mesh quality depending on more than one parameter; the important two parameters is meshed elements and maximum mesh skewness ratio to ensure that:

The mesh density should be high enough to capture all relevant flow features.

The mesh adjacent to the wall should be fine enough to resolve the boundary layer flow.

The best method for the greenhouse geometry is tetrahedral patch independent with 4.4 million elements with maximum skewness 0.599 which falls into the “good” range, according to the software standard.

The inlet air conditions are taken as the experiment conditions 33.25ºC. The inlet is set as velocity inlet conditions with velocity inlet 0.25 m/s and the turbulence intensity could be assumed to be 5%, and the hydraulic diameter is assumed to be 0.8949m.

The air outlets are set as pressure outlet conditions. Pressure outlet boundary conditions are used to define the static pressure at flow outlets (and also other scalar variables, in the case of backflow). The temperature of outlet air is 40°C, and the turbulence intensity could be assumed to be 5%, and the hydraulic diameter is assumed to be 0.35m.

The greenhouse roof and walls in the model are 0.006m thickness double layer polycarbonate glazing material and adding in ANSYS the material properties, it is properties is 1210 kg/m^3 density, 1200 J/kg-k specific heat and 0.21 w/m-k thermal conductivity. The walls temperature condition shown in table 4-4 as the experimental measurements.

Table 2 Greenhouse walls temperature measured at 12:00 pm for case 2.

Wall	Temperature (°C)
Right roof temperature	42.75

left roof temperature	41.75
Floor temperature	33.75
Front wall temperature	45.75
Right wall temperature	41
Back wall temperature	45.75
Left wall temperature	36.75
Outside temperature	42.75

Results and discussion

The working of the greenhouse started at 9 am on the day of the 25 August to ensure that the best representation of the mechanical ventilation inside the greenhouse kept at the peak time in the experimental measurements. The location of the greenhouse (latitude and longitude) and the experiment time introduced in the CFD program to show the radiation effect inside the greenhouse theoretically.

One of the most important applications of this study is to investigate the best turbulence model can use through CFD to control the temperature distribution inside the greenhouse.

The first three models (Standard K-ε, RNG K- ε and Reynolds Stress Model (RSM)) compared with the experimental work as shown in figure 3. The second three models (Transition Shear-Stress Transport (SST), Standard K-ω and K-KL-ω) compared with the experimental work as shown in figure 4.

The Reynolds Stress Model (RSM) seems to have the nearest results comparing which the experimental results. In horizontal line 1, the average temperature difference between the experimental measurements and numerical calculations is about 9%. The largest temperature difference percent is 18.6% in the middle of the horizontal line. The least difference is 0.7% on the west wall.

For the vertical line 1 in figure 3, the RNG K- ε has the nearest results comparing to the experimental measurements. The temperature difference percent in the range of 0.9% to 19% with an average value of 10.6%.

The percentage difference value calculated as:

$$\%\ value = \frac{t_{num} - t_{exp}}{t_{exp}} \times 100$$

Where:

t_{num} : the numerical temperature results

t_{exp} : the experimental temperature measurements

Horizontal Lines	Vertical Lines

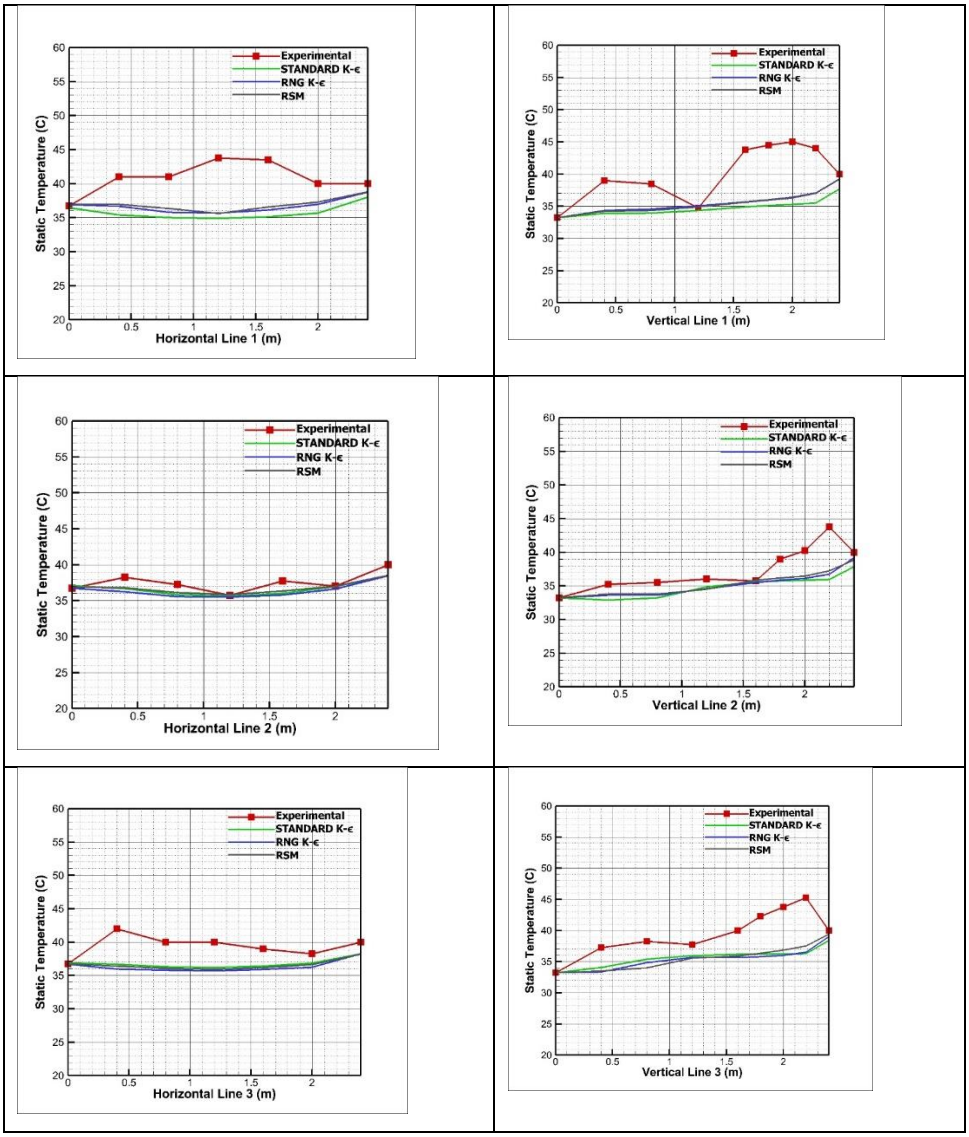

Figure 3 Experimental and numerical comparison for temperature variation at horizontal and vertical lines.

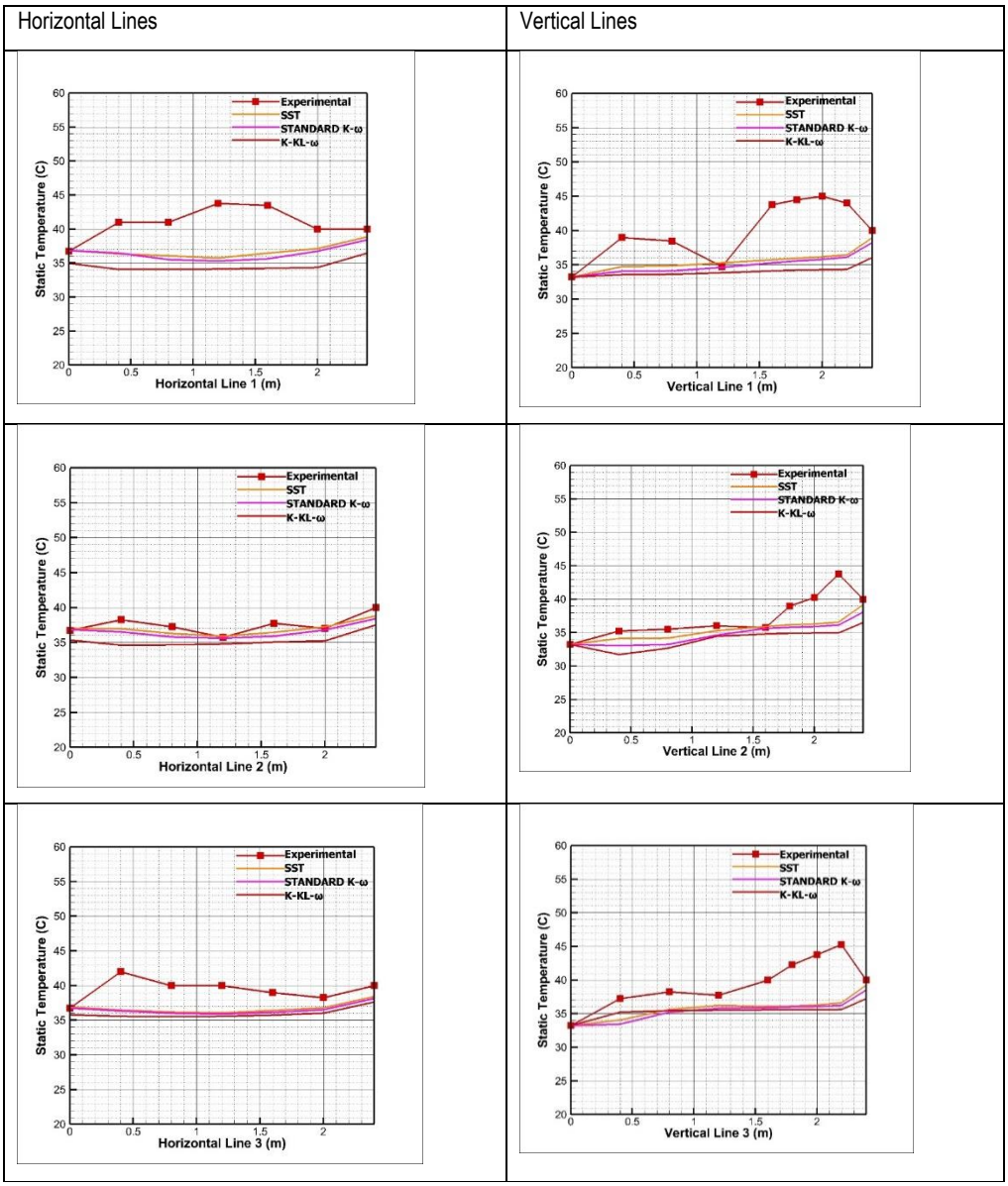

Figure 4 Experimental and numerical comparison for temperature variation at horizontal and vertical lines.

The highest temperature difference found at height 2m in the triangle zone under the even span roof. This increase is due to the effect of the greenhouse effect at the top of the greenhouse. Therefore, there is always a discrepancy between the experimental measurements and the numerical calculations in this region. The temperature difference between the experimental measurements and numerical solution is about zero at the points 0 m, 1.2 m, and 2.4 m.

In horizontal line 2, it can notice that small average temperature difference between the experimental measurements and numerical calculations especially for SST model as shown in figure 4, the average percentage difference is 1.48%. The largest temperature difference is 3.39%, and the minimum is 0.75%.

For the vertical line 2 the lowest temperature difference between the experimental measurements and numerical calculations for SST model as shown in figure 4, the average temperature difference is 4.85%, where the least and the greatest values are 0.49% and 16.38% respectively.

As shown in figure 3 in the third horizontal line, the nearest solution to the experimental results applying the standard K-ε model. The average temperature difference is 6.5% where the least temperature difference is 0.45%, and the maximum is 12.6%.

SST model is the nearest solution for the third vertical line. The average temperature difference is 9% for the highest value of the temperature difference which is 19%, and the lowest value is 1.9%.

The effect of the sun's movement between east and west shown in the horizontal lines in figure 3 and 4. There is a temperature difference between the east and west sides is 3.25°C in the experimental measurements. The corresponding value for the numerical study is 1.4°C.

Also saw on the vertical lines in figure 3 and 4 the temperature difference is raised from the surface of the ground and the greatest height of the greenhouse and significantly the greenhouse effect, especially from the height of 1.5 m to the highest level of the greenhouse.

Comparison between all models, the results are shown in figure 5, one can conclude that the most efficient turbulence models in the SST model.

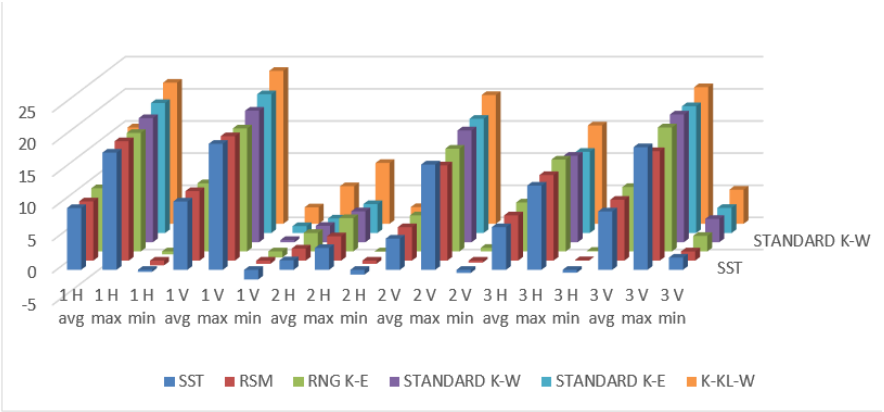

Figure 5 Percentage temperature difference between the experimental measurements and different turbulence models.

Conclusion

The influence of mechanical ventilation of an even-span greenhouse is numerically investigated using commercial fluid dynamics code. A good qualitative and quantitative agreement is found between the numerical results and the experimental measurements.

Must check different turbulence modules to find the suitable one, so six turbulence models applied in the present theoretical study: Standard K-ε, RNG K- ε, Reynolds Stress Model (RSM) and Transition Shear-Stress Transport (SST), Standard K-ω and K-KL-ω.

The effect of mechanical ventilation of an even-span greenhouse numerically investigated using commercial fluid dynamics code. A good qualitative and quantitative agreement found between the numerical results and the experimental measurements. The deviation between the two results was about 8% for all traversed lines.

The more efficient turbulence model in the present study is the SST model which gives nearly approaching results with the experimental measurements.

A good agreement between experimental measurements and numerical calculations, it can rely more on theoretical solutions.

References

[1] L. Okushima, S. Sase and M. Nara, "A support system for natural ventilation design of greenhouses based on computational aerodynamics," Acta Horticulturae , vol. 284, p. 129–136, 1989.

[2] S. Sase and T. Takakura, "Wind tunnel testing on airflow and temperature distribution of a naturally ventilated greenhouse," Acta Horticulturae , vol. 148, p. 329–336, 1984.

[3] I. B. Lee and T. H. Short, "Verification of Computational Fluid Dynamic Temperature Simulations in A Full–Scale Naturally Ventilated Greenhouse," Transactions of the ASAE, vol. 44, no. 1, p. 119–127, 2000.

[4] J. B. Campen and G. P. A. Bot, "Determination of Greenhouse-specific Aspects of Ventilation using Three-dimensional Computational Fluid Dynamics," Biosystems Engineering , vol. 84 , no. 1, p. 69–77, 2003.

[5] T. Bartzanas, T. Boulard and C. Kittas, "Effect of vent arrangement on windward ventilation of a tunnel greenhouse," Biosystems Engineering, vol. 88, p. 479–490, 2004.

[6] V. J. Flores, J. I. Montero, E. J. Baeza and J. Lopez, "Mechanical and natural ventilation systems in a greenhouse designed using computational fluid dynamics," Int J Agric & Biol Eng, vol. 7, no. 1, p. 1—16, 2014.

Eigenfrequency and Euler's Critical Load Evaluation of Transversely Cracked Beams with a Linear Variation of Widths

Matjaž Skrinar

Department of Structural Mechanics Faculty of Civil Engineering,

Transportation Engineering and Architecture University of Maribor

Abstract

For a truthful evaluation of the mechanical response of structures reliable and adequate computational models are essential. Consequently, various researches have been devoted to the mathematical representation of cracked structures. This paper studies the performance of the simplified crack model in estimations of fundamental eigenfrequency as well as elastic Euler's critical load for transversely cracked beams of rectangular cross-sections with linearly-varying widths. To obtain these solutions for different beams with diverse boundary conditions Rayleigh's energy method which requires an assumed transverse displacement function can be applied. After the appropriate displacement function is being selected, kinetic and strain energy, as well as the work done by an external axial compressive force P are evaluated. From these values, the estimations of the fundamental eigenfrequency, as well as the critical load, are assessed. To obtain these preliminary estimates, static deflection functions were applied initially. These functions represent a wide group of suitable functions since they automatically satisfy the required kinematic boundary conditions. Afterwards, alternative functions constructed from a dedicated polynomial solution were applied. Since this mathematical form offers straightforward integration, the genuinely applied displacement functions were further upgraded, separately for eigenfrequency as well as for critical load estimation. All obtained simplified model's solutions were afterwards compared to the results from equivalent and more detailed 3D finite models of the examined structures. The comparisons of the results demonstrated very fine agreements with the results from 3D FE models for all performed analyses. The considered simplified model thus clearly yields a suitable alternative in modelling of cracked beams with a linear variation of width in those situations, where cracks have to be considered within the analysis.

Keywords: Cracked beams with transverse cracks; linear cross-sections' variations; simplified computational model; transverse displacements- functions; fundamental eigenfrequency evaluation; Euler's critical load.

1. Introduction

Any degenerative effect in structures during the utilization alters their mechanical reaction by considerably decreasing the stiffness and potentially leading to their failure. Therefore, several studies consider the detection and identification of stiffness reductions in engineering structures. Such approaches for damages recognition and classification are often based on the measured structure's answer since the occurrence of damage changes the structures' response parameters. However, the efficiency of these strategies depends on the quality of measured data as well as on computational models implemented.

When analyzing cracked structures' response thorough meshes of 2D or 3D finite elements offer the finest description of a general structure, as well as of the cracks and their surroundings. Despite this, simplified models requiring fewer data are usually implemented in structural health monitoring techniques. The "discrete spring" model presented by Okamura et al. (Okamura et al., 1969) is the model that has been implemented in numerous research studies. Due to its simplicity this simplified model has been intensively applied in vibration analysis of cracked beams (F. Bakhtiari-Nejad et al., 2014), new various approaches for inverse identification of cracks (Labib et al., 2015), as well as in experimental inverse identifications of a crack (Cao et al., 2014) or a concentrated damage (Greco and Pau, 2011). Further, several papers were devoted to Euler–Bernoulli beam's finite element having an arbitrary number of transverse cracks differing in the principles of mechanics applied to obtain closed-form solutions of the genuine governing differential equation for transverse displacements (Biondi and Caddemi, 2007; Palmeri and Cicirello, 2011; Skrinar, 2009; Skrinar and Pliberšek, 2012).

The majority of the research has been limited to structural elements with constant rectangular cross-sections. Skrinar and Imamović (Skrinar and Imamović, 2018) studied bending of beams of various heights' variations along the length implementing a multi-stepped multi-cracked beam finite element (Skrinar, 2013) where the genuine continuous variation of height was modelled by an adequate series of steps. Although this model offers good (but approximate) results, it is limited to bending analyses only.

In this paper, the area of utilization of the simplified crack model is expanded to beams with linearly-varying widths where Rayleigh's energy method is being implemented for fundamental frequency and Euler's critical load estimations.

2. Simplified Computational Model

As a crack in a beam alters the local compliance, the crack is in Okamura "discrete spring" mathematical representation modelled as a massless rotational linear spring of appropriate stiffness. The neighbouring non-cracked parts of the beam to the left and to the right of the crack are modelled as elastic elements, connected by a linear spring. For the first definition for rotational spring's stiffness (given by Okamura et al. for a rectangular cross-section) as well as for all other definitions, the linear moment-rotation constitutive law is adopted. The model thus allows for a rather effortlessness description of a crack as only two parameters are required: its location L_1 from the left end of the beam, and its depth which governs the spring stiffness K_r.

3 Implementation of Rayleigh's Energy Method for Fundamental Frequency and Euler's Critical Load Estimations

Structural analysis is mainly concerned with the determination of a physical structure's response when subjected to some action. Each new computational model's behaviour must be therefore tested in various engineering situations such as static, dynamic or buckling analyses.

In dynamic analysis, eigen or natural frequencies are one of the basic properties of elastic dynamic systems. Each such system has one or more natural frequencies i.e. frequency at which it tends to vibrate freely in the absence of any driving or damping force. Therefore, the simplified model's abilities in the first natural frequency prediction were studied as they dependent only on the structure's properties (its stiffness and participating mass) and not on the load function.

There are many available methods for determining the natural frequency (Newton's Law of Motion, Rayleigh's Method,...). Some of these methods yield a governing equation of motion (from which the natural frequency may be determined afterwards), and the others produce the natural frequency only.

In this study, which examines the behaviour of the simplified computational model, Rayleigh's method (also known as the energy method), which reduces the dynamic system to a single-degree-of-freedom system consequently yielding just the first natural frequency is being utilised.

Rayleigh's method requires an assumed displacement function $w(x)$. If this function is identical to the solution of the corresponding differential equation of motion (i.e. mode shape), the true fundamental frequency is being obtained. As this is seldom true, the assumed displacement function introduces additional constraints. Because they increase the stiffness of the system, Rayleigh's method overestimates the true fundamental frequency. The fundamental lemma of the method thus states that the total energy of the system is equal to the maximum kinetic energy which also equals the maximum deformation (potential) energy.

For the situation where the breathing of the crack is not considered i.e., the crack remains open, the "strain" energy (the potential energy stored as elastic deformation of the structure including crack) is approximated as:

$$U_{strain} = \frac{1}{2}\cdot\left(\int_{x=0}^{L_1} EI(x)\cdot(w_1''(x))^2\cdot dx + \int_{x=L_1}^{L} EI(x)\cdot(w_2''(x))^2\cdot dx + K_r\cdot(w_1'(L_1)-w_2'(L_1))^2\right) \quad (1)$$

In Eq.(1) functions $w_1(x)$ and $w_2(x)$ are functions that represent the transverse displacements and must satisfy the most important kinematical boundary conditions, such as displacement and rotation. The more accurate displacement function also provides a more accurate result. In the absence of an exact solution of the differential equation (mode shape), approximate functions are applied, where static deflection functions $v(x)$ represent a wide group of suitable functions since they automatically satisfy the required kinematic boundary conditions.

To obtain the first eigenfrequency estimation the beam's kinetic energy is approximated as

$$U_{kin} = \frac{\omega_1^2}{2} \cdot \left(\int_{x=0}^{L_1} m(x) \cdot (w_1(x))^2 \cdot dx + \int_{x=L_1}^{L} m(x) \cdot (w_2(x))^2 \cdot dx \right) \quad (2)$$

implementing the same displacement functions.

Afterwards, the first in-plane vibrations eigenfrequency estimate is obtained from the total mechanical energy conservation law:

$$U_{strain} = U_{kin} \quad (3)$$

The results from these functions *w(x)* can be improved by evaluating new upgraded displacement functions due to a transverse load, given as $q(x)=m(x)\cdot\omega^2\cdot w(x)$.

The strain energy approximation can be also applied in the energy method for the buckling load evaluation. The method assumes that the elastic system is a conservative system in which energy is not dissipated as heat, and, therefore, the energy added to the system by the applied external forces is stored in the system in the form of strain energy. The work (i.e. "applied" energy) done on the system by an external axial compressive force P is evaluated by applying the same transverse displacements functions:

$$U_{app} = \frac{P}{2} \cdot \left(\int_{x=0}^{L_1} (w_1'(x))^2 \cdot dx + \int_{x=L_1}^{L} (w_2'(x))^2 \cdot dx \right) \quad (4)$$

The energy conservation law states:

$$U_{strain} = U_{app} \quad (5)$$

from which the estimate of the buckling load P_{crit} can be evaluated.

Therefore, although the same static transverse displacements function due to bending allow for a very straightforward implementation either in natural frequency as well as in buckling analysis, their solutions are not the finest.

Therefore, the assumed displacement functions *w(x)* are usually constructed from the analysed problem's dedicated polynomial solution, primarily due to ease of their integration which is essential for a successful subsequent upgrade of the solutions. Among the results obtained by implementing various assumed displacement functions, the smallest value yields an upper limit of the true fundamental frequency or buckling load.

4. Numerical Validations

Four cracked fundamental beam-structures were analyzed in order to investigate the effectiveness of the simplified model. For all four structures that differed only in boundary conditions, the length *L* was 10 m and the Young modulus was 30 GPa with Poisson's ratio 0.3. The cross-section was a rectangle with height *h* = 0.2 m where the width *b* was linearly increasing from 0.1 m at the left-end to 0.2 m at the right-end. A single transverse crack of the depth of 0.1 m was located at the mid-span to maximise its impact on the results for the majority of the examples, and the rotational spring's definition given by Okamura was selected.

The obtained results were further compared with the values from a commercial finite element program COSMOS/M where corresponding 3D finite models of the considered structures were established and analyzed. The computational model consisted of 48,000 3D solid finite elements with almost 75,000 nodal points. In each node, three degrees of freedom were taken into account – vertical and two horizontal displacements. The model's vertical and horizontal displacements were obtained in discrete points by solving more than 220,000 linear equations. Since this model allows for a realistic description of the crack those results further served as the reference values.

In the first phase, the first eigenfrequency and the buckling load estimations were obtained by implementing static deflection functions due to a downward vertical uniform load q=2000 N/m along the complete structure. These functions were further introduced into Eqs.(1)-(5).

Afterwards, basic polynomial functions were constructed for each of the considered structures considering general boundary conditions only. The implementation of these functions in Eqs.(1)-(5) yielded new sets of results for the first eigenfrequency and the buckling load.

These basic general polynomial functions were also upgraded accordingly to the specific problem to see the impact of functions' improvement to the quality of the results for both studied problems.

In the penultimate step, special polynomial functions devoted exclusively to buckling analyses were created by considering additional boundary data. Ultimately, also these functions were upgraded.

4.1 Simply Supported Beam

Initially, the governing differential equation of the elastic line for a slender beam subjected to bending in the plane of symmetry was solved. This equation, known also as Euler–Bernoulli equation of bending, relates transverse displacement $v(x)$, the coordinate x, the geometrical and mechanical properties of the cross-section (unified in flexural rigidity $EI(x)$), and the applied transverse load $q(x)$. For the case considered where the flexural rigidity $EI(x)$ is not a constant value this relation yields a fourth-order ordinary differential-equation with non-constant coefficients. However, the crack, located arbitrarily within the beam ($0 \le L_1 \le L$), separates the beam into two elastic parts, and to obtain the transverse displacements two coupled differential equations had to be solved. Consequently, two displacement functions for the parts on the left ($v_1(x)$) and right ($v_2(x)$) side of the crack were obtained:

$$v_1(x) = 145.087 + 15.476 \cdot x + 0.05 \cdot x^2 - 8.333 \cdot 10^{-4} \cdot x^3 - 10 \cdot \mathrm{Ln}\left(2 \cdot 10^6 + 200000 \cdot x\right) - x \cdot \mathrm{Ln}\left(2 \cdot 10^6 + 200000 \cdot x\right) \qquad 0\ \mathrm{m} \le x \le 5\ \mathrm{m}$$

$$v_2(x) = 145.060 + 15.481 \cdot x + 0.05 \cdot x^2 - 8.333 \cdot 10^{-4} \cdot x^3 - 10 \cdot \mathrm{Ln}\left(2 \cdot 10^6 + 200000 \cdot x\right) - x \cdot \mathrm{Ln}\left(2 \cdot 10^6 + 200000 \cdot x\right) \qquad 5\ \mathrm{m} \le x \le 10\ \mathrm{m}$$

The quality of these solutions was verified by analysing the considered structure by implementing the COSMOS/M commercial finite element program. This model produced the midpoint's vertical displacement of -0.1009 m thus confirming excellent result from the simplified model which has produced the value of -0.1013 m (with 0.34 % discrepancy). Matching of the results between the two models was also very good for all other points along the beam as the discrepancy nowhere exceeded the value at the crack location.

The initial eigenfrequency estimation was generated by inserting bending solutions into Eqs.(1)-(3). This resulted in the value ω_1 = 18.53651 rad/s for the first eigenfrequency estimation. On the other hand, the 3D FE model produced the value of 18.53429 rad/s again confirming excellent quality of the result from the simplified model as the discrepancy between the two models' results was very low (0.01198 %).

Afterwards, also the buckling load P_{crit} was approximated from Eqs. (4)-(5) by implementing the same transverse displacements functions. The buckling load estimation was 258,229 N. Alternatively, the 3D FE model produced the value of 256,693 N thus showing that the simplified model produced the results with a moderately small discrepancy (0.5985 %).

Afterwards, general basic polynomial functions $w_1(x)$ and $w_2(x)$ were constructed by considering specific boundary conditions only (implementing zero boundary displacements as well as bending moments):

$$w_1(x) = 0.339 \cdot x - 8.328 \cdot 10^{-3} \cdot x^3 + 5.552 \cdot 10^{-4} \cdot x^4 \qquad 0\ \mathrm{m} \le x \le 5\ \mathrm{m}$$

$$w_2(x) = -8.194 \cdot 10^{-2} + 0.563 \cdot x - 8.328 \cdot 10^{-2} \cdot x^2 + 2.776 \cdot 10^{-3} \cdot x^3 \qquad 5\ \mathrm{m} \le x \le 10\ \mathrm{m}$$

The implementation of these functions into eigenfrequency computation resulted in the value of ω_1 = 18.6983 rad/s for the first eigenfrequency estimation which is clearly an inferior result to the value from the bending functions as discrepancy increased to a (still quite acceptable) value of 0.885 %.

The same basic polynomial displacement functions were further implemented in the buckling load analysis already producing an acceptable value for the buckling load: 259,238 N with a discrepancy of almost 1 % (which was again higher than at static bending functions' utilisation).

Since the displacement functions were simple polynomials, the upgrading of basic polynomial functions was afterwards separately performed for first eigenfrequency estimation as well as for buckling estimation without any mathematical issues, yielding the following functions:

$$w_{d,1}(x) = -0.204\cdot\omega^2 - 2.838\cdot10^{-2}\cdot\omega^2\cdot x - 4.436\cdot10^{-4}\cdot\omega^2\cdot x^2 - 3.777\cdot10^{-6}\cdot\omega^2\cdot x^3 + 1.889\cdot10^{-7}\cdot\omega^2\cdot x^4$$
$$+ 5.925\cdot10^{-8}\cdot\omega^2\cdot x^5 - 1.597\cdot10^{-9}\cdot\omega^2\cdot x^6 - 1.338\cdot10^{-10}\cdot\omega^2\cdot x^7 + 5.901\cdot10^{-12}\cdot\omega^2\cdot x^8$$
$$+ 8.873\cdot10^{-3}\cdot\omega^2\cdot(10+x)\cdot\mathrm{Ln}(10+x) \qquad 0\ \mathrm{m} \le x \le 5\ \mathrm{m}$$

$$w_{d,2}(x) = 0.188\cdot\omega^2 + 2.7554\cdot10^{-2}\cdot\omega^2\cdot x + 4.192\cdot10^{-4}\cdot\omega^2\cdot x^2 - 3.419\cdot10^{-5}\cdot\omega^2\cdot x^3 + 1.624\cdot10^{-6}\cdot\omega^2\cdot x^4$$
$$+ 1.820\cdot10^{-8}\cdot\omega^2\cdot x^5 - 3.084\cdot10^{-9}\cdot\omega^2\cdot x^6 + 5.508\cdot10^{-11}\cdot\omega^2\cdot x^7$$
$$- 8.122\cdot10^{-3}\cdot\omega^2\cdot(10+x)\cdot\mathrm{Ln}(10+x) \qquad 5\ \mathrm{m} \le x \le 10\ \mathrm{m}$$

The newly derived at upgraded polynomial approximations $w_d(x)$ (obtained through four consecutive integrations of genuine basic polynomial functions) for the first eigenfrequency estimation produced the value ω_1 = 18.51594 rad/s, which has a rather low discrepancy (-0.099 %) against the 3D model value. However, it should be noted that the obtained value underestimated the value from the 3D model which is not consistent with the theory. Nevertheless, this divergence was a consequence of the computational model and not of the method, as the approximate method is being applied to a simplified model. It should be also noted that the upgrading process could have been further repeated. However, this was not executed due to the already low discrepancy achieved.

The separate upgrade of original polynomial function was executed also for the buckling problem. A new set of transverse displacements functions were derived at by realising that in buckling the transverse displacements are a sole function of axial compressive force P_{crit}. Therefore, the bending moments' functions were expressed as functions of applied axial force and transverse displacements. The considered problem's specific relation was $M_z(x) = -P_{crit}\cdot v(x)$. After two consecutive integrations the following functions were obtained:

$$w_{b,1}(x) = 1.208\cdot10^{-3}\cdot P_{crit} + 1.745\cdot10^{-4}\cdot P_{crit}\cdot x + 2.623\cdot10^{-6}\cdot P_{crit}\cdot x^2 - 1.157\cdot10^{-7}\cdot P_{crit}\cdot x^3 + 5.783\cdot10^{-9}\cdot P_{crit}\cdot x^4$$
$$- 1.388\cdot10^{-10}\cdot P_{crit}\cdot x^5 - 5.246\cdot10^{-5}\cdot P_{crit}\cdot(10+x)\cdot\mathrm{Ln}(10+x) \qquad 0\ \mathrm{m} \le x \le 5\ \mathrm{m}$$

$$w_{b,2}(x) = -1.934\cdot10^{-3}\cdot P_{crit} - 2.766\cdot10^{-4}\cdot P_{crit}\cdot x - 4.1845\cdot10^{-6}\cdot P_{crit}\cdot x^2 + 9.253\cdot10^{-8}\cdot P_{crit}\cdot x^3 - 1.157\cdot10^{-9}\cdot P_{crit}\cdot x^4$$
$$+ 8.410\cdot10^{-5}\cdot P_{crit}\cdot(10+x)\cdot\mathrm{Ln}(10+x) \qquad 5\ \mathrm{m} \le x \le 10\ \mathrm{m}$$

With these two new functions the "strain" energy, Eq.(1), as well as the "applied" energy, Eq.(4), were re-evaluated. Finally, Eq.(5) yielded the improved value for the buckling load of P_{crit} = 257,606.5 N with a decreased discrepancy of 0.356 %.

In the last part, special alternative functions constructed from a dedicated polynomial solution were applied exclusively for the buckling analysis. These functions were constructed by additionally considering boundary information regarding shear forces which resulted in the unknown buckling load P_{crit} to be included in the displacement functions $w_s(x)$ (due to their complexity these functions are not presented here). The buckling load obtained from these functions was 258,346.2 N (with the discrepancy of 0.644 %). These functions produced the result which was better than the value obtained from the original basic general polynomial function, but worse from those from the improved general polynomial solution. Consequently, it was expected that the upgrading of these dedicated functions will result in the best approximation. However, the integration of these functions (that included the unknown buckling load P_{crit}) initially failed. Therefore, in the integrations within the upgrade process, the value of the unknown buckling load was taken as 258,346.2 N. Consequently, the bending functions become simple polynomials which allowed the integrations to be completed resulting in functions $w_{su}(x)$. The obtained buckling load was 257,557.4 N which became the simplified model's best results as the discrepancy was 0.3369 % (which is just slightly better than the value that resulted from the upgrading of basic general polynomials).

Afterwards, the above-described analyses were repeated for several locations of the crack along the beam, and the essential results are given in Tables 1 and 2.

It is obvious from Table 1 that almost all the simplified model's solution overestimate the corresponding "exact" values (i.e. values from the 3D FE model) as there are just two cases where the results just slightly underestimate the values from the 3D FE model. Initial simple general polynomial solutions $w(x)$ mostly provided the least accurate results. However, these

functions allowed for upgrading ($w_d(x)$) that provided the situation's lowest values that, according to the theory, should also be the most accurate.

Similarly, Table 2 apparently shows that all the simplified model's solutions overestimate the corresponding values from the 3D FE model also in buckling analyses. Basic general polynomial solutions $w(x)$ initially provided results with less accuracy than the static bending displacement functions $v(x)$ for almost all locations. However, general polynomial solutions also allowed for the upgrade ($w_b(x)$) that in most case further produces slightly better results than the static bending displacement functions.

Furthermore, original special polynomial approximations $w_s(x)$ performed somehow better than general basic approximations. Ultimately, the best results for almost all locations were obtained from the upgrades ($w_{su}(x)$) of these special dedicated polynomials. The only exception is the case where the crack was 1 m from the weaker part of the structure where the static bending displacement functions produced just a slightly better result.

4.2 Cantilever, Clamped at the Right End

As the second structure, a cracked cantilever was examined. Again, derived at bending GDE's solutions $v(x)$ were compared against the 3D FE model solutions. The simplified model produced the free end's vertical displacement of -0.7272 m with a rather small discrepancy (0.032 %) against the 3D FE model result. However, it is interesting to note that the discrepancy at the crack location is slightly higher (0.142 %) as the discrepancy actually increased with the distance from the free end. Nevertheless, the general matching of the results between the two models was actually very good for all the points along the cantilever as the maximum discrepancy was everywhere below 1 %. After the verification of the simplified model's displacement functions, the initial eigenfrequency, as well as buckling load values were calculated and compared to the matching values from the 3D FE model. All these values are given in Tables 3 and 4.

After that, general basic polynomial functions $w(x)$ were constructed by considering example's specific boundary conditions only (considering zero boundary displacement and rotation as well as bending moment). These functions, as well as their upgrades ($w_d(x)$ and $w_b(x)$) , produced new values of the fundamental eigenfrequency and buckling load (see Tables 3 and 4).

The cantilever's study was completed by obtaining a buckling analysis dedicated polynomial solutions $w_s(x)$. These functions were constructed by considering additional boundary information regarding shear forces at the clamped end. In contrast to the simply supported beam structure, the inclusion of this additional information did not result in the unknown buckling load to be included in the newly derived at displacement functions. Consequently, the integration of these functions ($w_{su}(x)$) in the upgrading process did not cause any numerical problems. Both obtained values for the fundamental buckling load are given in Table 4.

It is evident from Tables 3 and 4 that static bending functions $v(x)$ produced a very decent result in the fundamental eigenfrequency estimation and, on the other hand, were quite unsuccessful in the buckling load analysis. Similarly, also general basic polynomials $w(x)$ performed well in dynamic analysis and were slightly less efficient in Euler load evaluation. Nevertheless, separate upgrades of basic polynomial approximations for both kinds of problems brought evident improvement of the results where the results for eigenfrequency once more exhibited slightly better agreement with the results from the 3D FE model. However, the special polynomial approximations $w_s(x)$ for buckling analysis already initially provided a decent result which was further efficiently improved with the upgrade process.

4.3 Propped Cantilever

All the above-described procedures were also repeated for the third structure, a propped cantilever with clamped-simply supported boundary conditions. The main results are summarised in Tables 5 and 6.

4.4 Clamped-clamped Beam

As the last a clamped-clamped beam was examined. The key results from the procedures already explained above are given in Tables 7 and 8.

5 Conclusions

The fundamental eigenfrequency, as well as Euler's critical load determination for transversely-cracked slender beams with a linear variation of width, was studied by implementing the simplified Okamura's computational model of cracked beams.

The solutions for four beam structures were obtained through Rayleigh's energy method where kinetic and strain energy, as well as the work done by an external axial compressive force P, were evaluated by applying appropriate transverse displacement functions. In the paper, various displacements functions were applied. The results obtained with the implementation of the simplified model with the combination of various functions were afterwards compared to the results obtained from the pure numerical approach implementing 3D finite elements within the framework of the finite element method.

Initially, transverse displacements' functions $v(x)$ due to transverse load were implemented. Although they produced good values for the first eigenfrequency (with the discrepancy below 0.4 %) the quality of the results for the buckling load was not very consistent as for some cases they have produced very low discrepancies (0.6 %), but for some other examples, the discrepancy was evidently higher (up to 18 %). Furthermore, since these functions are not given as plain polynomials their upgrade through their integrations was not possible. Afterwards, alternative general polynomial functions $w(x)$ were constructed. Also these functions exhibited better results for eigenfrequency estimations. The maximum discrepancies were namely up to 3.8 % for eigenfrequency analysis and up to 10.8 % for buckling load analysis. However, their mathematical form allowed for integration and, therefore, the genuine polynomial functions were further upgraded, separately for eigenfrequency ($w_d(x)$) as well as for critical load ($w_b(x)$) estimation. These separated upgrades for eigenfrequency and buckling analyses have evidently improved the quality of the results. The discrepancies in eigenfrequency analysis almost vanished (below 0.1 %) while the discrepancies for the buckling load dropped below 1.5 %.

In the end, special polynomial functions $w_s(x)$ were constructed just for buckling analyses producing evidently better results than the general polynomial functions $w(x)$ with the maximum discrepancy around 2.1 %. These functions have been further upgraded. Although these improved functions ($w_{su}(x)$) generally produced the best results their improvement was not as apparent as in the previous cases as their discrepancies were already rather low prior to upgrading.

Despite the clear differences in the mathematical form and computational efforts between both computational models considered, the considered examples have thus shown that the application of the simplified model produces adequately matching of the results as no major differences are noticeable against 3D FE solutions. It can be thus concluded that the model is suitable for free vibration analyses with non-breathing crack as well as for buckling load evaluation. It is even reasonable to assume that by applying appropriate transverse displacement functions even higher eigenfrequencies could be evaluated.

The Okamura's computational model has thus proved itself to be usable for beams with linear variations of widths even by applying rather simple analysis methods. Nevertheless, it is rational to expect that by implementing more dedicated computational methods for eigenfrequency analysis as well as for buckling analysis this would also reflect in better results from the simplified model.

Acknowledgement

The author acknowledges the partial financial support from the Slovenian Research Agency (research core funding No. P2-0129 (A)).

References

[1] Bakhtiari-Nejad, F., Khorram, A., Rezaeian, M. (2014). Analytical estimation of natural frequencies and mode shapes of a beam having two cracks. *International Journal of Mechanical Sciences, 78*, 193–202.

[2] Biondi, B., Caddemi, S. (2007). Euler-Bernoulli beams with multiple singularities in the flexural stiffness". *European Journal of Mechanics - A/Solids, 26*(5), 789-809.

[3] Cao, M., Radzieński, M., Xu, W., Ostachowicz, W. (2014). Identification of multiple damage in beams based on robust curvature mode shapes. *Mechanical Systems and Signal Processing, 46*, 468–480.

[4] Greco, A, Pau, A. (2011). Detection of a concentrated damage in a parabolic arch by measured static displacements. *Structural Engineering & Mechanics, 39*(6), 751-765.

[5] Labib, A., Kennedy, D., Featherston, C. A. (2015). Crack localisation in frames using natural frequency degradations. *Computers and Structures, 157*, 51–59.

[6] Okamura, H., Liu, H.W., Chorng-Shin, C. (1969). A cracked column under compression. *Engineering Fracture Mechanics, 1*(3), 547-564.

[7] Palmeri, A., Cicirello, A. (2011). Physically-based Dirac's delta functions in the static analysis of multi-cracked Euler-Bernoulli and Timoshenko beams. *International Journal of Solids and Structures*, *48*(14-15), 2184-2195.

[8] Skrinar, M. (2009). Elastic beam finite element with an arbitrary number of transverse cracks. *Finite Elements in Analysis and Design, 45*(3), 181-189.

[9] Skrinar, M., Pliberšek, T. (2012). On the derivation of symbolic form of stiffness matrix and load vector of a beam with an arbitrary number of transverse cracks. *Computational material science, 52*(1), 253-260.

[10] Skrinar, M. (2013). Computational analysis of multi-stepped beams and beams with linearly-varying heights implementing closed-form finite element formulation for multi-cracked beam elements. *International Journal of Solids and Structures, 50*(14/15), 2527-2541.

[11] Skrinar, M., Imamovic, D. (2018). On the Bending Analysis of Multi-Cracked Slender Beams with Continuous Height Variations. *Periodica Polytechnica Civil Engineering*, *62*(4), 873-880. https://doi.org/10.3311/PPci.11897

Table 1: Results for fundamental eigenfrequency ω_1 [rad/s] for the simply supported beam

	Functions/model			
L_1	$v(x)$	$w(x)$	$w_d(x)$	3D FE
1 m	19.52986	22.49288	19.51193	19.48735
2 m	19.19155	20.77441	19.17580	19.14632
3 m	18.83349	19.65291	18.81885	18.78653
4 m	18.59319	18.99199	18.57628	18.58736
5 m	18.53651	18.69833	18.51594	18.53429
6 m	18.67056	18.70218	18.64743	18.62232
7 m	18.95363	18.93382	18.93022	18.91004
8 m	19.29570	19.29387	19.27301	19.25661
9 m	19.57118	19.62610	19.54853	19.53399

Table 2: Results for buckling load P_{crit} [N] for the simply supported beam

	Functions/model					
L_1	$v(x)$	$w(x)$	$w_b(x)$	$w_s(x)$	$w_{su}(x)$	3D FE
1 m	285104.3	339121.8	287056.7	308723.4	285468.7	283826.0
2 m	273286.9	294491.2	273529.8	282226.0	272810.7	271407.9
3 m	263088.2	271730.4	262402.4	266115.2	262117.1	260947.2
4 m	257902.7	261355.8	257111.3	258784.3	256987.0	255966.7
5 m	258229.1	259237.6	257606.5	258346.2	257557.4	256692.7
6 m	263352.1	263245.0	262925.0	263204.4	262921.3	262201.6
7 m	271791.8	271816.4	271538.2	271615.0	271524.6	270944.1
8 m	281167.4	282875.9	281011.4	281076.4	280880.7	280389.8
9 m	288346.3	292723.4	288132.0	288365.6	287851.1	287389.3

Table 3: Results for the fundamental eigenfrequency ω_1 [rad/s] of the cantilever

Method/model	ω_1	discrepancy
COSMOS 3D FE model	8.494559 rad/s	-
bending functions $v(x)$	8.519639 rad/s	0.295 %
general basic polynomial approximations $w(x)$	8.529249 rad/s	0.408 %
upgrade of general polynomial approximations $w_d(x)$	8.492690 rad/s	-0.022 %

Table 4: Results for buckling load P_{crit} [N] of the cantilever

Method/model	P_{crit}	discrepancy
COSMOS 3D FE model	76724.8 N	-

bending functions $v(x)$	90559.3 N	18.031 %
general basic polynomial approximations $w(x)$	81818.4 N	6.639 %
upgrade of basic polynomial approximations $w_b(x)$	76856.7 N	0.172 %
special polynomial approximations $w_s(x)$	78086.7 N	1.775 %
upgrade of special polynomial approximations $w_{su}(x)$	76809.6 N	0.110 %

Table 5: Results for the fundamental eigenfrequency ω_1 [rad/s] of the propped cantilever

Method/model	ω_1	discrepancy
COSMOS 3D FE model	27.95442 rad/s	-
bending functions $v(x)$	28.02343 rad/s	0.247 %
general basic polynomial approximations $w(x)$	29.02114 rad/s	3.816 %
upgrade of general polynomial approximations $w_d(x)$	27.94767 rad/s	-0.024 %

Table 6: Results for buckling load P_{crit} [N] of the propped cantilever

Method/model	P_{crit}	discrepancy
COSMOS 3D FE model	530869.9 N	-
bending functions $v(x)$	548504.2 N	3.322 %
general basic polynomial approximations $w(x)$	588154.4 N	10.791 %
upgrade of basic polynomial approximations $w_b(x)$	537350.8 N	1.221 %
special polynomial approximations $w_s(x)$	542066.3 N	2.109 %
upgrade of special polynomial approximations $w_{su}(x)$	533636.5 N	0.521 %

Table 7: Results for the fundamental eigenfrequency ω_1 [rad/s] of the clamped-clamped beam

method	ω_1	discrepancy
COSMOS 3D FE model	42.56036 rad/s	-
bending functions $v(x)$	42.72411 rad/s	0.385 %
general basic polynomial approximations $w(x)$	43.54528 rad/s	2.314 %
upgrade of general polynomial approximations $w_d(x)$	42.56100 rad/s	0.0015 %

Table 8: Results for buckling load P_{crit} [N] of the clamped – clamped beam

method	P_{crit}	discrepancy
COSMOS 3D FE model	1044774.0 N	-
bending functions $v(x)$	1101546.7 N	5.434 %
general basic polynomial approximations $w(x)$	1082479.2 N	3.609 %
upgrade of basic polynomial approximations $w_b(x)$	1030595.4 N	-1.357 %
special polynomial approximations $w_s(x)$	1052194.1 N	0.710 %
upgrade of special polynomial approximations $w_{su}(x)$	1028921.5 N	-1.517 %

Effectiveness of Active Confinement Techniques with Steel Ribbons: Masonry Buildings

Elena Ferretti

DICAM – Department of Civil, Chemical, Environmental, and Materials Engineering, Alma Mater Studiorum, Università di Bologna, Italy

Abstract

In the present paper, we analyzed the main advantages of the active confinement techniques with a particular focus on the CAM system, which is an Italian reinforcement technique with pre-tensioned stainless steel ribbons. Italian seismic codes classify the CAM system as belonging to the strengthening category of "horizontal and vertical ties". Therefore, we compared the CAM system to the reinforcement techniques with horizontal and vertical ties in order to understand the actual similarities and possible differences between them. Moreover, we offered a deep analysis of the main critical issues of the CAM system, distinguishing between geometrical and mechanical weak-points. In particular, we analyzed the strengthening mechanism of the CAM system, still poorly understood, by performing a static analysis in the Mohr/Coulomb plane. Finally, we provided suggestions for future developments.

Keywords: CAM system, masonry walls, in-plane loading, out-of-plane loading

Attaining a Beam-Like Behavior with FRP Strips and CAM Ribbons

Elena Ferretti

DICAM – Department of Civil, Chemical, Environmental, and Materials Engineering, Alma Mater Studiorum, Università di Bologna, Italy

Abstract

One of the major concerns in the seismic retrofitting of masonry walls is that of increasing the ultimate load for out-of-plane forces. In multi-story buildings, these forces may originate from the hammering actions of floors, when the earthquake direction is orthogonal to the wall. A possibility for counteracting the out-of-plane displacements is retaining the wall by building some buttresses, that is, some beams lean against the wall and disposed vertically. Another possibility is to make the buttress in the thickness of the wall. In this second case, we must cut the wall for its entire height, realize the buttress, and restore the masonry wall around it. In both cases, the interventions are highly invasive. The first intervention also leads to increments of mass that enhance the attraction of seismic forces. The aim of this paper is to find a less invasive and lighter alternative for realizing buttresses. We proposed to use FRP strips and steel ribbons in a combined fashion, so as to realize an ideal vertical I-beam embedded into the wall, without requiring to cut the masonry. We also provided some experimental results for verifying the effectiveness of the model.

Keywords: CAM system, masonry walls, seismic retrofitting, out-of-plane loading, hammering action.

Integrated biostratigraphy of the Tarasci Formation of the Central Taurides (Turkey) and its implication for the regional correlation of Sultan Mts time-equivalent deposits

Ali Murat Kılıç

Balikesir University Faculty of Engineering Dept of Geological Eng, Balikesir Turkey

Zeki Unal Ümün

Namik Kemal Uni., Faculty of Corlu Engineering, Dept of Environmental Eng, Corlu-Tekirdag, Turkey

Abstract

Nearly four decades having passed, it was imperative to launch a new campaign to study the Tarasci Formation. In the scope of this project, well dated conodont elements are the object of a systematic paleontologic and phylogenic study. Members of the subfamily Marquezellinae found in of the Central Taurus may contribute to the understanding of the Geology of Turkey. The subfamily Marquezellinae originated in the Family Gondolellidae during the Pelsonian (late Anisian) and was extinct during the early Julian (early Carnian), at the time that the "Sephardic Province" is replaced by dominantly evaporitic facies. Marquezellinae faunal elements spread during Late Ladinian–Early Carnian to the Southern Alps, Dinarids, Taurides and the Cimmerian terranes (Malayan Peninsula and SW China). The facies of the "Sephardic Province" represented here in Southern Turkey (WNW of Seydişehir, Konya) has been recognised in South-Eastern Spain, North Africa (Algeria, Tunisia and Egypt) and the Near East (Israel, Jordan). To date, specimens of the conodont subfamily Marquezellinae were recovered Early and Late Ladinian sediments of Spain, Tunisia, Egypt and Israel, Jordan, Slovenia, Croatia, Serbia, Turkey, and Sicily. Late Ladinian to early Carnian occurrences of the subfamily are known from the Southern Alps of Italy, Dinarides as well as displaced terranes in Hungary and the Cimmerian terrane of Sibumasu in South-West China and the Malayan Peninsula. It is of special significance that the key index fossil of the basal Ladinian GSSP (Curionii Zone) in the Southern Alps has been found in SE Spain as well as Israel. This ammonoid zone also includes the Fassanian (Lower Ladinian) FO (first occurrence) of *Pseudofurnishius murcianus* [1], [2], [3]. The area of Seydisehir (Konya) is considered as a fragment of the African - Arabian plate below the Taurus Nappes. Its Triassic sequence yields fauna's characteristic for the "Sephardic Province" that is restricted to the Southern Tethys. A number of alpinotype Tethyan faunal elements provide clues as to their age, including Late Anisian, Fassanian, Longobardian and Julian. When examining Triassic sections in Turkey, Assereto and Monod collected a few samples for conodonts from the Middle and Upper Triassic Taraşçı Limestone [4], [5]. The Tarasci Limestone consists of dark well bedded protected-bay limestones with intercalated lenses of white massive biogenic Emir Kaya Limestone (Ladinian). The Toptaş Limestone, the uppermost Ladinian white biogenic massive reefoidal top of the Tarasci Limestone, is directly overlain by the Sarpyar Dere Formation of Carnian age that consists of turbiditic marls, sandstones and microbreccias. The samples yielded only few conodonts except for one from the upper Tarasci Limestone in the Tepearasi Valley, Osmanin Dag. This sample with abundant *Pseudofurnishius murcianus* was not in place, but contains the ammonoid *Protrachyceras* sp. of Longobardian age. Out of the four superposed fossiliferous horizons distinguished in the Tarasci Limestone, the three lower are of Early Ladinian age, while the Upper Ladinian age of the upper fauna was determined but Assereto and Monod (1974), following Tozer [6]. [a]

Keywords: Triassic, Conodonts, *Pseudofurnishius*, Taurus, Turkey

[a]Thıs Study Was Supported by Tubıtak Grant 116y374

A Backstepping Approach for of longitudinal Aircraft

Labane Chrif

PhD, Algeria

Abstract

For transportation aircraft, the primary control objective for an autopilot system engaged during approach and landing is relative to the flight longitudinal tracking on the basis of highly simplified linear models of flight dynamics. The dynamics governing the flight longitudinal of an aircraft are in general highly nonlinear and involve complex physics for which no accurate models are available. In this paper a nonlinear model describing the longitudinal equations of motion in strick feedback form is derived. Backstepping is utilized for the construction of a globally stabilizing controller with a number of free parameters. It is implemented a controller with an internal loop controls involving the pitch rate of the aircraft and an external loop which includes angle of attack, path angle and pitch angle. Finally, nonlinear simulation results for a longitudinal model of a transportation aircraft are displayed and discussed.

Keywords: backstepping, approach, longitudinal, aircraft

Assessment of Alternative Policy Strategies towards a Decarbonised Energy System: A Fuzzy - Promethee Approach

Aikaterini Papapostolou

National Technical University of Athens

Charikleia Karakosta

National Technical University of Athens

Haris Doukas

National Technical University of Athens

Abstract

Recent political discussions and research interest focus on ways to accelerate the development and deployment of low-carbon technologies with respect to the targets set for 2030 and 2050. Although targets are well defined, extensive uncertainties exist in the European energy future necessitating the identification and analysis the parameters affecting several decarbonization options. In this framework, a set of alternative strategies were designed by identifying outcomes that conform to the objectives of European energy and climate policy. These strategies are positioned under two key uncertainties; the level of cooperation (i.e. cooperation versus entrenchment) and the level of decentralisation (i.e. decentralisation versus path dependency). This study presents a multi-criteria approach in order to assess alternative decarbonization strategies for achieving a sustainable energy system in EU. To cope with the disparate preferences of decision-makers, as well as to manage the uncertainty that arises when solving decision problems, a methodological assessment framework is developed based on an extension of the Preference Ranking Organization METHod for Enrichment of Evaluations (PROMETHEE) for group decision-making. Making use of the popularity and suitability of Fuzzy PROMETHEE in managing energy sector problems, this study offers an original work able to shed light in the policy-making problem related to sustainable energy transition.

Keywords: Energy and Climate Policy; Low-carbon Transition; Group Decision Making; Fuzzy PROMETHEE; Europe; Policy Recommendations

Experimental Study on Influence of Pressure Holding Time on Strain Generation in the Hydraulic Autofrettage Process

Hakan Çandar

University of Gaziantep, Turkey

Abstract

In this study, the effect of pressure holding time on strain generation in hydraulic autofrettage process is investigated. Experiments are performed in a hydraulic autofrettage test stand available in Delphi Automotive Systems. AISI 4140 steel is used as the test material which exhibits similar mechanical properties with common rails. The test samples are held on 8 different autofrettage pressures varying between 530 and 666 MPa for 180 seconds. During the experiments 90° rosette gauges are mounted on the surface of the cylinders and both axial and tangential strains are recorded in 100Hz frequency. It is found that, there is an increase in the tangential strain with respect to holding time until few seconds and then it stays constant. The time period increases for higher pressures and there is no significant effect of time on axial strain.

Keywords: Hydraulic autofrettage, common rail, pressure holding time, strain gauge measurement.

Determination of Grave Locations in War Cemeteries with High Resolution GPR (Ground Penetrating Radar)

Erdem Gündoğdu

Çanakkale Onsekiz Mart University, Çan Vocational School, Department of Mining and Mineral Extraction, Turkey

Yunus Can Kurban

Eskişehir Osmangazi University, Graduate School of Natural and Applied Sciences, Department of Geological Engineering, Turkey.

Cahit Çağlar Yalçıner

Çanakkale Onsekiz Mart University, Çan Vocational School, Department of Mining and Mineral Extraction, Turkey.

Abstract

As in the whole world, in Turkey the burial and later determination of the grave locations of soldiers who lost their lives during war involves many deficiencies in terms of the historical record. Though there is very valuable information like maps and writings from the time of war, due to the intense and violent passage of war, much important information is not directly communicated to the present day. The most controversial of this information is probably the locations of war graves. The main reason can be considered the excessive numbers of the dead and the excessive loss of soldiers in very short periods. In spite of these problems, the locations of many war cemeteries have been determined due to detailed research by historians and maps drawn during the war. However, the locations of graves within the war cemeteries are only roughly determined and in line with this, areas were fenced off as cemeteries. The high-resolution, non-destructive shallow geophysical method of ground penetrating radar (GPR) has been used for many years with the aim of identifying structural elements that are buried (graves, tunnels, archeological remains, etc.). In this context, its use in studies to research the locations of graves in areas known to be war cemeteries will illuminate the past and re-organization of war cemeteries according to the locations of the graves will contribute to the importance and respect that should be shown to the soldiers or martyrs who died. This work was supported by Çanakkale Onsekiz Mart University The Scientific Research Coordination Unit, Project number: FBA-2018-2485

Key words: war cemeteries, grave locations, ground penetrating radar (GPR).

The Effects of Toxic Element Pollutions on Benthic Foraminifers in the Eastern Mediterranean

Zeki Ünal Yümün

Namık Kemal University, Çorlu Engineering Faculty, Environmental Engineering Depertmant, Tekirdağ

Ali Murat Kılıç

Balikesir University, Engineering Faculty, Geology Engineering Depertmant, Balikesir, Turkey

Abstract

In study, foraminiferal assemblages and the pollution results of heavy metal concentrations obtained from drilling samples in the Eastern Mediterranean have been examined. In this way, three sea drilling works have been carried out in the study area and Quaternary sediments taken as the core from the driling. Benthic foraminifers have been identified from all three samples. In addition, horizontal and vertical distributions of toxic element concentrations of the same samples determined. In thise study, a large foraminiferal assemblages "Adelosina duthiersi, Adelosina mediterranensis, Ammonia compacta, Ammonia tepida, Cibicidoides cicatricocus, Elphidium charlottense, Elphidium complanatum, Elphidium crispum, Eponides concameratus, Lachlanella carinata, Massilina secans, Quinqueloculina seminula, Planorbulina mediterranensis, Rosalina brody, Spiroloculina angulosa, Spiroloculina antillarum, Spiroloculina dilatata, Spiroloculina ornata, Triloculina bermudezi" have been defined. Concentrations of 28 toksic elements (Fe, Zn, Al, Mn, As, B, Co, Cr, Cu, Ni, Sb, Na, Mg, K, Ca, P, Pb, Hg, Cd, Ag, Bi, Cd, Mo, Pb, Pt, Sn, Se, Hg) have been determined but the concentrations of 9 toxic elements (Cu, Zn, Pb, Ni, Cr, Fe, As, Se, and Mn) evaluated. In addition, surface element analyzes have been carried out to reveal the causes of color changes in the shell structure of Ammonia compacta. Surface element analysis was performed with Scanning Electron Microscope, it was determined that the color change in the Ammonia compacta tests originated from Mn and Fe elements. in some of the foraminifera shells which morphological changes observed in, Color changes also have been observed. Especially at the upper levels of the drilling samples the concentration values of the elements are higher. These top levels, where the elements are intensive, represent the current environment, and the foraminifers identified at these levels were more discolored. It is thought that the main cause of the polluting element densities in the upper levels representing the current environment is agricultural activities and geological formations (Upper Meastrihtian Ophiolitic Rocks) located neighbor area.

Keywords: Eastern Mediterranean, Foraminifera, toxic elements, heavy metals, bio-ecology

An Empirical Investigation into the Notes of Financial Reporting - Case of Albania

PhD Cand. Juna Dafa
Faculty of Economy, University of Tirana, Albania

Prof. Assoc. Diana Lamani
Faculty of Economy, University of Tirana, Albania

Abstract

The year 2008 determined the transition in Albania from *Plan Comptable Général,* a fiscal – oriented system based on accounting rules to the IFRS system which is known as an investor-oriented system. The implementation of the IFRS resulted in a qualitative improvement of the Albanian financial reporting of banks, insurance companies, and other large companies. The purpose of this paper is to verify the level of compliance with the disclosures requirements of financial statements (hereinafter FS) made in accordance with IAS 1, providing an empirical evidence for this specific area of financial reporting. In order to fulfil the aim of this study, 41 large companies, that meet the criteria for applying IFRSs according to the Accounting Law of Albania, are considered. The paper reveals through empirical analysis that only one of the entities taken into consideration does not present the basis of preparation and does not make a summary of significant accounting policies applied. All the entities give supporting information for the items presented in the FS. 26% of the entities do not present information related to commitments and contingent liabilities. 6 entities out 41 do not present information about risk management. 5 entities out 41 do not cross-reference the notes with the respective items presented in the FS. The updating terminology is made by more than 70% of the entities. The level of compliance with disclosure requirements is measured by a self-constructed unweight index (DI). The average overall compliance is 92%, which is considered as a satisfactory level for our country.

Keywords: financial reporting, IAS 1, mandatory disclosures.

Introduction

International Financial Reporting Standards (IFRS) is that set of standards enables obtaining better information, as a result of using recognition and measurement criteria that better reflect the economic reality of companies and providing a wide range of information in the notes (Lourenço & Branco, 2015).

The implementation of IFRS in our country, started with the adoption of the Law No. 9928 "On accounting and financial statements", in 2004, by the Albanian Parliament. Since the year 2008, bank and insurance companies, and some other large private companies (even if they are not listed in any stock exchange) in Albania, prepare Financial Statements, including notes, in accordance to the IFRS. The law defined which entities have to present FSs using full IFRSs or the Accounting National Standards (prepared by the National Accounting Council in compliance with the IFRSs). Based on this law, the financial reporting structure in Albania is organized in three levels. At the first level are included entities that apply IFRSs (issued by IASB and translated into Albanian, without any changes to the original text in English). At the second level are included the small and medium-sized private and public sector for-profit entities that use 14 National Accounting Standards (NAS) issued in accordance with IFRSs. At third level are the micro-entities, which reports on the basis of a single standard issued specifically for them (NAS 15-For Accounting and Financial Reporting of micro-entities).

The implementation of the IFRS/NAS determined the transition of our country from *Plan Comptable Général* (known as French accounting model) based on accounting rules, fiscal – oriented system, to the IFRS system (the Anglo-Saxon accounting model) which is known as investor-oriented system. The implementation of the IFRS resulted in a qualitative improvement of the Albanian financial reporting of banks, insurance companies, and other large companies.

It is generally recognized that IFRS contain so many requirements relating to the information to provide in the notes to financial statements that they result in information overload and increased complexity (Blanchette et al., 2013). The Notes

to the Financial Statements are components of a complete set of FSs that provide important disclosures and details related to the information reported in them. They make up an integral part of the financial reporting, prepared at the end of the reporting period. The demand for financial reporting and disclosure arises from information asymmetry and agency conflicts between managers and outside investors (Healy & Palepu, 2001).

A lot of the information that needs to be presented in the notes is specifically described in the requirements of mandatory disclosures by accounting standards. But IFRSs only prescribe the format and order of the notes to a limited degree. Other aspects of the notes depends from management's assessment in what is important for a user to understand FSs.

Healy & Palepu (2001) point out that managers' presentation decisions within the financial statements reflect informational motivations (that is, revealing the underlying economics of the firm) or opportunistic motivations (that is, attempts to bias perceptions of firm performance). Riedl & Srinivasan (2008) suggest managers to use income statement presentation as a mechanism to assist users in better identifying and understanding the firm's underlying performance. On the other hand, in order to process financial statement information appropriately, users must understand that information which is relevant, discover that information in the financial statements and asses the implications of that information for judgments and decisions, both alone and in conjunction with other information (Hodge et al., 2004).

In recent years, the authors see that the financial statement presentation is one of considerable importance issue of those addressed by the IASB in the context of the Disclosure Initiative for better communication. "The Board has been clear that the Disclosure Initiative is not about reducing disclosures per se—it is about making disclosures more meaningful by improving their communication value while simplifying the preparation process" (Kabureck[a], 2016).

In the context of the most recent developments at international level as a reflection on Disclosure Initiative, the authors study the level of compliance with mandatory disclosures requirements as per IAS 1, of some Albanian large companies. Since IAS 1 includes the general disclosure requirements in the FS, the main purpose of this study is to provide evidence regarding the way that those companies are disclosing information in compliance with the overall requirements of that standard.

Considering the gap that exists in our country with regards to studies involving mandatory disclosure and more importantly on company disclosure levels, this paper intends to contribute to the topic by addressing some identified issues in this specific area of financial reporting.

Literature review and Theoretical background

Financial statements are a primary means for management to communicate financial information about an enterprise to the external parties. The basis for the presentation of the general-purpose financial statements in accordance with IFRS are prescribed in International Accounting Standard 1 (IAS 1) "Presentation of Financial Statements", which sets out the overall requirements for the presentation of financial statements, the guidelines for their structure and minimum requirements for their content.

The usefulness of financial statements is believed to be increased by explanations and details outside the body of the statements themselves. For this reason, financial statements are accompanied by notes and other additional disclosures when necessary providing a variety of information that would otherwise not be available. Through these disclosures, managers provide information that facilitates external users of financial reports to better understand the true economic picture of the business (Kothari & Short, 2003).

The key role of the notes in the financial statements is to provide further information explaining the amounts presented in the financial statements as well as the information about items that have not been recognized, aimed to be useful for decision-making. There is a degree of fluidity between showing information "on the face of the accounts" (i.e., directly in the statement of financial position or income statement) and in the notes: the main categories have to be preserved, but the detail underlying the reported amounts may be shown in the notes (Epstein & Jermakowicz, 2010).

In accordance with IAS 1, the notes should: (1) present information about the basis of preparation of the financial statements and the specific accounting policies used; (2) disclose the information required by IFRS that is not presented elsewhere in

[a] Mr. Kabureck is a Member of the International Accounting Standards Board.

the financial statements, and (3) provide information that is not presented elsewhere in the financial statements, but is relevant to an understanding of any of them.

IFRS are principle-based rather than rule-based, which are characterized by less precise guidance and fewer bright-line rules (Barth *et al*. 2008). The IASB's Conceptual Framework states that "To a large extent, financial reports are based on estimates, judgements and models rather than exact depictions" and "The usefulness of financial information is enhanced if it is comparable, verifiable, timely and understandable." This means that preparers and auditors would, therefore, need the courage to exercise and defend their professional judgements in performing their roles in this simplified accounting world (Shields[a], 2006; Tweedie[b], 2007).

IAS 1 is not prescriptive in nature. Rather, IAS 1 confess that judgement is required in determining the best manner in which information is presented. The standard has two separate paragraphs regarding the requirements to present two types of judgements made by management that have the most significant effect on the amounts recognised in the financial statements:

1. Judgements that management has made in the process of applying accounting policies (IAS1:122); and
2. Judgements that management makes about the future and estimations (IAS 1:125).

To be a key judgement disclosed under IAS 1: 122, the subject matter must relate to something other than assumptions about the future or making estimates (Deloitte, 2017). The separation of generic from the specific accounting policies has been shown to be difficult to make. Disclosures of key judgements do not usually address measurement although they may do when the issue relates to determining the appropriate measurement basis (e.g. fair value, amortized cost etc.) rather than what goes into arriving at the amounts recognized (Deloitte,2017). It happens quite often that useful information is lost in technical disclosure, but in the same time it is accepted that making disclosures on recognition and measurement without being technical is challenging (IASB, 2013).

Second type judgements are considered as sources of estimations uncertainty. Actually, making such estimates is a difficult task as long as a subjective assessment of many things is required at the reporting date and in the future. For this reason, information about these judgements is usually included in the form of a special note. These estimates include professional judgments that are made to set amortization rates, as well as an assessment of whether the entity meet the assumption of going concern and will continue in operation for the foreseeable future. It is obvious that there is a risk of making "mistakes" when assumptions have a high degree of subjectivity and complex "guesswork" about uncertainties (e.g. the life of an asset, future selling prices, future costs, and future interest rates). There also needs to be a significant risk that a material adjustment to the carrying amount of assets or liabilities may be required as a result of changes in those assumptions or estimates in the next period, not just in any future period whenever that might be (Deloitte, 2017).

According paragraph 113 in IAS 1, an entity should, as far as practicable, present notes in a systematic manner and should cross-reference each item in the statements of the financial position and the comprehensive income, in the separate income statement (if presented), and in the statements of changes in equity and of cash flows to any related information in the notes.

Up to 2016, an entity is required by paragraph 114 to present notes in the following order, to help users understand the financial statements and to compare them with financial statements of other entities:

1. Statement of compliance with IFRS;
2. Summary of significant accounting policies applied;
3. Supporting information for items presented in the financial statements;
4. Other disclosures, including contingent liabilities and unrecognized contractual commitments; and nonfinancial disclosures.

[a] Director and Head of Financial Reporting at Barclays Capital, a division of Barclays Bank.

[b] Sir David Tweedie is the former chairman of the International Accounting Standards Board.

Now, in the context of the Disclosure Initiative, this order is only an example of how notes can be ordered. It is required by the revised standard that the notes be ranked based on the qualitative characteristics of understandability and the comparability of information.

The way in which some Standards are designed hint the perception that specific requirements of those Standards override the general statement in IAS 1:31 that an entity need not provide information that is not material. Materiality has been and remains an important concept in the centre of attention of the IASB itself, closely related to the importance of information that is useful for user decision-making. However materiality is very important in practice for its implications for the preparers of financial statements and auditors.

One of the underlying requirements for financial statement preparation in compliance with the IFRSs is that an entity should make an explicit and unreserved statement of such compliance in the notes. This means that financial statements and the notes and other supplemental information accompanying them must include all available relevant information to keep them from being misleading (Carmichael & Graham, 2007). There is a risk that an immaterial information that is not deemed necessary to be present in primary statements, can be found unnecessarily in notes. The presence of immaterial information and the omission of material information results in a decrease of the decision-usefulness of the financial statements. The inappropriate application of "materiality" from entities is considered to be one of the reasons of disclosure ineffectiveness. As a consequence, the IASB has addressed materiality as part of the Disclosure Initiative. The amendments to the definition of material in IAS 1 must be applied prospectively for annual periods beginning on or after 1 January 2020.

Methodology

The main purpose of this paper is to verify the level of compliance with the disclosures requirements of financial statements made in accordance with IAS 1, providing an empirical evidence for this specific area of financial reporting in our country.

This study is carried out using primary as well as secondary data sources which are available on World Wide Web. The authors have primarily worked with secondary data, i.e. papers published by foreign authors, IAS 1 disclosure requirements, and discussions done related to Disclosure Initiative.

Based on Law No. 9228 dated 29.04.2004[a] "On accounting and financial statements", the financial reporting structure in our country is organized in three levels. Only those entities categorized as first level are required to apply IFRSs issued by IASB and translated into Albanian without any changes to the original text in English. This category includes:

a) the entities listed on an official stock exchange and their subsidiaries, subject to the consolidation of the accounts; and
b) of important general interest (second level banks, financial institutions, similar to banks, insurance and reinsurance companies, securities funds and all companies licensed to carry out investment activities in securities, even when they are not listed on an official stock exchange;) and
c) other large unlisted entities when they meet the last two years these both criteria set by the Council of Ministers: 1) annual income over 1,250,000,000 ALL; 2) average annual number of employees over 100.

In selecting the sample the authors referred only to the entities of group (c). There are no listed entities in our country as predicted in category (a). Since the drafting of the Law on Accounting, the creation of the stock exchange in our country was made possible after 13 years, in July 2017, when it was licensed "Albanian Stock Exchange (Albanian Stock Exchange) - ALSE" as the first Albanian stock exchange with private capital licensed in the country. The stock exchange ALSE started its activity, officially, in February 2018 with a limited activity only in the trading of government securities, but with the aim of further expansion of the financial market as a whole in the future. On the other hand there is no published information about any Albanian entities listed on any international stock exchange. Entities included in category (b), in addition to reporting under IFRSs, also have specific reporting requirements set by the supervisory boards of the respective markets, which are likely to impact the level of disclosures.

[a] This law is superseded by Law No. 25/2018 "On accounting and financial statements" ("New Law"), published in the Official Gazette no. 79, dated 30.05.2018, with effect as of 01.01.2019. The New Law is partly harmonized with the European Union legislation on financial statements and other reports of economic entities.

The authors provided the annual reports and relevant data of the entities of category (c) referring to the National Business Center (NBC) web site. NBC is the institution where entities have the legal obligation to publish valuable financial information for use by the general public. So, the primary data are provided on official way from the only source where the Certified Financial Statements can be found.

The authors have manually downloaded notes of the FS, from NBC, for 41 Albanian large non-listed companies using IFRS, for the year ended 31 December 2016. To measure the level of the compliance with the disclosure mandatory requirements, as per IAS 1, the authors have used a self-constructed unweight disclosure index. The index includes the following 8 items of information:

1. Reference number – The authors have verified if the entities have the column reference in the FSs, as well as, if the items are cross-referenced with the information given into the notes. If the entities cross reference the information in the notes with the respective item in the FSs the authors put 1, otherwise 0. Except of being a mandatory element of FSs, the reference number enables the realization of the enhancing sub characteristic of understandability.
2. A summary of significant accounting policies applied – Do the entities make a summary of significant policies applied, for example, do they specify the method used to depreciate the intangible assets, the method used to evaluate the inventory, etc.
3. Basis of preparation – Do the entities make an explicit and unreserved statement of compliance with IFRS?
4. Judgements and estimates - Do the entities make judgements in the process of applying the entity's accounting policies that have the most significant effect on the amounts recognised in the financial statements?
5. Supporting information for the items presented in the FS – Do the entities provide breakdown of line items in FSs into the notes?
6. Commitments and contingencies – Do the entities disclose in *other disclosure* section, commitments or contingent liabilities?
7. Comparative information – Do the entities provide comparative figures in the notes, i.e. the notes of the previous year? Providing comparative information enables the fulfillment of the enhancing sub-characteristic of comparability.
8. Business risk information – Do the entities disclose in *other disclosure* section, nonfinancial risk management?

Disclosure index (DI) =$\sum_{i=1}^{n} di$ /n

If the item i is disclosed, di=1,

if the item i is not disclosed di=0.

n=number of items which might be disclosed by a sample company, i.e. 8.

In addition to the items included in the DI, the authors have verified some other items in the Notes in the FSs. This verification is done through the compilation of a list of questions which represent the chosen disclosure requirements assessed in our research. The compiled questions are as follows:

- In how many pages are the notes disclosed? – In some studies, the number of pages of notes has been taken as a factor that may affect the quality of them, although it mainly measures the quantity of disclosures (Beretta & Bozzolan, 2008).
- Does the entity use an updated/partially updated/old terminology? The terminology is updated if the companies use the new terminology introduced by IASB in 2007. Regarding the terminology we have verified whether the entities have been updated with the new terminology announced by the National Accounting Council, which is based on that published by IASB in 2007. We have verified terms like:
    - Balance Sheet or Statement of Financial Position
    - Income Statement or Financial Performance Statement
    - Passive or liabilities and equity

- Does the entity recognize a provision? - The authors have verified if the entities describe provision in the summary of significant accounting policy applied and applies it, i.e. recognize a provision, or just describe it.
- Does the entity recognize an allowance for doubtful accounts? The authors have verified if the entities describe impairment of receivables in the summary of significant accounting policy applied and applies it, i.e. recognize an allowance for doubtful accounts, or just describe it.
- Does the entity continue to present disclosures in the same order as prescribed by IAS 1:114? - The authors have verified if the entities continue to present disclosures in the same order as prescribed by IAS 1:114 or have reflected the amendments done in 2014.

Analysis

The primary data were elaborated through excel spreadsheets. Our sample comprise 41 large companies.

General characteristics of the sample

Through descriptive analysis the authors will describe the main characteristics of the sample selected (Table 1, Table 2 and Table 3).

Table 3: Sample by industry

Industry	*Number of companies*	*Percentage*
Petroleum	*3*	*7%*
Gaming industry	*3*	*7%*
Mining industry	*2*	*5%*
Construction	*8*	*20%*
Production	*5*	*12%*
Service	*7*	*17%*
Telecommunication	*5*	*12%*
Trade	*8*	*20%*
Total	*41*	*100%*

Source: prepared by authors

The major part of the companies studied (56%) operate in the construction, service and trade sector while the other 44 % operate in petroleum, gaming, mining, production and telecommunication industry.

Table 4: Sample by legal form

Legal form	*Number of companies*	*Percentage*
Corporation	*21*	*51%*
Limited liability company	*20*	*49%*

Source: prepared by authors

According to the legal form, 51% of the companies are limited liability companies, and the other 49% are corporations.

Table 5: Sample by company size

Company size (measured by total assets)	*Number of companies*	*Percentage*
500 million-5 billion	*28*	*68%*
5 billion-10 billion	*6*	*15%*
over 10 billion	*7*	*17%*

Source: prepared by authors

The total assets of the major part of the companies studied (68%) are in the interval 500 million ALL – 5 billion ALL.

Analysis of the items included in the Disclosure index

After the verification of each item included in the Disclosure Index with the notes of each company, the authors reveals that:

- 36 out of 41 entities comprise cross-references with Notes, 5 out of 41 do not have a column of reference in their FSs.
- 40 out of 41 entities make an explicit and unreserved statement of compliance with IFRS in the notes.
- 40 out of 41 entities make a summary of significant accounting policies applied.
- 34 out 41 entities apply their judgements and make estimates for the preparation of FS.
- All the entities present supporting information for the line items presented in the FS.
- Commitments and contingencies have the lowest level of compliance, only 30 entities present notes according to this requirement by IAS 1.
- Only one entity does not present the comparative information related to the previous year figures.
- 35% of the entities present non-financial disclosure, such as business risk management.

The graph below summarize these findings.

Graph 1: Percentage of companies that disclose the items of DI

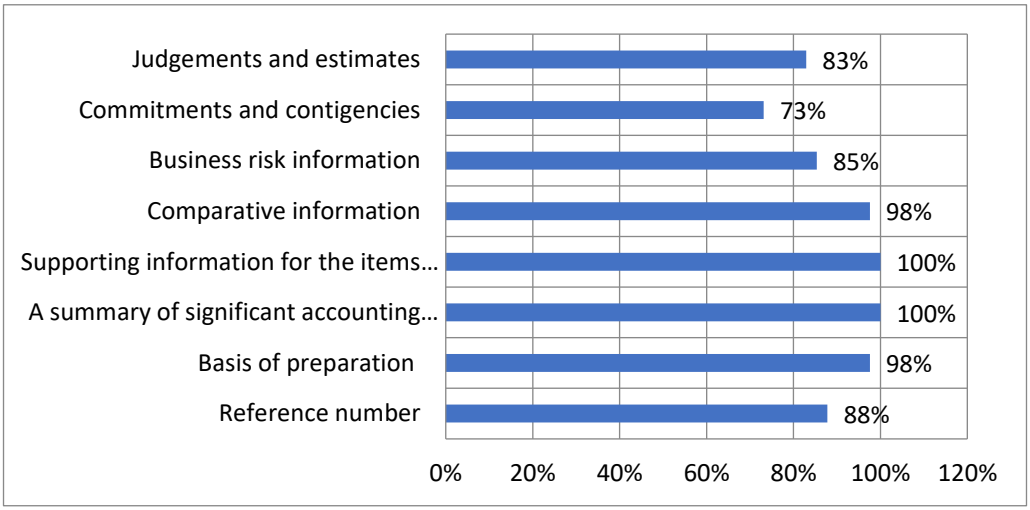

Source: prepared by authors

The study reveals that companies, on average, report 92% of the mandatory information.

Other items verified

- Number of disclosure pages varies between 8 and 40, with an average of 22 pages. The number of disclosure pages is too low compared to that of developed countries. According to the study by Beattie, Dhanani & Jones (2008) this figure in England in 1965 was approximately 26.
- 71% of the companies use the new terminology introduced by the IASB. 29% of them do not use the updated terminology.
- 24 out of 41 companies describe provisions in the summary of significant accounting policies applied, 15 out of 24 recognize a provision and 2 out of 41 companies do not mention provisions.

- 25 out of 41 companies describe impairment of receivables in the summary of accounting policies applies. 13 out of 25 companies test receivables for impairment, i.e. create an allowance for doubtful accounts, or make an explicit statement that their receivables are not impaired at the end of the reporting period. 3 companies do not mention impairment of receivables.
- Only 2 out of 41 entities do not continue to present notes in the same order as prescribed in unrevised IAS 1.

Conclusions

- The main objective of this paper was to verify the compliance with the mandatory disclosure requirements as per IAS 1, by large companies using IFRS in Albania. Moreover, we wanted to contribute with an up to date knowledge regarding the Disclosures and Disclosure Initiative. In order to meet the main objective, a data set for year 2016 was analyzed with 41 large companies. The empirical results indicate that the average disclosure level among Albanian companies investigated was 92%, while the minimum and maximum level were 50% and 100% respectively. This indicates the need for regulatory bodies to start enforcing laws that assure the compliance with mandatory requirements. However, we can say that 92% is considered to be a satisfactory level for our country.
- Only one of the entities taken into consideration does not present the basis of preparation and does not make a summary of significant accounting policies applied. All the entities give supporting information for the items presented in their FS. 26% do not present information related to commitments and contingent liabilities. 6 entities out 41 do not present information about risk management. 5 entities out of 41 do not cross-reference the notes with the respective items presented in FS. The terminology used in the preparation of the notes is updated for more than 70% of the entities studied.
- The major part of the companies describe the impairment of accounts receivable and provision in the summary of significant accounting policies applied session, but only half of them test the receivables for impairment and recognize provision. This means that, in reality they do not use those accounting policies.

Recommendations

- For a sustainable disclosure environment in the developing countries like Albania, more attention should be given on organizational culture, monitoring and enforcement by the regulatory body.
- Regulators body and government should enforce laws and regulations that guarantee full compliance with the mandatory requirements, reflecting in time the related amendments made in standards during the improvement process.
- Continuous training to the preparers of the notes, about the procedure of the compiling notes of the FSs.

References

[1] Barth, M., Landsman, W., & Lang, M. (2008). International accounting standards and accounting quality. *Journal of Accounting Research 46*(3), 467- 498.

[2] Beattie, V., Dhanani , A.,& M.J. Jones. (2008). Investigating presentational change in UK annual reports: A longitudinal study. *Journal of Business Communication 45*(2), 181 - 222.

[3] Beretta, S., & Bozzolan, S. (2008). Quality versus Quantity: The Case of Forward-Looking Disclosure. *Journal of Accounting, Auditing and Finance 23*(3), 333 - 376.

[4] Blanchette, M., Racicot F.E., & Sedzro K. (2013). L'adoption des IFRS au Canada: une analyse empirique de l'incidence sur les états financiers = IFRS adoption in Canada: an empirical analysis of the impact on financial statements. Association des comptables généraux accrédités du Canada. Available at: http://citeseerx.ist.psu.edu/viewdoc/download?doi=10.1.1.660.1220&rep=rep1&type=pdf (Accessed:2018-12-02).

[5] Deloitte (May,2017). Spotlight on key judgments and estimates.

[6] EFRAG. (July, 2012). Towards a Disclosure Framework for the Notes. Discussion paper.

[7] Epstein, J.B., & Jermakovicz, E.K.(2010). *International Accounting Standards and Application of International Financial Reporting Standards*.Wiley&Sons, Inc, Somerset, NJ 08875.

[8] Graham, L., & Carmichael,D.R. (2007). *Accountant's Handbook,* Financial Accounting and General Topics.Vol I.,12th ED, 10-3. John Wiley & Sons, Inc., Hoboken, New Jersey.

[9] Healy,P.,& Palepu,K. (2001). Information asymmetry, corporate disclosure, and the capital markets: A review of the empirical literature, *Journal of Accounting & Economics 31*(1-3), 405 - 441.

[10] Hodge,F., Jollineau, J.,& Laureen, M.A. (2004). Recognition versus Disclosure in Financial Statements: Does Search-facilitating Technology Improve Transparency? *The Accounting Review 79*(3), 687 - 703.

[11] Hope, O.K. (2003). Firm-Level Disclosures and the Relative Roles of Culture and Legal Origin. *Journal of International Financial Management and Accounting 14*(3), 218 - 248.

[12] IAS 1 International Accounting Standards 1 – Presentation of Financial Statements. Online Available (login required): http://eifrs.ifrs.org/eifrs/Menu Acquired: 2018-11-27.

[13] IASB (International Accounting Standards Board). (2013).Discusssion-Forum – Financial Reporting Disclosure:Feedback statement. The International Financial Reporting Foundation, May 2013. Available at: https://www.ifrs.org/-/media/project/disclosure-initative/feedback-statement-discussion-forum-financial-reporting-disclosure-may-2013.pdf (Accessed: 2018-11-27).

[14] Jaggi, B. , & Low, P.Y. (2000). Impact of Culture, Market Forces, and Legal System on Financial Disclosures. *The International Journal of Accounting 35*(4), 495 - 519.

[15] Kabureck, G.K. (2016, March). Footnotes of the Future—Reflections from the Disclosure Initiative.The article was first published on Compliance Week. Available at: https://www.complianceweek.com/sites/default/files/March%202016%20Digital%20Issue.pdf (Accessed:2018-12-02).

[16] Kothari, S.P., & Short,J.E. (2003). The Effect of Disclosures by Management, Analysts, and Financial Press on the Equity Cost of Capital. Paper 195 at ebusiness@mit.edu or 617-253-7054.

[17] Lourenço, I., & Branco, M. (2015). Main Consequences of IFRS Adoption: Analysis of Existing Literature and Suggestions for Further Research. *Accounting & Finance Review 26*(68), 126 - 139.

[18] Riedl E.J., & Srinivasan, S.(2010). Signaling Firm Performance Through Financial Statement Presentation: An Analysis Using Special Items. *Contemporary Accounting Research 27*(1), 289 - 332.

[19] Shields,H.(April, 2006). Introduction to a research report called “Principles not Rules: A Question of Judgement. (ICAS).

[20] Tweedie,D.(2007). Can Global Standards Be Principle Based? *Journal of Applied Research in Accounting and Finance 2*(1), 3 - 8.

[21] The Conceptual Framework form Financial Reporting (2010). Available at: https://dart.deloitte.com/resource/1/7036afd8-3f7e-11e6-95db-2d5b01548a21(Accessed:2018-12-02).

Synthesis of ZnO Nanorods by Chemical Bath Deposition Route: The Seed Layer Effects on Photovoltaic Performance

D. Gültekin

Sakarya University, Metallurgy and Materials Engineering Department, Esentepe Campus, Serdivan, Sakarya, Turkey

Abstract:

ZnO has been considered as one of the most proposed photo-anode materials [1] with wide bandgap (3.37 eV) and high exciton binding energy (60 meV) [2]. One-dimensional ZnO is among the most promising nanostructures due to their exceptional properties in wide range of applications such as electronic, optoelectronic, electrochemical, electromechanical and photoelectrochemical devices [3]. Dye sensitized solar cell as the third generation of solar photovoltaic device has attracted considerable interest during the past two decades, due to its low fabrication cost, simple manufacturing process and higher energy conversion efficiency. A perfect nano-structure of ZnO is required, which could provide the direct pathway for electron transmission. The typical one dimensional nano-structure of ZnO such as nanowires, nanorods and nanotubes, which can be beneficial to electron transport and can reduce the probability of charge recombination [1]. The ZnO nanorods have been synthesized by hydrothermal method. The seed layer properties are vitally important to control the structural, morphological, and optical features of the ZnO nanorods [3]. In this study, the effects of seed layer on the growth of ZnO nanorods during hydrothermal process and also on the photovoltaic properties of ZnO nanorod-based dye sensitized solar cells have been examined. The ZnO seed layers have been deposited on FTO coated glass substrates by sol-gel dip coating and preheated at 400°C. Zinc acetate dihydrate as precursor, monoethanolamine as an additive and ethanol as an solvent have been used to provide the sol to synthesize the seed layers. ZnO nanorods have been produced by hydrothermal route from precursor solution contains Zinc nitrate, hegzamethilenetetramine and water. General morphologies and detailed structural characterizations have been obtained by using scanning electron microscope, X-ray diffractometer, Raman spectroscopy, Open-circuit photovoltage measurements have been performed to investigate the photoelectrochemical characteristics of ZnO nanorod-based dye sensitized solar cells.[a]

Keywords: ZnO, nanorods, hydrothermal process, seed layer effects

[a] 1. Y. Dou, F.Wu, C. Mao, L. Fang , S. Guo, M. Zhou, Journal of Alloys and Compounds, 633, 2015, p. 408 - 414.
2. Y-C. Yoon, K-S. Park, S-D. Kim, Thin Solid Films, 597, 2015, p. 125 -130.
3. E. Pourshaban, H. Abdizadeh, M.R. Golobostanfard, Procedia Materials Science, 11, 2015, p. 352 - 358.

A Finite Difference Spectral-Collocation Method for Fractional Reaction-Diffusion Systems

Angelamaria Cardone

Dipartimento di Matematica, Università di Salerno, Italy

Abstract

This presentation deals with the numerical solution of a reaction-diffusion problems, where the time derivative is of fractional order. Since the fractional derivative of a function depends on its past history, these systems can successfully model evolutionary problems with memory, as for example electrochemical processes, porous or fractured media, viscoelastic materials, bioengineering applications. On the side of numerical simulation, the research mainly focused on suitable extensions of methods for PDE. This approach often produced low accuracy and/or high computational methods, due to the lack of smoothness of the analytical solution and to the long-range history dependence of the fractional derivative. Here we consider a finite difference scheme along space, to discretize the integer-order spatial derivatives, while we adopt a spectral collocation method through time. A suitable choice of the function basis produces an exponential convergence though time at a low computational cost, since the spectral method avoids the step-by-step methods.

Keywords: A Finite Difference Spectral-Collocation Method for Fractional Reaction-Diffusion Systems

Contrast of the Use of Open Educational Resources, in the Students of System Engineering of the Tecnologico Nacional De Mexico, Campus Mexicali

Dr. Jesus Francisco Gutierrez Ocampo

LSC. Hector Alejandro Pelaez Molina

M.C. Corina Araceli Ortiz Perez

M.C. Jose Antonio Camaño Quevedo

Tecnologico Nacional de Mexico, Campus Mexicali, Mexico

Abstract.

The open educational resources are a movement that has impacted the communities of students and teachers around the world, and the Tecnologico Nacional de Mexico, Campus Mexicali seeks to contrast it in the Systems Engineering students, with a research where the answers obtained as result of the survey on Open Educational Resources, were very important for the results.Paris Declaration on open educational resources, was the beginning of this movement that has impacted the communities of students and teachers around the world, and Tecnologico Nacional de Mexico, Campus Mexicali has not been left behind because of the importance of contrast of the use of Open Educational Resources, in the students of System Engineering of the Tecnologico Nacional de Mexico, Campus Mexicali. The design of the research and the idea of carrying out this important research was planned, first defining the problem of the research, and defining the objectives of the research, formulating the research questions; and following the methodology, we will focus on the specific description of our study population, define the technique and the instrument used for the compilation of the information, and finally, we will detail the assumptions used in the research, as well as the analytical techniques for compare them statistically.

Keywords: Open Educational Resources, MOOCS, Ingenieria de sistemas.

DLC Coatings on Spherical Elements of HIP Endoprostheses

Vasylyev V.V.
National Science Center «Kharkiv Institute of Physics and Technology», Kharkiv, Ukraine

Strel'nitskij V.E.

National Science Center «Kharkiv Institute of Physics and Technology», Kharkiv, Ukraine

Makarov V. B.

State Specialized Multidisciplinary Hospital No.1, Ministry of Health of Ukraine, Dnipro, Ukraine,

Skoryk M.A.

[3]NanoMedTech LLC, Kyiv, Ukraine

Boyko I. V.

SSI "Scientific and Practical Center for Preventive and Clinical Medicine", Scientific Department of Minimally Invasive Surgery, Kiev, Ukraine

Lazarenko G.O.

SSI "Scientific and Practical Center for Preventive and Clinical Medicine", Scientific Department of Minimally Invasive Surgery, Kiev, Ukraine

Abstract

Hard coatings are increasingly being used in medicine to protect metal endoprostheses The experimental process for the high-productive synthesis of high-quality diamond-like carbon (DLC) coatings with high hardness and a sufficiently high level of adhesion to the spherical shaped parts of the hip joint made from the stainless steel or cobalt-chrome alloy have been developed. DLC coating deposition was performed by vacuum-arc method from a high-productive source of the filtered vacuum-arc carbon plasma of rectilinear type with a "magnetic island". The high degree of thickness uniformity in the coating on the head of the hip joint with a high adhesion to the metal joint base was developed. Modernization of the vacuum arc plasma source allowed to accelerate the cathode spot motion, exclude substrate overheating and increase the diamond-like carbon hardness up to 30-40 GPa. The high adhesion level was achieved as a result of the high voltage pulsed of substrate bias potential use and multilayer architecture of DLC coating. The DLC coating on the heads of hip endoprosthesis did not peel off when boiling endoprosthesis or when immersing it into the liquid nitrogen.

Keywords: diamond-like carbon, head of hip joint, vacuum-arc, filtered plasma source, adhesion.

JEL O31

Determination of Insecticide Residues in European Honey Bees: Exposure in Conventional and Organic Cropping Systems

Míriam Gurpegui

Department of the Environment, National Institute for Agricultural and Food Research and Technology (INIA), 28040 Madrid, Spain

Manuel González-Núñez

Department of Plant Protection, National Institute for Agricultural and Food Research and Technology (INIA), 28040 Madrid, Spain

Ismael Sánchez-Ramos

Department of Plant Protection, National Institute for Agricultural and Food Research and Technology (INIA), 28040 Madrid, Spain

Ana I. García-Valcárcel

Department of the Environment, National Institute for Agricultural and Food Research and Technology (INIA), 28040 Madrid, Spain

Concepción Ornosa

Department of Biodiversity, Ecology and Evolution, Complutense University of Madrid, 28040 Madrid, Spain.

María Dolores Hernando

Department of the Environment, National Institute for Agricultural and Food Research and Technology (INIA), 28040 Madrid, Spain

Abstract

Bees play such an essential role as crop pollinators that it is crucial to preserve their diversity and to encourage the conservation of their populations. The decline of European honey bees (*Apis mellifera* L.) has many possible causes, including pathogens, parasites, malnutrition, habitat loss, climate change or the incorrect use of phytosanitary products. This study is intended to acquire knowledge on the degree of exposure of *A. mellifera* to Plant Protection Products (PPPs) in agronomic systems by comparing conventional versus organic production crops. Forager bees may be exposed to residues of PPPs when they collect nectar or pollen from flowers of crops previously treated. Bees may intercept pesticide residues via consumption of guttation droplets from plants, via contact with the dust drift originating from sowing treated seeds or via inhalation of high vapour pressure compounds during spray treatments. A particular concern has been raised about some systemic insecticides, such as neonicotinoids, which are used to control a wide range of insect pests. This 3-year field study was carried out in peach and apricot orchards in the Region of Murcia (Spain). The methodological approach involved an Ultrasound Assisted Extraction (UAE) and mass spectrometric analysis of insecticide residues in samples of honey bees.[1]

Keywords: European honey bee, insecticide residues, field study, cropping systems, mass spectrometric analysis.

[1] Acknowledgements: The authors acknowledge funding support from the National Plan for Scientific and Technical Research and Innovation 2013-2016; National Institute for Agricultural and Food Research and Technology – INIA, Ref. Project RTA2013-00042-C10-01.

Gaussian Noise Reduction in Images Using Non-Local Means Filter And Variational Methods

Ş. G. Kıvanç

Ankara Yıldırım Beyazıt University, Ankara/Turkey

B. Şen

Ankara Yıldırım Beyazıt University, Ankara/Turkey

F. Nar

Konya Food and Agriculture University, Konya/Turkey

Abstract

Noise is an unwanted signal resides in images that deteriorates the crucial information and structures in images. In this study, the advantages of Non-local Means filter and Total Variation based Sparsity Driven Despeckling with Quadratic Linear term is combined in a single cost function. NL means is used on texture areas and SDD-QL is used on homogeneous areas. Gaussian noise is artificially added to test images. The results of applying proposed method to noisy images are showed both qualitatively and quantitatively.

Keywords: NLTV, SDD-QL, NL Means, Gaussian Noise

Detection of Pesticide Residues in Honeybees in a Cropping System Under Integrated Pest Management

Patricia Plaza-Córdoba

National Institute for Agricultural and Food Research and Technology - INIA, 28040 Madrid, Spain

Ana I. García-Valcárcel

National Institute for Agricultural and Food Research and Technology - INIA, 28040 Madrid, Spain

María Teresa Martínez-Ferrer

Institute of Agrifood Research and Technology, IRTA, E 43870 Amposta, Tarragona, Spain

José Miguel Campos

Institute of Agrifood Research and Technology, IRTA, E 43870 Amposta, Tarragona, Spain

María Dolores Hernando

National Institute for Agricultural and Food Research and Technology - INIA, 28040 Madrid, Spain

Abstract

Pollination of crops is possible due to the action of pollinators, so honeybees have a very important role. The honeybee population is facing growing threats. Various factors have been identified in causing the reduction in pollinators including an expansion of pathogens, the incorrect use of phytosanitary products and environmental contaminants, along with other factors such as loss or fragmentation of habitat, invasive species and climate change. In economic terms, agriculture is a key sector in the EU; the estimated value of pollination is around 22 billion euros annually. In the Spanish agricultural sector, the citrus cultivation has a great socio-economic importance. In citrus, integrated pest management (IPM) attempts the most available use of strategies for the control of pests populations by means of taking actions that prevent problems, remove levels of damage and use of chemical control only when and where is necessary. The purpose of this work is to evaluate the exposure of honeybees to the usage of plant protection products (PPPs). Honeybees may intercept residues of PPP via consumption of nectar or pollen of plants treated by foliar spray or, via inhalation of high vapor pressure compounds during spray treatments. Due to the foliar spray in the crops, it is produced the absorption of hydrophobic PPPs, capable of crossing the cuticle of the plants or of entering through the stomata of the leaf, occurs mainly. The work presented here is a three-year field study, an approach to improve knowledge about exposure to PPPs on citrus orchards on honeybees. The methodological approach involves a generic extraction and mass spectrometric analysis of pesticide residues in samples of pollen collected from treated plants and in the honeybees themselves.[1]

Keywords*: pollinators, pesticide residues, field-study, citrus, exposure vias.*

[1] Acknowledgments: The authors acknowledge funding support from the National Plan for Scientific and Technical Research and Innovation 2013-2016; National Institute for Agricultural and Food Research and Technology – INIA, Ref. Project RTA2013-00042-C10-01 and RTA2013-00042-C10-04.

The Visualization of the Swirling Structures and the Swirling Burst of a Revolution Warhead

Dr (HDR) Abderrahmane Abene

ISTV Universite polytchnique de hauts de France

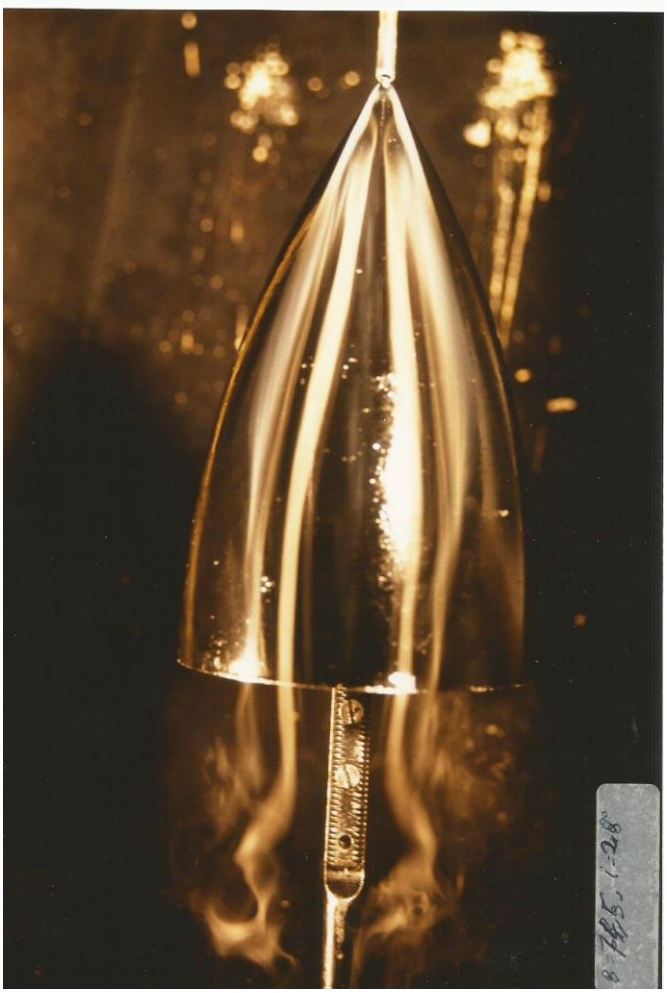

New Approach to Basel IV using AI

Pallav Kumar

Masters of Business Administration – Finance

Bachelor of Engineering – Computer Science

Dhrubajyoti Dey

Masters of Business Administration - Finance

Bachelor of Engineering – Computer Science

Abstract

The Basel Committee on Banking Supervision (BCBS) has released the Basel IV standards in December 2017. The major focus of the Basel committee has always been to improve capital and manage risk in the Banks. Basel IV, in this regards, targets the calculation of risk weighted assets for now and the capital floors by the end of 2022. In order to be compliant to this, the banks can either go the conventional way, which is not only cost heavy but also is a massive amount of manual work or the banks can strive for innovative solutions to cater to the requirement. Off late, Artificial Intelligence (AI) has been a major game changer in the fin-tech area. This paper is to showcase the capability of AI to eliminate manual effort and optimize the Basel IV implementation. AI can help in the real time assessment and consolidation of data from various sources to standardize the same and transmit the reports to the regulators in the required formats. AI can also anticipate the liquidity scenarios (based on trends, events etc.) and provide solutions to control the crests and troughs of the same. AI also helps data governance by generating reliable self-service data insights to make better decisions. Moreover, AI will help to optimize the operational procedures required to run the bank. All these along with an analytical engine put on the top can prove to be a breakthrough in the Basel IV implementation. Our paper explains in detail about how each of the Basel IV requirements can be implemented through Artificial Intelligence, thus proving to be a cost effective and optimized solution.

Keywords: new, approach, Basel IV, AI

Exponentially Fitted Quadrature Formulae for Oscillatory Problems

Dajana Conte

Dipartimento di Matematica, Università di Salerno

Abstract

Gaussian-type quadrature rules for oscillatory integrand functions are presented. The weights and nodes depend on the frequency of the problem and they are constructed by following the exponential fitting theory. The error analysis proves that the exponentially fitted Gaussian rules are more accurate than the classical Gaussian rules when oscillatory functions are treated. Some numerical tests are reported.

Keywords: exponentially, fitted, quadrature, formulae, oscillatory, problems